The development of an optimization procedure for the drivetrain of large-scale offshore wind turbines

Jasper Daneels

Abstract

List of symbols

A	Availability	(-)
c	Wind speed distribution scale factor	(-)
C	High voltage cable capacitance	(µF/km)
c(r)	Chord distribution along the blade	(m)
C_{blade}	Total blade costs	($)
$C_{blade\ labor}$	Blade labor costs	($)
$C_{bu\text{-}gen}$	Back-up generator costs	(k€)
$C_{blade\ material\ 1}$	Baseline blade material costs	($)
$C_{blade\ material\ 2}$	Advanced blade material costs	($)
c_{cable}	Specific cost of the submarine cable	(€)
$c_{converter}$	Specific converter cost	(€/kW)
$C_{converter}$	Converter costs	(€)
$c_{gearbox1}$	Specific cost for a single stage gearbox	(€/kg)
$C_{gearbox1}$	Single stage gearbox costs	(€)
$c_{gearbox3}$	Specific cost for a three stage gearbox	(€/kg)
$C_{gearbox3}$	Three stage gearbox cost	(€)
$C_{hc\ system}$	Costs of the hydraulics and cooling systems	($)
$C_{l,max}$	Lift coefficient for maximal L/D	(-)
$C_{ls\text{-}shaft}$	Cost of the low-speed shaft	($)
$C_{main\ bearings}$	Cost of the main bearings	($)
$C_{main\ frame}$	Cost of the main frame	($)
$c_{MV,install}$	Medium voltage cable installation cost	(€/m)
$C_{MV/HV\ trans}$	Cost of the MV/HV transformer	(k€)
C_{naelle}	Cost of the nacelle cover	($)
$C_{pitch\ mechanism}$	Pitch mechanism cost	($)
$C_{sg,MV}$	Medium voltage switchgear cost	(k€)
$C_{sg,HV}$	High voltage switchgear cost	(k€)
C_{SR}	Shunt reactor cost	(k€)
C_{SS}	Substation structural cost	(k€)
$C_{support\ structure}$	Support structure costs	(k€)
C_p	Coefficient of power	(-)
$C_{p,est}$	Estimated coefficient of power	(-)
C_{pcc}	Total costs of the power collection cables	(€)
c_{vessel}	Installation vessel dayrate	(k€/day)
$C_{yaw\ drive}$	Cost of the yaw drive	($)
D	Rotor diameter	(m)
$D_{default}$	Default rotor diameter	(m)
D_{seabed}	Depth of the seabed	(m)
E_{year}	Annual energy yield	(MWh)
f	Grid frequency	(Hz)
F_s	Single stage gearbox service factor	(-)
F_w	Single stage gearbox weight factor	(-)
H_{hoist}	Hoisting height	(m)
H_{hub}	Hub height	(m)
H_{ref}	Wind speed reference height	(m)
K	Wind speed distribution shape factor	(-)
$I_{n,MV}$	Maximal current in the medium voltage cable	(A)
$I_{n,HV}$	Maximal current in the high voltage cable	(A)
LCOE	Levelized cost of energy	(€/MWh)
L_{SCC}	Length of the shore connection cable	(km)

L_{string}	Length of the cable that connects a string of turbines	(m)
m_{1blade}	Mass of one blade	(kg)
m_{cone}	Mass of the spinner and nose cone	(kg)
m_{hub}	Hub mass	(kg)
$m_{gearbox1}$	Single stage gearbox mass	(kg)
$m_{gearbox3}$	Three stage gearbox mass	(kg)
$m_{main\ bearings}$	Mass of the main bearings	(kg)
m_{tower}	Tower mass	(kg)
N	Number of blades	(-)
N_{gear}	Number of gearbox stages	(-)
N_{rows}	Number of rows of turbines in the wind farm	(-)
$N_{turbines}$	First estimate of the number of turbines in the reference wind farm	(-)
P	Rotor power	(W)
P_{avg}	Average power output at a specified site	(MW)
P_i	Gearbox input power	(kW)
$p_{converter}$	Load through the converter	(W)
$P_{converter}$	Converter size	(kW)
$p_{conv,,rated}$	Losses in the converter at rated power	(W)
$P_{loss,converter}$	Converter losses	(W)
$p_{loss,copper}$	Generator copper losses at rated power	(W)
$P_{loss,copper}$	Generator copper losses	(W)
$P_{loss,gearbox}$	Gearbox losses	(kW)
$p_{loss,iron}$	Generator iron losses at rated power	(W)
$P_{loss,iron}$	Generator iron losses	(W)
P_{rated}	Rated power	(MW)
P_{SR}	Required size of the shunt reactor	(MVAr)
P_{target}	Target rotor aerodynamic power	(MW)
P_{trans}	Transformer substation rating	(MVA)
R	Rotor radius	(m)
R_{min}	Minimum rotor size	(m)
R_{max}	Maximum rotor size	(m)
r_{ratio}	Single stage gearbox gear ratio	(-)
r_w	Single stage gearbox sun-wheel ratio	(-)
T_I	Threestage gearbox input torque	(kNm)
T_m	Single stage gearbox output torque	(Nm)
T_{year}	Amount of hours in one year	(hours)
$U_{n,MV}$	Voltage of the MVAC cables	(V)
$C_{inst,HV}$	Voltage of the HVAC cable	(V)
V	Wind speed	(m/s)
$V_{cut\text{-}in}$	Cut-in wind speed	(m/s)
$V_{cut\text{-}out}$	Cut-out wind speed	(m/s)
V_{hub}	Wind speed at hub height	(m/s)
V_{rated}	Rated wind speed	(m/s)
$V_{rated,\ default}$	Default rated wind speed	(m/s)
V_{ref}	Wind speed at reference height	(m/s)
Z	Number of planet wheels in a gearbox stage	(-)
α	Cable cost coefficient	(€/m)
α_{shear}	Wind shear exponent	(-)
β	Cable cost coefficient	(€/m)

γ	Cable cost coefficient	(1/A)
λ	Tip speed ratio	(-)
λ_{max}	Maximal tip speed ratio	(-)
λ_r	Local tip speed ratio	(-)
$\varphi(r)$	Twist distribution along the blade	(°)
ρ	Air density	(kg/m^3)

List of abbreviations

AEP	Annual energy production
BEM	Blade element momentum theory
DC	Direct current
DD	Direct drive
DFIG	Doubly fed induction generator
DFIG-1G	Doubly fed induction generator - single stage gearbox system
DFIG-3G	Doubly fed induction generator - three stage gearbox system
DOWEC	Dutch offshore wind energy converter
EESG	Electrically excited synchronous generator
EESG-DD	Electrically excited synchronous generator – direct drive system
FCR	Fixed charge rate
HTS	High temperature superconducting synchronous generator
HVAC	High voltage alternating current
HV	High voltage
ICC	Initial capital costs
IEC	International electrotechnical commission
ISA	International standard atmosphere
LCOE	Levelized cost of energy
LRC	Levelized replacement costs
MVAC	Medium voltage alternating current
MV	Medium voltage
MV/HV	Medium to high voltage
NREL	National Renewable Energy Laboratory
O&M	Operation and maintenance
PMSG	Permanent magnet synchronous generator
PMSG-1G	Permanent magnet synchronous generator - single stage gearbox system
PMSG-3G	Permanent magnet synchronous generator - three stage gearbox system
PMSG-DD	Permanent magnet synchronous generator - direct drive system
PWM	Pulse-width modulation
SCIG	Squirrel cage induction generator
SG	Synchronous generator
WRIG	Wound rotor induction generator
XLPE	Cross-linked polyethene

Table of contents

1 Introduction

1.1 Goal of this thesis

The wind turbine drive train is one of the most important parts of the wind turbine. In literature, the term drive train is often used for the gearbox and generator combination inside the nacelle of the turbine. In this report however, the term 'drive train' is used for the entity of the rotor, the gearbox (if present) and the generator with converter. These are the main moving components of the wind turbine that harvest the energy from the wind and convert it to electrical energy. Figure 1 shows the cost breakdown of a wind turbine. From this figure can be seen that the drive train takes up almost half of the costs of the turbine, which adds to the importance of adequate design of this group of components.

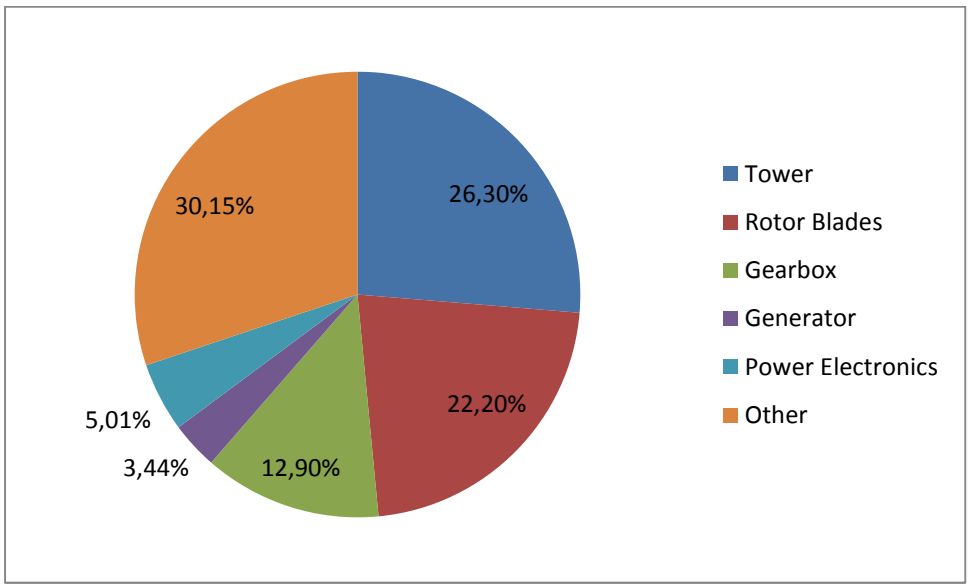

Figure 1: Cost breakdown of a REpower MM92 wind turbine [37]

One segment of wind turbine markets which is heavily growing is the market for offshore turbines. In early offshore projects, onshore turbines were used with only slight modifications. The harsh offshore environment resulted in high failure rates for these onshore models that were used offshore, which lead to the need and development of dedicated offshore wind turbines. This offshore market is growing rapidly over the last years with around 4 GW of installed capacity, around 5 GW under construction and up to 18 GW of consented projects in Europe [1]. Almost all these projects use turbines which have a conventional three bladed, variable speed and fully geared drive train.

Figure 2 depicts the average turbine sizes over the recent years. From this figure can be seen that the average wind turbine size has been around 3 MW for years. In 2007, the first 5 MW turbines were installed offshore and these very large wind turbines are being used more often, which is why the average size has risen to about 4 MW for the turbines currently under construction. Wind turbine manufacturers anticipate this trend of increasing turbine sizes, which is why 78% of the offshore wind turbine models under development are in the 5 MW or more size range [1].Within this growing segment of very large wind turbines, a larger differentiation in drive train configurations can be seen. Table 1 gives an overview of large turbines currently being manufactured or being developed and their main drive train specifications.

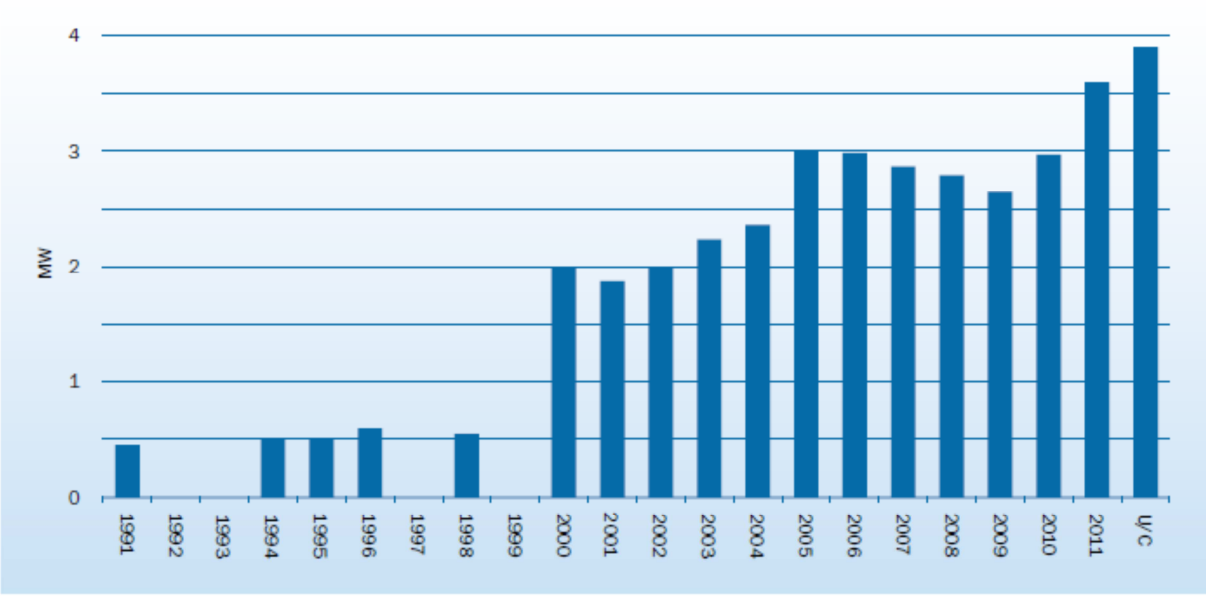

Figure 2: Annual average size of installed offshore wind turbines in MW [1]

From table 1 can be seen that there is a large differentiation in drive train configurations and sizes:

- *Rated Power*: The rated power ranges from 4.1 MW to 10 MW. It can be seen that the new 'industry standard' size could be around 5-6 MW as this is the range wherein most turbines are being manufactured and developed.

- *Rotor Size*: The rotor sizes range from 113 m to 190 m diameter. One would expect that increased rotor size would also mean increased rated power and this was a general trend of turbines in the past [2]. However, this is not always the case. For example, in the 5 MW size, there are rotors diameters ranging from 115 m to 135 m and for the 6 MW size, the rotor diameters range from 120 m to 154 m. This means that there are 5 MW turbines with a larger rotor diameter than some turbines with 6 MW rated power. This diversification is done in order to make turbines more attractive for locations with either high or low wind speeds. For two turbines with the same rated power but with a different rotor size, the one with the larger rotor will be more interesting for low wind speed locations while the turbine with the smaller rotor will be more interesting for the high wind speed locations.

- *Gearbox technology*: The large offshore wind turbines that are currently available are all geared turbines. Areva works with medium speed, single stage gearboxes, while Bard and REpower work with high speed, fully geared (three stage) gearboxes. Many turbines currently being developed will use direct drive (DD) systems, although there are also a considerably amount of medium and high speed, geared systems being developed. The direct drive has the advantage of having fewer moving parts, which is thought to improve the reliability of the turbines as the gearbox is considered a component with a high failure rate and repair cost [3].

- *Generator technology*: The current offshore turbines use either doubly fed induction generators (DFIG) or permanent magnet synchronous generators (PMSG). The turbines in development will all use PMSG technology, with only a handful exceptions.

- *Number of blades*: The 3-bladed turbines have become an industry standard for both onshore and offshore turbines due to their better performance and the fact that they are dynamically more balanced than 2-bladed turbines. However, in the future, we might see some 2-bladed offshore turbines appearing as there are a few manufacturers developing such turbines. This is because two-bladed turbines have a lower total blade cost, lower tower head mass and the rotor plus nacelle can be fully assembled in one time during installation, which is interesting for offshore applications [4].

- *Top mass*: The top mass is the mass of the rotor blades, hub and nacelle (which houses a.o. the gearbox and generator). Lower top mass leads to lower turbine installation costs as smaller installation vessels and cranes can be used. It also leads to lower loads on the tower and thus smaller tower wall thickness, reducing the tower cost.

- *Tip speed*: For onshore wind turbines, the tip speed is limited to approximately 80 m/s due to noise constrictions. For offshore wind turbines this restriction does not apply, which can be seen from the variation in tip speeds. Current large turbines operate at tip speeds between 80-100 m/s. Most turbines in development will also operate in this range except for two-bladed rotors. These two bladed rotors operate at high tip speeds in order to increase their power production.

There will thus be a very wide range of drive train configurations possible. Especially the selection of the number of blades, rotor size, gearbox type and generator type offer many possibilities and determine the power production to a large extent. For wind turbine designers and project developers, it could be useful to be able to compare many of these configurations to one another and study the impact of specific, site-related, wind conditions on the optimal design of the drive train configuration. It could therefore be useful to have an automated tool that compares the different drive train options for offshore wind turbines and estimates and optimizes some preliminary design variables. Developing such a tool will therefore be the goal of this thesis.

1.2 Project approach

There are many ways to model the components of the wind turbines drive train and the behavior of these components, each with its own level of detail and accuracy. Since the tool is developed for conceptual design studies, it should work relatively fast with very little input. This means that there has to be a trade-off in the models between complexity, level of accuracy and computational time.

There can be several objective functions for which the design is optimized. Since we are dealing with a sustainable source of electrical energy, one could set the objective function to maximize the amount of energy captured and converted to electricity. However, in most cases this objective function is not the most interesting from an investor's point of view. His interest will mainly be in maximizing the return on his investments. The question is now: How can we determine which configuration will maximize the return on investment? When reading articles and reports about different drive train configurations, it is often read that '*Generator system A has a larger reliability than generator system B. But generator system B is more cheap than generator system A*.' or '*Rotor configuration A has a lower energy yield than rotor configuration B, but rotor configuration A has lower installation costs*'. Such statements give notion of which configurations will increase or decrease energy yield with a change in cost at the same time. But is does not say if the cost decrease of a specific configuration is enough to make up for the loss in energy yield. Making a design choice purely based on such statements is therefore very difficult. To compare configurations with a different performance and different cost, the concept of levelized cost of energy will be introduced in Chapter 3 as this concept gives the possibility to combine the cost and performance of a turbine in an economic parameter. Therefore, the objective function of the design tool is set to minimize the levelized cost of energy as this gives a good estimate for maximizing the return on investment.

As was already mentioned, the rotor blades, the gearbox and the generator are parts with a wide range of design possibilities. These components also have a very large effect on the operation of the turbine and, as will be seen in Chapter 3, they also have a large effect on the economic performance of the turbine.

The goal of the study can now be defined as:

'Develop a fast engineering tool that optimizes the design of an offshore wind turbines drive train with the objective of minimizing the levelized cost of energy while taking into account the different configurations that are possible for the main components of the drive train.'

Obviously, the optimization of the main components of the drive train has already been subject of many research projects. Several design studies have done optimization studies for parts of the drive train or have even made optimization tools and models of drive train components. The WindPACT Turbine Rotor Design Study made a design model which optimizes the rotor design for cost of energy for medium to large size wind turbines [5].P. Fuglsang et al. made a model which optimizes the rotor for cost of energy for 1.5-2MW turbines with special attention to the specific wind conditions at the site for which the turbine is designed [6]. Martin Kirk investigated the effect of site-specific wind conditions on the rotor and generator size using an optimization tool [7]. Michael Schmidt conducted a similar research to find the optimum specific rating (kW/m²) of a turbine and included a cost model for offshore wind turbines [8]. However, all these studies only looked at one wind turbine layout: a three bladed, upwind, variable speed, fully geared wind turbine with a high speed wound rotor and variable speed electronics.

In the Upwind project, a tool was created which optimizes the drive train of a wind turbine consisting of a gearbox (if present) and a generator [9]. An optimization routine was developed for a number of gearbox-generator topologies, while having the turbines rotor topology and wind distribution as an input variable. This study also didn't account for the effects of different gearbox and generator topologies on the reliability and the availability of the wind turbine and it only optimized the gearbox and generator for one rotor design per turbine size.

All of the above research studies only focused on optimizing one component or subsystem of the offshore turbine or the offshore windfarm. It is thought that this will not lead to the optimal wind turbine layout as all the components of the drive train, the blades, gearbox and generator, should be treated as a complete system that needs to be optimized. An integrated design is thought to give better results than the sum of separately optimized subsystems [10].Therefore, the optimization of the blades, gearbox and generator should be done in one multidisciplinary design optimization which optimizes all the components of the drive train simultaneously while taking into account all other aspects of the turbine and wind farm. To the knowledge of this author, no record of a study that developed such a multidisciplinary design optimization tool for multiple drive train configuration options is available.

A similar study was performed as a master thesis by Bram Derks, another student at TU Delft [11]. His optimization procedure consisted of a complex (Matlab) optimization routine that used a complex gearbox model in combination with a rather simple rotor and generator model. The model faced convergence problems and did not yield any suitable results. To avoid such problems, the approach in this project will be to first set-up a first simple, working model after which improvements can be added to obtain better results. The results of both the first and the second model will be analyzed in order to see if the results correspond to what is expected and in order to see if the results can be used to make any relevant conclusions about the optimal drive train configuration, given the level of accuracy that is reached.

In Chapter 2, the components and variables which are subject to optimization will be analyzed. In Chapter 3, the framework for analyzing the economics of each design is given. Chapter 4 sets the framework to analyze the performance of each design. The optimization procedure is explained in Chapter 5 after which a first set of results is analyzed in Chapter 6. The work shown in Chapter 3 to 6 forms the first, simple model. In Chapter 7, the model limitations are summed up and some improvements to this first model are suggested and Chapter 8 shows results of an improved model in which some of these suggestions are implemented.

Table 1: Overview of large offshore wind turbine's drive train technology

Existing models									
Manufacturer	**Type**	**P rated (MW)**	**D rotor (m)**	**Hub height (m)**	**Gearbox stages**	**Generator type**	**Blades**	**Top mass (t)**	**Tip speed (m/s)**
Areva	M5000 - 116 [12]	5	116	90	1	PMSG	3	345	89,9
	M5000 - 135 [12]	5	135	90	1	PMSG	3	375	95,4
Bard	Bard 5.0 [13]	5	122	90	3	DFIG	3	350	100
Repower	5M [14]	5,075	126	85-95	3	DFIG	3	410	79,8
	6M [15]	6,15	126	85-95	3	DFIG	3	450	79,8
In development									
Alstom	Haliade [16]	6	150	100	DD	PMSG	3	390	90,8
AMSC	Sea Titan [17]	10	190	125	DD	HTS	3		
Bard	Bard 6.5 [18]	6,5	122		3	2 x PMSG	3	350	/
Condor	Condor 5 [19]	5	120		2,5	SCIG	2	266	126,9
DSME	DSME 7MW [20]	7	160	106	2	PMSG	3		
Gamesa	G128 [21]	5	128	120-140	2	PMSG	3		
	G14X [22]	7	145				3		
GE	4,1-113 [23]	4,1	113		DD	PMSG	3		
Mitsubishi	Sea Angel [24]	7	165		Hydraulic	Brushless SG	3		
Nordex	N150 [25]	6	150	100	DD	PMSG	3	330	95
SCD Technology	SCD 6 MW [26]	6	140				2	205	99,6
Siemens	SWT 6.0 120 [27]	6	120		DD	PMSG	3	350	
	SWT 6.0 154 [27]	6	154		DD	PMSG	3	360	88,7
Vestas	V164 [28]	7	164	104	3	PMSG	3	390 (+ blades)	90,2
XEMC DarWinD	DD115 [29]	5	115		DD		3	265	
2-B Energy	2B6 [30]	6	130				2		

2 Drivetrain system description

In this chapter, the main components of the drive train will be described together with the most common technology that is used today or is expected to be used in the near future for these components.

As was mentioned in the introduction, the main components which form the drive train are the rotor, consisting of the rotor blades and the hub, the gearbox (if present) and the generator. And although there are many more components determining the performance and the costs of a turbine, the focus will be on these component technologies as the rest of the components are not subject to optimization.

The rotor captures part of the energy from the wind and converts it to rotational energy. The main shaft, sometimes called the rotor shaft or low-speed shaft, transfers the rotor torque to the gearbox while rotating at the same rotational speed as the rotor. In the gearbox, this rotational speed is stepped-up to a higher rotational speed which is more suitable for the generator. Finally, the generator converts the mechanical energy from the high-speed shaft, which comes out of the gearbox, into electrical energy. For some configurations, an electronic power converter is needed in order to improve the power quality to a level which is suitable for the electrical grid and to allow variable speed operation. The transformer is considered not to be part of the wind turbine drive train, but part of the electrical transmission system.

Each design choice for the components has its advantages and its disadvantages. Since the optimization procedure only accounts for costs and energy yield of the design options, the main focus of the comparison of different concepts was on (dis)advantages of the concepts that could be quantified by changes in cost or energy.

2.1 The rotor

2.1.1 Speed regulation

The rotational speed of a rotor can either be fixed speed, meaning that the rotor rotates at a constant rotational speed over the entire range of wind speeds for which the turbine operates, or it can be variable speed, meaning that the rotational speed of the blades varies with the wind speed. Many fixed speed turbines were manufactured during the 1980's and 1990's. The use of fixed speed turbines became less popular since this type of speed regulation has some downsides. One major downside is that the performance of the rotor is only optimal at one speed [31].

During the previous decade, most large turbines of over 1,5MW use the variable speed concept. The reasons for this are [31]:

- Improved output power quality which is increasingly important due to grid requirements.
- Increased energy capture because the turbine can operate at optimal performance for the entire range of wind speeds between cut-in and rated wind speed.
- Reduced noise.
- Reduced mechanical stress in the drive train. This is because a varying rotor speed can dampen the power and torque peaks caused by wind gusts through storage of kinetic energy in the rotor.

One drawback of using variable speed is that a power electronic converter is required to alter the generator frequency to the correct grid frequency, which is not the case for fixed speed turbines. However, since the price of power electronic converters has dropped drastically over the recent years, this disadvantage became a smaller problem.

Since nearly all turbines that are currently being produced or being developed have variable speed operation, only variable speed machines are considered for the optimization of the offshore wind turbine drive train.

2.1.2 Rotor power control

Two ways of power control are quite common: passive stall control and active pitch control. In stall control, the blades are designed such that they stall at high wind speeds, reducing the aerodynamic performance at these wind speeds and therefore lowering the power. The advantage of such power control is that the blade can be connected to the hub through a rigid connection. One disadvantage of stall control is that stall properties of blades are difficult to predict. This could lead to inaccurate estimations of the loads encountered by the rotor and the rest of the drive train [32]. Another disadvantage is that the maximum power usually occurs at relatively high wind speeds. And although such wind speeds are infrequent, all the components must be sized for the loads occurring at this wind speed [2].

The most common way of power control today is through active pitch control. With active pitch control, the entire blade is rotated at wind speeds above rated wind speed such that the angle of attack and hence the lift coefficients along the blade decrease. Such a rotation is called pitch to feather. This type of control has the advantages of having a higher total energy capture, the ability to work as an aerodynamic brake and the ability to reduce loads at extreme wind speeds. The disadvantages are that a complex blade-hub connection is needed in order to allow for the blade to pitch. Both this complex connection and the necessary pitch system increase the cost of the rotor [32].

There is also a more exotic way of controlling the power and this is by means of active yaw control. For this type of control, the rotor is yawed out of plane of the incoming wind, therefor reducing the effective area facing the wind and hence lowering the power. One offshore turbine is under development that will use this kind of power control, the Condor 5.

It is thought that the active pitch control system is the best system and since almost all current turbines use this type of power control, only pitch controlled turbines are considered in the optimization procedure.

2.1.3 Number of blades

Most modern turbines have a three-bladed rotor. This is because their polar moment of inertia is constant during yawing, making the rotor dynamically more balanced [2]. Another benefit is that three-bladed rotors perform slightly better than two-bladed rotors due to lower tip losses [32].

Two-bladed rotors have the advantage of being cheaper as less blade material is needed. Another cost advantage is that two-bladed rotor turbines can be fully assembled and loaded on a ship which takes them to the installation site where they are installed in a single hoist, which saves both time and cost [4].

In order to achieve performance that is comparable to three-bladed rotors, two bladed rotors either need a much larger blade planform or a higher tip-speed. Since increasing the blade planform area would cancel out the benefit of using less material and thus having a cheaper rotor, two-bladed rotors usually operate at a higher tip-speed [2]. Due to these larger tip-speeds, two-bladed rotors produce much more noise. These noise restrictions are a major issue for onshore turbines, however, for offshore turbines, this is less of a drawback [4]. Another disadvantage is that two bladed rotors introduce higher loads on the main shaft. This is a reason why teetered hubs are being used for two-bladed rotors as this relieves some of these higher loads [2]. Such teetered hubs are more expensive than the conventional hubs which can be used for three-bladed turbines.

Both rotor concepts are evaluated in the optimization process.

2.1.4 Tip speed ratio

As was mentioned in Section 2.1.1, the turbine will operate at variable speed. When designing a blade, the blade twist angles and chord distribution will be optimized for a specific tip speed ratio. The power coefficient will therefore only be at its maximum for this design tip speed ratio. For a fixed blade solidity, an increase of the tip speed ratio will lead to a decrease in chord lengths along the blade. This could lead to lower blade weight although a smaller chord length doesn't have to mean that the blade mass will be lower. Another benefit of a higher design tip speed ratio is that the rotational speed of the rotor will be higher, leading to a lower torque for a given power level. This leads to a decrease in the mass and cost of the main shaft, the gearbox and the generator [2].

2.1.5 Rotor diameter

In the past, increasing the rotor diameter usually was accompanied by an increase in rated power. However, in recent years, interest has risen for wind turbines with rotor diameters suitable for specific sites.

The commonly used formula for power delivered by a wind turbine up to rated wind speed is:

$$P = \frac{1}{2}\rho C_p \pi R^2 V^3 \qquad (2.1)$$

Where:

P= Rotor power (W)

ρ = Air density (kg/m³)

C_p = Power coefficienct at the design tip speed ratio (-)

R = Rotor radius (m)

V = Wind speed (m/s)

From this formula, it can be seen that (with an unchanged coefficient of power) if the diameter is increased, lower wind speeds are required to meet a certain power level. This is interesting for locations with lower wind speeds. The increased rotor diameter of course comes at a higher cost as more blade material is needed. The increase in energy harvested at the lower wind speeds must therefore be enough to account for this increase in rotor cost.

Similar to the reasoning above, the same can be done for high wind speed locations. In such locations, it could be worth it to decrease the rotor diameter and thus lower the rotor costs.

2.2 The gearbox

The gearbox is a component in between the rotor and the generator. The function of the gearbox is to increase the rotational speed of the main shaft. In this way, you actually get two shafts: the low-speed shaft, connecting the rotor to the gearbox, and the high-speed shaft, connecting the gearbox to the generator. Since the high-speed shaft has a higher rotational speed, the torque will be lower as rotational speed and torque vary inversely for a given power level. Since the size of the generator is proportional to the mechanical input torque, the presence of a gearbox will decrease the size and cost of the generator [9]. A gearbox consists of several stages, each increasing the rotational speed step by step. A three-stage gearbox, sometimes called high speed gearbox or fully geared system, is commonly used in both onshore and offshore turbines.

A disadvantage of the three-stage gearbox is that there are some losses in the gearbox, decreasing the efficiency of the drive train. Another major disadvantage is the fact that historically, gearboxes have been a component with a relatively high failure rate. Due to the large size and weight of gearboxes, gearbox failure is a costly problem, especially offshore.

An alternative to using a gearbox in between the rotor and generator is by using a direct drive system. In such a system, the rotor is directly connected to the generator by use of a single low-speed shaft. Such a system has the advantages of omitting the complex gearbox. This leads to a system with a higher overall efficiency and reliability and a higher availability. However, since the generator operates at such a low rotational speed, the generator will have a very large diameter and a high weight. This leads to a high cost of such drive systems [9].

A solution in between the direct drive technology and the high speed gearbox is the single-stage, medium speed gearbox. It has the advantages of working at a higher rotational speed than the direct drive technology while keeping the number of components relatively low, thereby hopefully assuring a higher reliability than the fully geared concept. The losses are also less than the losses in a three-stage gearbox.

All three configurations will be investigated in the optimization routine.

2.3 The generator

The generator is the component in the wind turbine that transforms the mechanical energy into electrical energy. Historically, many types of generators have been used and tested in wind turbines. These generator types include squirrel cage induction generators (SCIG), wound rotor induction generators (WRIG), doubly fed induction generators (DFIG), permanent magnet synchronous generators (PMSG) and electrically excited synchronous generators (EESG) [9]. Not all generators are suitable for each, geared or direct, drive system. Direct drive systems require a synchronous generator, while geared systems are usually equipped with induction generators [32]. In this optimization procedure, PMSG and EESG technology is analyzed for direct drive systems and DFIG and PMSG technology is analyzed for geared systems.

The sections concerning the design options for the generator are largely based on the research on generator systems done for the Upwind project [9].

2.3.1 Doubly fed induction generators

Since a DFIG does not require a full scale converter, but can be used with a 30% power rating electronic power converter, this technology is very popular for large wind turbines as power electronics are an expensive part of the generator system. An advantage of the DFIG is that the stator active and reactive power can be controlled independently by controlling the rotor currents with the converter. The grid-side converter can control the reactive power fed into the grid independently of the generator operation, which allows for voltage support towards the grid.

Disadvantages of the DFIG are that:

- A gearbox is necessary in the drive train as the speed range of a DFIG and the speed range of a typical large rotor do not match.
- The connection between the generator rotor and the converter is a connection between a stationary and a rotating part. In order to make this connection, carbon brushes and slip rings are used. These components require regular maintenance, are prone to failure and increase the electrical losses.
- DFIG requires complex control strategies in case of grid disturbances.

2.3.2 Electrically excited synchronous generator

Usually in an EESG, the rotor carries a DC system, which excites the rotor magnets. This type of generator requires a full scale converter, which is costly. However, the advantage of the use of a full scale converter is that at the generator side of the converter, the amplitude and frequency of the voltage can be fully controlled independent of the rotational speed of the generator rotor and thus independent of the turbines rotational speed. This allows the gearbox to be omitted and the use of direct drive technology instead. The generator active and reactive power can also be fully controlled. The main disadvantage is that both the generator and the power electronic converter are very expensive.

2.3.3 Permanent Magnet Synchronous Generator

PMSG technology works in a similar way to EESG. The main difference is that PMSG technology uses, as the name says, permanent magnets instead of electrically excited magnets. Permanent magnets used to be extremely expensive, but due to drastic price drops in the past decades, they have become an interesting alternative to EESG technology.

The advantages of PMSG over EESG are:

- Higher efficiency and energy yield due to removal of rotor windings, brushes and slip rings.
- Higher reliability due to fewer electrical components and due to the absence of brushes.
- A lighter weight can be achieved.

The disadvantages are the still relatively high costs of permanent magnets, the difficulties to handle these magnets in manufacture and the demagnetization of such magnets at high temperatures. Although the current price of permanent magnets is not so high, these prices could rise in the future as these permanent magnets use rare earth metals.

2.4 The design variables

In the previous sections, the main components of the drive train have been described together with the most feasible technologies. In this section, all this will be summarized and a list of the design variables will be given. There are two sorts of design variables: numerical design variables and conceptual design variables. Numerical design variables are variables for which the optimization procedure will vary the values over a specified range. Conceptual design variables are completely different from numerical design variables as they represent a choice between several concepts that are feasible for that 'variable'. An example of a conceptual design variable could be the choice of the generator technology.

The turbine will be an upwind, variable speed, pitch controlled turbine. The desired rated aerodynamic power will be used as input.

Numerical design variables:

- Tip speed ratio λ
- Rotor radius R (alternatively, the rated wind speed for the turbine could be used as a design variable as diameter and rated wind speed are interdependent for a fixed rated power).

Conceptual design variables:

- Number of blades N. Although the number of blades appears to be a numerical value, it is a choice between two concepts, either a two-bladed rotor or a three-bladed rotor and is therefore a conceptual design variable.
- Choice of direct drive technology or technology including a single stage or three stage gearbox
- Generator choice: PMSG, EESG and DFIG.

Constraints on these design variables will be given and explained in Chapter 5. However, some constraints on the conceptual design variables will already be applied. As explained in section 2.3, not all drive systems work with all types of generators. The gearbox-generator combinations will therefore be limited to:

- PMSG with direct drive, single stage gearbox or three stage gearbox
- EESG with direct drive
- DFIG with single stage gearbox and three stage gearbox

It could be argued that an EESG could also be used in combination with a gearbox. Such a system is not considered since is thought to be too expensive and have too high losses. The EESG direct drive combination is merely included to have more than one direct drive system under evaluation.

3 Wind Turbine Economics

In this chapter, some concepts which are used in the economical evaluation of the design are explained and the economic dynamics of designing a wind turbine will be explained as well. As mentioned in the introduction, the economic analysis will be done using the concept of the levelized cost of energy.

3.1 Objective Function: Levelized Cost of Energy (COE)

The objective function of the optimization tool is to minimize the COE. Dr. Stefan Thomas defines the levelized cost of energy as [33]:

Levelized Cost of Energy is equivalent to the average price consumers would have to pay to exactly repay the investor for capital, O&M and fuel costs with a rate of return equal to the discount rate. It is thus the minimum price at which energy must be sold for an energy project to break even.

This definition applies to all types of electrical energy generation. For wind energy, the fuel costs can be excluded as the wind is a free source of 'fuel'. Various approaches can be found in literature to calculate the levelized cost of energy. Some of them account for financing costs and inflation, others do not. In the WindPACT Alternative Drive Trains Design study, the COE was calculated using the following expression [34]:

$$LCOE = \frac{ICC \times FCR + O\&M + LRC}{AEP}$$

The COE is expressed in €/MWh. The contributions to the COE are:

- ICC (€): The initial capital costs (€) consist of the costs of all the offshore turbine system components and the balance of station costs [35]. Figure 3 gives an overview of the cost breakdown of an offshore wind farm. In this cost breakdown, the cost of the support structure, the grid connection, the turbine can be identified as costs contributing to the initial capital costs. The costs of the turbine itself can be broken down into several components. Figure 4 shows the cost breakdown of a REpower MM92 turbine. As opposed to Figure 1, the cost of the tower is excluded in Figure 4 as this was already included under 'Support Structure' in Figure 3. One cost contribution which is not included in Figure 3 or Figure 4 is the installation costs. This is also considered to be an initial capital cost and will be accounted for. For each configuration, the initial capital costs will have to be determined using available costs models for different components.
- FCR (%/year): The fixed charge rate can be described as [34]: *The FCR is the amount of revenue per dollar of ICC needed to pay the carrying charges for the investment. It includes return on debt, return on equity, taxes, depreciation, and insurance.* The fixed charge rate is independent of the drive train design and thus the same for each configuration, but it should be noted that in real life, the FCR changes over time do to the changing economic climate. In this report, it is assumed to equal 11.5%/year.
- O&M (€/year) stands for the levelized annual operation and maintenance costs per year. The annual operation and maintenance costs are the costs associated with both scheduled and unscheduled maintenance per year and with costs from administration and support. They consist of costs for labor, parts, equipment and supplies [35]. The unscheduled maintenance costs are influenced by the failure rate of the components, the mean time to

repair and the costs of spare parts. Different drive train configurations will therefore have an impact on the costs for operation and maintenance.

- LRC (€/year) are the levelized replacement costs. It accounts for the costs for major overhauls and replacements which will take place a few times over the lifetime of the wind turbine. The NREL cost model distinguishes these costs from the operation and maintenance costs. It could be argued that these costs are a part of the scheduled maintenance. In the O&M cost model described in Section 3.7, the levelized replacement costs are already accounted for as part of the O&M costs.
- AEP (MWh/year): The annual energy produced is the energy that is produced by a single turbine within one year and delivered to the electrical grid. It depends on the performance of the rotor, the wind speed distribution, the efficiency of the drive train components and the availability of the turbine.

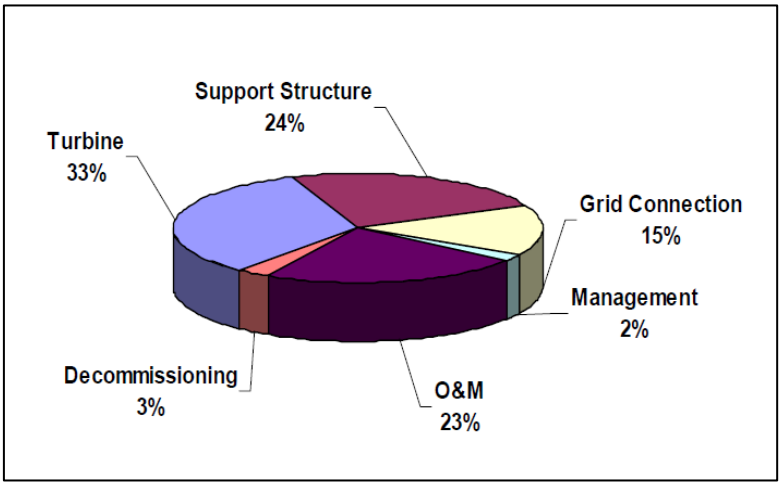

- Figure 3: Approximate cost breakdown for an offshore wind project in shallow water [36]

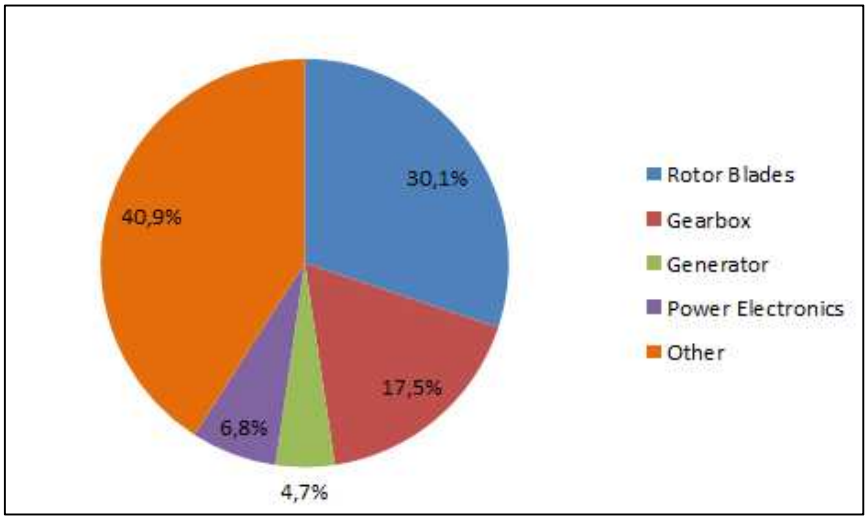

Figure 4: Cost breakdown of a REpower MM92 wind turbine excluding the tower. Reproduced from [17]

In order to clarify the interactions that contribute to the levelized cost of energy are shown in a schematic way in Figure 5.

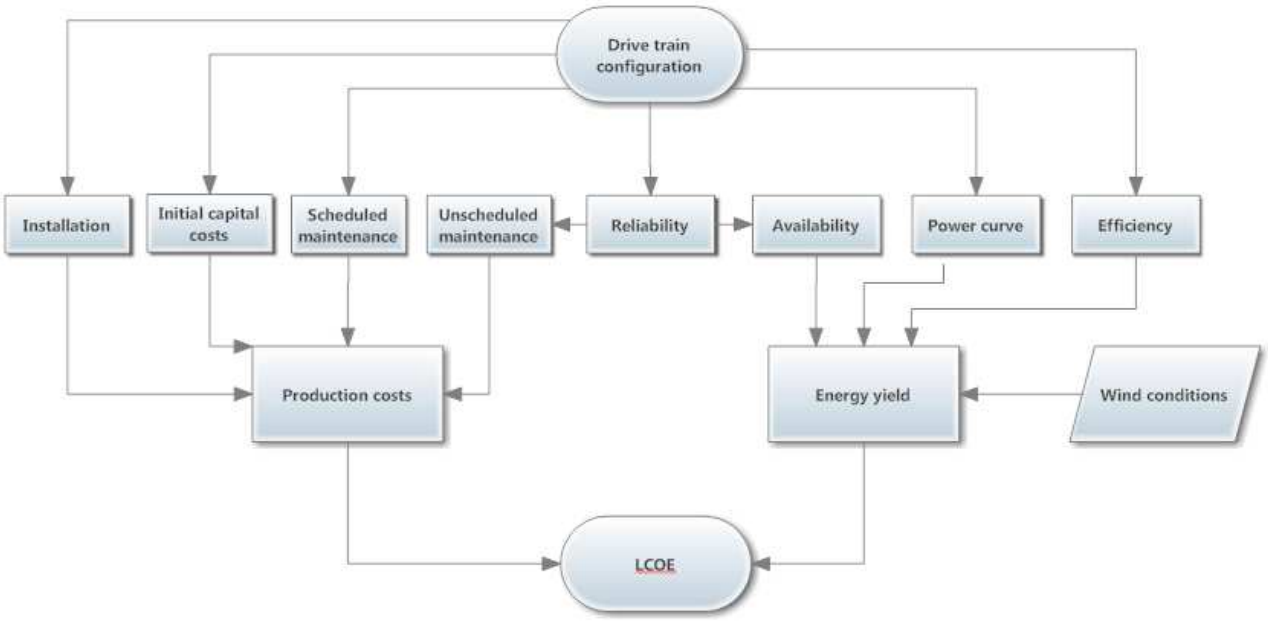

Figure 5: Overview of the contributions to the levelized cost of energy calculation

3.2 Currency and inflation correction

It should also be noted that many of the cost models that will be used in the following chapters, have been developed some years ago. The results therefore have to be corrected for cost changes over the years. Inflation can give a first estimate of the evolution of the costs from the date of publication of the models to the present. However, material and labor costs for each component can show different trends than the overall inflation, which causes the results to be incorrect. But since there is a lack of recent models for some components, this correction for inflation is the simplest solution to this problem. Another problem which has to be accounted for is that some models give results in US Dollars while others give results in Euro. All the values should be converted into Euro.

When a cost estimate needs to be converted from US Dollars to Euro and a correction for inflation is needed, two options are possible [51]. One is to correct for inflation using the inflation rate of the original currency (in this case US Dollar) and afterwards use the current exchange rate from US Dollar to Euro. This is called the inflate-first method. Another possibility is to exchange from US Dollar to Euro using the historical exchange rate first and afterwards correct for inflation using the inflation rate of the Euro. This method is called the exchange-first method.

Since the currency exchange rates show very large variations over time and the inflation rate of the US Dollar and the Euro show different trends, the two methods can show very different results. Figure 6 shows and example of the two methods being applied to a project that needs to be converted from year 2000 US Dollar to year 2009 Euro. In this report, the exchange-first method will be used.

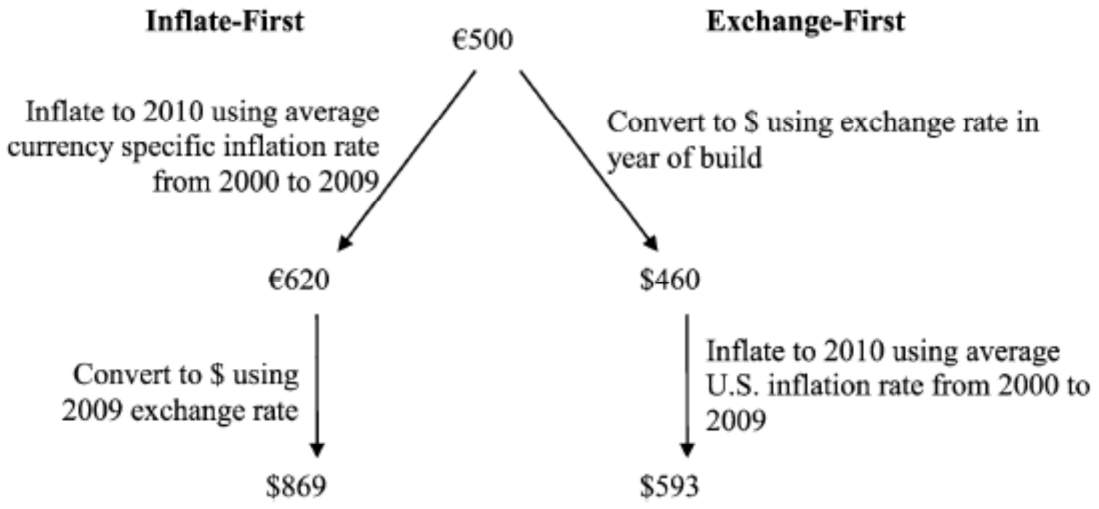

Figure 6: Example of the conversion from year 2000 US Dollar to year 2010 Euro using two different correction methods [51]

3.3 Initial Capital Costs

In this chapter, the cost models for all the components of the wind farm will be given. Although this study focuses on the optimization of the drive train components, the costs of all the components should be considered when determining the COE. The components that are accounted for in the cost model are:

Wind turbine components:

- The blades and hub
- The gearbox if a gearbox is present
- The generator, optionally with a power electronic converter
- The auxiliary components inside the nacelle
- The tower and support structure

Wind farm components:

- Offshore electrical network and transformer substation
- Development costs

Besides the component costs, the costs for installation will also be calculated.

Since the optimization procedure wants to find the optimal drive train configuration, the cost models should show the effects of changing the drive train variables on the costs of each component. In the first optimization model, cost models are taken from literature. Detailed cost models are very hard to find in literature as there is only a limited amount of cost information publicly available. Therefore, the found cost models do not always fully reflect the change in drive train variables as a change in costs. But they do suffice to form a first model. In Chapter 7, the limitations of these models are analyzed and improvements to the cost model are suggested and implemented.

3.4 Wind turbine costs

As was mentioned in the previous section, it is rather difficult to find detailed and up-to-date cost models for most components. It will be seen that due to the lack of detailed cost models, the chosen cost model do not always fully reflect the cost drivers that really determine the component costs but are subject to simplification. The limitations of the used cost models will be discussed more thoroughly in chapter 7.

3.4.1 Blade costs

The costs of the blade are made up out of two categories: the direct manufacturing costs and the indirect manufacturing costs. The direct manufacturing costs are the material and the labor costs. The indirect manufacturing costs consist out of overhead costs, development costs and facilities costs [38]. The transportation costs are not included in the blade cost model. An example of the different cost contributions for different blade sizes is given in Table 2. The contribution of the 'other costs' consists mainly of the development costs. As can be seen, the major cost contribution comes from the material costs and the labor costs.

Blade radius	30 m	50 m	70 m
Material costs	32,9%	38,5%	40,7%
Labor costs	39,4%	33,4%	30,6%
Overhead costs and profit	23,1%	23,0%	22,7%
Other costs	4,6%	5,2%	6,0%

Table 2: Blade costs contributions (excluding transportation costs) [38].

3.4.1.1 Material costs

The amount of blade material is determined from the aerodynamic blade shape and from the structural requirements.

An example of a typical layout of a blade section is shown in Figure 7. The desired aerodynamic shape is formed by the balsa-core skins. The amount of skin material for the aerodynamic shape can be determined from the airfoil and chord distribution over the length of the blade.

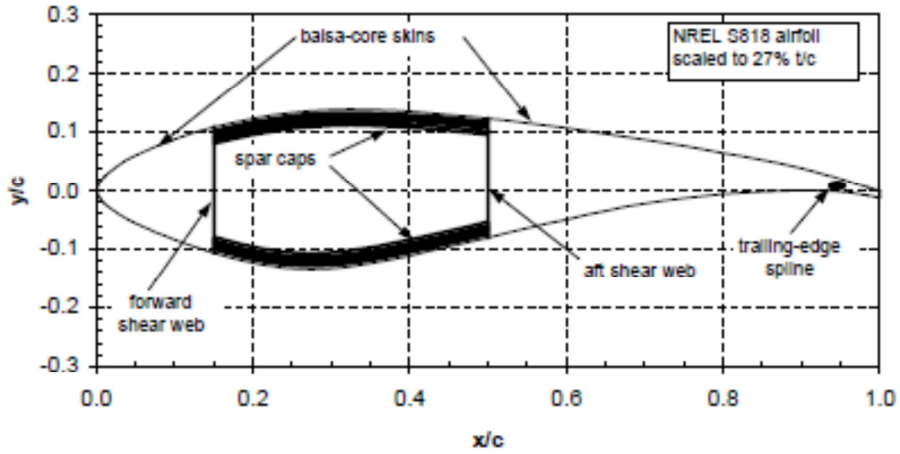

Figure 7: Typical cross section of a wind turbine blade [40]

Although the blade skin will carry some loads, the bulk of the loads will be carried by the main structural element. This structural element could be described as a box-beam consisting of two shear

webs and two spar caps as shown in Figure 7. The dimensions of the main structural element are determined by a number of operational constraints:

- The maximal tip deflection of the blade should be controlled. This is done by controlling the blade stiffness.
- The natural frequencies of the blade should be checked. The natural frequencies of the blade are controlled through the stiffness and mass distribution.
- Buckling should be avoided. This is done by controlling the blade stiffness and providing enough strength.
- The extreme loads should be carried. This means that the blade should ensure sufficient ultimate strength.
- The variable loads should be carried in order to avoid fatigue damage. The blade must therefore have sufficient fatigue strength.

The structural element should be sized in order to meet all of the above constraints and this should be done for each planform design. This would require a detailed design of the blade as many of these constraints are dependent on the material selection and on the exact layout of the blade sections and structural elements. However, a full detailed design of a wind turbine blade is out of the scope of this project. A simplified approach will therefore be used in order to obtain the necessary blade material and hence material cost for the different planforms.

3.4.1.2 Labor costs

The manufacturing of wind turbine blades is still a process which requires much man labor and therefore takes up a large share of the blade costs.

Larger blades, having a larger planform surface area, or blades with a larger material thickness will require more labor and have higher labor costs. Different manufacturing techniques will also influence the labor costs. However, analyzing the exact effects of each blade planform on the labor costs is out of the scope of this project. Again, a simplified scaling relation will be used to estimate the labor costs.

3.4.1.3 Blade cost model

As was mentioned, a simplified cost scaling model is needed for the blade costs. The blade cost model presented here is based on the '*NREL wind turbine cost and scaling model*' [35]. The NREL cost model used the results from a blade cost scaling report written by TPI Composites [38] in order to find a scaling function. The model described the blade costs as a function of the rotor radius.

In the TPI studies, rotors with a similar blade planform were scaled and the effects on the costs were analyzed. The non-dimensional blade planform that was used in these studies is shown in Figure 8. The non-dimensional characteristics of the same blade planform are given in Table 3.

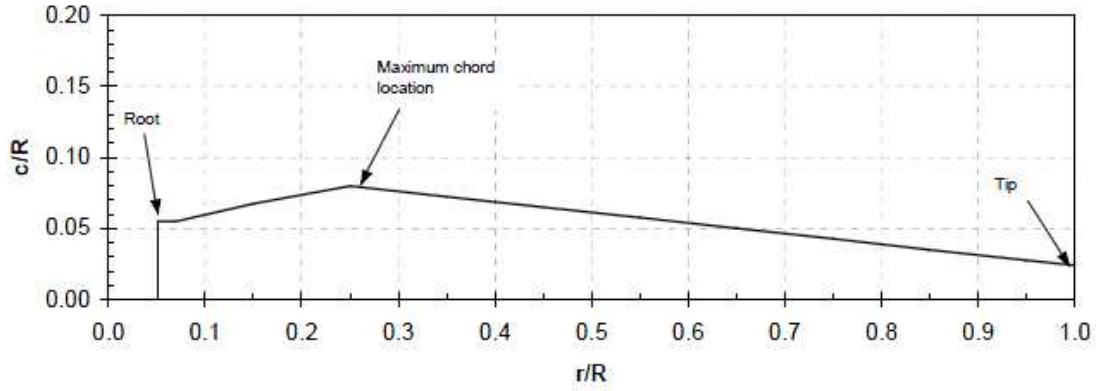

Figure 8: TPI study blade planform [39]

Radius Ratio	Chord Ratio	Twist (deg)	Thickness Ratio
5%	5.2%	29.5	100%
15%	7.8%	19.5	42%
25%	8.6%	13.0	28%
35%	7.6%	8.8	24%
45%	6.6%	6.2	23%
55%	5.7%	4.4	22%
65%	4.9%	3.1	21%
75%	4.0%	1.9	20%
85%	3.2%	0.8	19%
95%	2.4%	0.0	18%

Table 3: Non-dimensional blade planform characteristics used in the TPI study [40]

The design loads for which the blades are dimensioned are extreme wind design loads. In this load case, a wind speed of 70 m/s at the hub is assumed in accordance to IEC class 1 specifications. The blades are in fully feathered position. The wind shear exponent is 0.11 in accordance to Germanisher Lloyd rules [38].

The blade material was now calculated as a function of the blade planform and the calculated extreme loads.

The NREL baseline cost model for blade material costs was based on the results of this study and the cost, $C_{\text{blade material 1}}$ ($), are identified using the following expression [35]:

$$C_{\text{blade material 1}} = 0.4019R^3 - 955.24 \qquad (2.2)$$

This NREL defined a cost model for advanced blades on this expression together with the results from the TPI innovative blade study [41]. The average costs of the four innovative designs was taken as a starting point and scaled using the same scaling exponent as the baseline blade material cost expression. This gave an expression for the cost of advanced blades, $C_{\text{blade material 2}}$ ($) [35]:

$$C_{\text{blade material 2}} = 0.4019R^3 - 21051$$

Besides the material costs, the labor costs will also be considered. The TPI large blade cost study [38] also modeled the labor costs for large wind turbine blades. In order to calculate these costs, 12 manufacturing tasks which required labor were identified. These tasks are listed Table 4. The blade labor cost, $C_{\text{blade labor}}$ ($), scaling expression is given as [35]:

$$C_{\text{blade labor}} = 2.7445R^{2.5025}$$

Again, this cost scaling relation is only dependent on the rotor radius while the labor costs are dependent on the blade planform size.

No.	Manufacturing Task
1	Material
2	High Pressure Skin
3	Low Pressure Skin
4	Leading Edge Shear Web
5	Trailing Edge Shear Web
6	Assembly Prep
7	Bonding
8	Root Attachment System
9	Finishing
10	Inspection
11	Testing
12	Shipping

Table 4: Blade manufacturing tasks [38].

The indirect manufacturing costs were assumed to be 28% of the total blade costs. This gives the following expression for C_{blade} ($), the total blade costs (excluding transportation):

$$C_{blade} = \left(0.4019R^3 - 21051 + 2.7445R^{2.5025}\right)\frac{1}{0.72}$$

3.4.2 Gearbox costs

Both in the Upwind project [42] as in the NREL cost model project [35], expressions for gearbox cost models were given. However, the NREL cost model is less recent than the Upwind model and the Upwind model provided a more detailed (yet very simple) model for a single-stage gearbox. The cost expressions presented below are all taken from the Upwind model.

3.4.2.1 Single stage gearbox

Figure 9 shows a configuration of a turbine with a single-stage gearbox. The single-stage gearbox consists of one planetary gear stage.

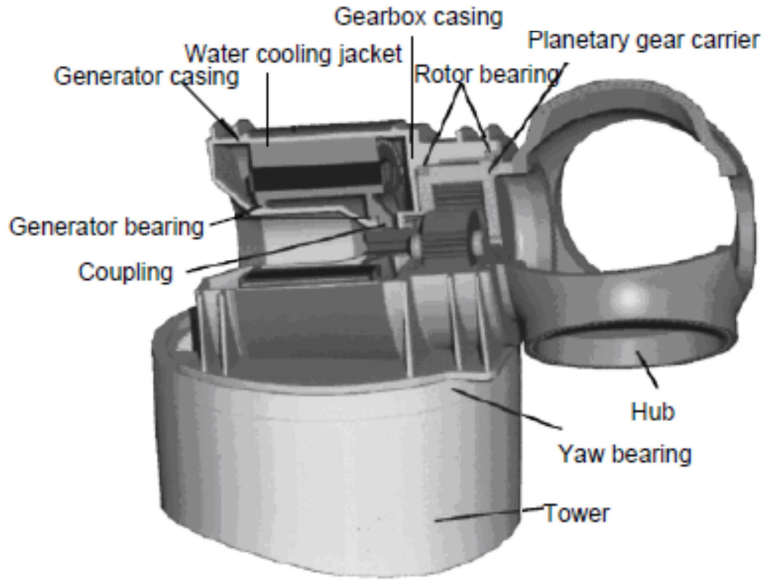

Figure 9: Configuration of the drive train containing a single-stage gearbox [42]

The gearbox cost model is entirely mass based. This means that the gearbox cost is a direct function of the gearbox mass. The gearbox mass, $m_{gearbox1}$ (kg), can be expressed as a function of the gearbox ratio and the rotor shaft torque [43]:

$$m_{gearbox1} = 3.2\frac{T_m F_s F_w}{1000}$$

Where:

T_m= Output torque (Nm)

F_s= Service factor=1.25 (-)[9]

F_w= Weight factor (-) which is given as:

$$F_w = \frac{1}{Z} + \frac{1}{Z r_w} + r_w + r_w^2 + 0.4\frac{1+r_w}{Z}\left(r_{ratio} - 1\right)^2$$

Where:

Z= Optimal number of planet wheels in a stage= 6 (-)

$r_w = \frac{r_{ratio}}{2} - 1$ =Sun-wheel ratio (-)

r_{ratio}= Single stage gear ratio (-)

The cost of the gearbox equals:

$$C_{gearbox1} = c_{gearbox1} m_{gearbox1}$$

Where:

$C_{gearbox1}$=Single stage gearbox specific cost= 6 (€/kg) [9]

3.4.2.2 Three stage gearbox costs

In Figure 10, a typical three-stage gearbox which is used in wind turbines is shown. This gearbox consists of one stage with planetary gears and subsequently two stages of helical gears.

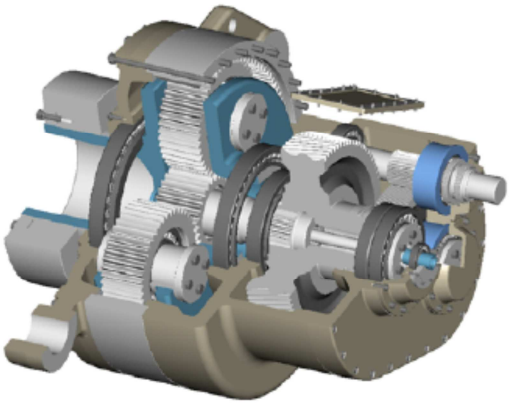

Figure 10: Typical configuration of a three-stage gearbox [42]

Again the gearbox cost is directly linked to the gearbox mass for a three stage gearbox. The gearbox mass, $m_{gearbox3}$ (kg), is dependent on the input torque and can be found using the following expression:

$$m_{gearbox3} = 10.35 T_l + 1950$$

Where:

T_l= Gearbox input torque (kNm)

The cost of the gearbox equals:

$$C_{gearbox3} = c_{gearbox3} m_{gearbox3}$$

$C_{gearbox3}$=Three stage gearbox specific cost= 10 (€/kg) [9]

3.4.3 Generator and converter costs

The NREL cost model gives very straightforward cost relations for high-speed generators, single-stage generators and direct-drive generators [35]. However, this study does not hold different models for PMSG, EESG and DFIG generators. Since this is needed, the NREL generator cost expressions are not used. Instead, the results from the report on the optimization of wind turbine generator systems by Upwind [9] are used. This study used very detailed generator models in order to find the optimal gearbox-generator designs for different configurations for generator sizes between 0.75 – 10MW. The study uses a genetic optimization routine to find the optimal generator designs. For a detailed description of the models and routines used, the interested reader is referred to the Upwind report on the model description [42] and the report on the optimization routine and the results [9]. Setting up such an optimization routine is out of the scope of this report and instead, the results from the Upwind study will be used to estimate the generator size and costs for all the configurations. The following sections are thus entirely based on descriptions and results given in the two Upwind reports.

The generator costs are made up of active material costs and structural costs of the generator. The active material costs are the costs for the active electrical material such as copper, iron and permanent magnets if permanent magnets are used.

The cost estimations for the active material and structural material of all the different generator systems can be found in Appendix A.

3.4.3.1 Converter costs

Back-to-back PWM power converters are assumed to be used in this model. The functions of this power converter is to supply correct voltage frequency under variable speed operation and to control the active and reactive power supplied by the generator. The generator systems under investigation either use a full scale power converter, meaning that 100% of the power is passed through the converter, or use a partial power converter, where only 30% of the power is passed through the converter.

The costs of the power converter, $C_{converter}$, are linearly dependent on the required size of the converter [42]:

$$C_{converter} = c_{converter} P_{converter}$$

Where:

$C_{converter}$= The specific converter price per kW = 40 (Euro/kW) [9]

$P_{converter}$= The converter size in kW

3.4.3.2 Permanent magnet synchronous generator – Direct drive (PMSG-DD) system costs

Figure 11 shows a scheme of the PMSG-DD system under consideration. Since no gearbox is present, the generator rotor speed equals the rotational speed of the blades. A full scale converter is needed in order to deliver the correct voltage frequency and to control the active and reactive power that is delivered.

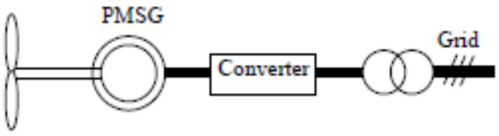

Figure 11: Scheme of a PMSG-DD system [42]

The results of the different contributions are shown in Figure 12. This figure shows the costs of the generator active material (iron, copper and permanent magnets), the generator structural costs and the converter costs as a function of the rated power. The exact results are given in more detail in Appendix A. The costs are a function of the rated power and are estimated by interpolating between the results presented in Figure 12.

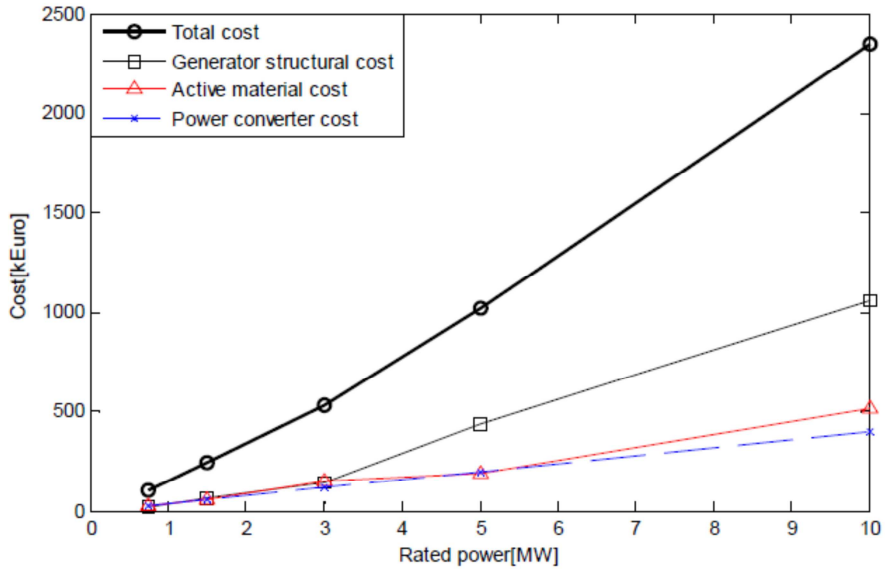

Figure 12: Cost contributions for a PMSG-DD system as a function of rated power [9]

3.4.3.3 Permanent magnet synchronous generator – Single-stage gearbox (PMSG-1G) system costs

Figure 13 shows a scheme of a PMSG-1G system. This system consists of a single-stage planetary gearbox (for which the cost expression was already given), the PMSG and a full scale converter.

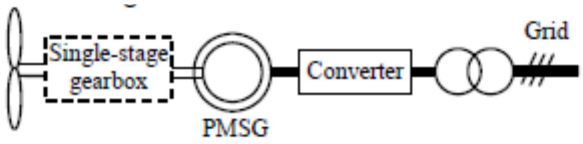

Figure 13: Scheme of a PMSG-1G system [42]

The costs of the gearbox are a function of the gear-ratio and a higher gear ratio will lead to a more expensive gearbox. The generator cost on the other hand is dependent on the rotational speed of the generator rotor (and thus of the shaft coming out of the gearbox). A higher rotational speed means a lower required generator torque and thus a smaller generator size. Therefore, a higher gear ratio (which leads to higher rotational speed of the generator rotor) will lead to a less expensive generator. This means that an optimal gear ratio needs to be found in order to have the minimal combined cost of the gearbox and generator. An example of how the optimal gear ratio is determined is shown in Figure 14 which shows the cost contributions of the PMSG-1G system for a 1.5MW turbine. The optimal gear ratio is different for systems of different size. Figure 15 shows the total system costs over a range of gear ratios and levels of rated power.

It should be noted that this optimization of the generator-gearbox system costs only holds for turbines operating at a tip speed ratio which equals 7. If the tip speed ratio is different, the rotational speed and torque will be different leading to new system costs and a new optimal gear ratio. This is not accounted for in the model and instead, the gear ratios that were determined in the Upwind project are used.

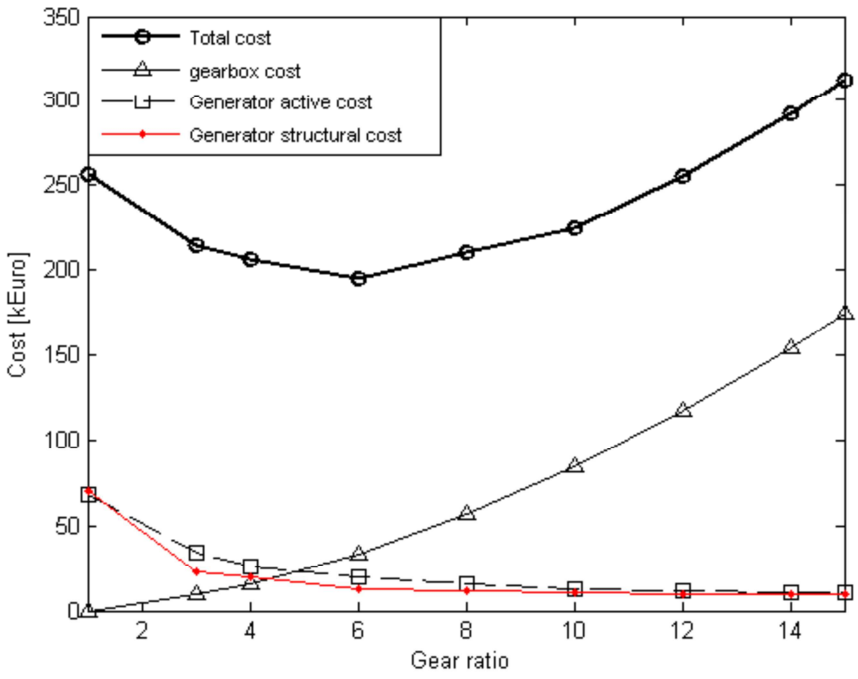

Figure 14: Gearbox, generator and total cost as a function of the gear ratio for a 1.5 MW turbine [9]

The development of an optimization procedure for the drivetrain of large-scale offshore wind turbines

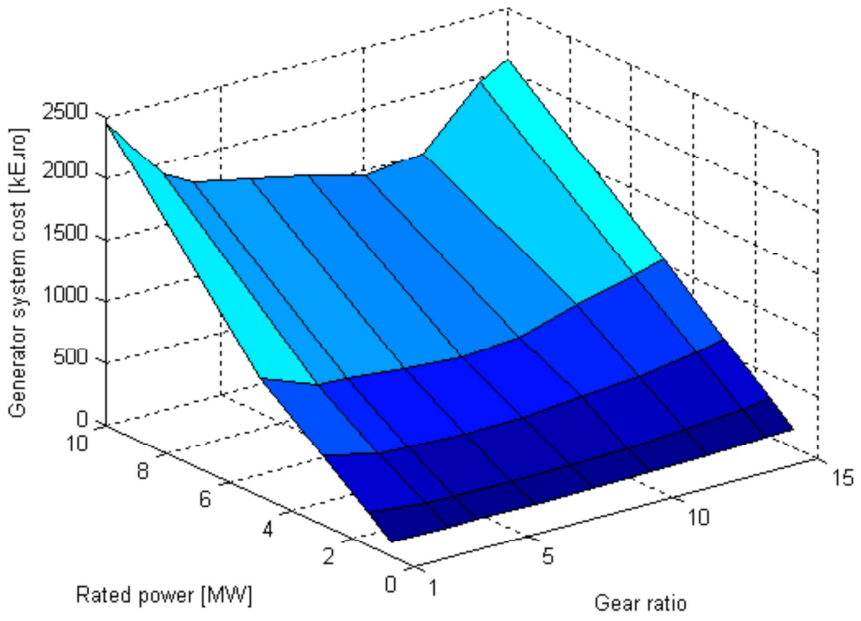

Figure 15: Three-dimensional visualisation of the optimized system costs for different gear ratios and different levels of rated power [9]

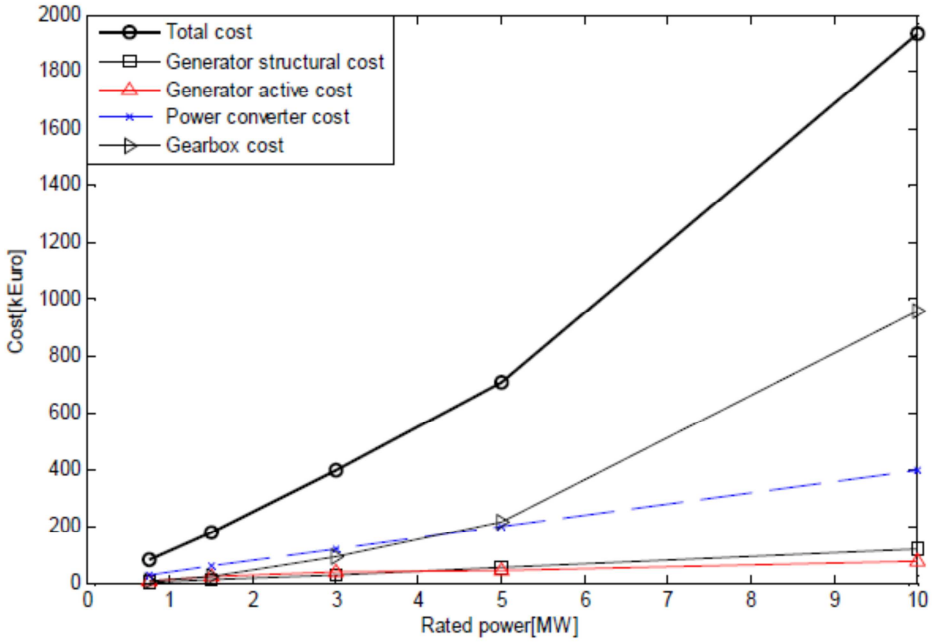

Figure 16: PMSG-1G system cost contributions as a function of rated power [9]

Figure 16 shows the cost contributions to the PMSG-1G system. The components in this figure are the active generator material costs, the generator structural costs, the gearbox costs and the converter costs. The exact results are presented in Appendix A and will be used to interpolate for the correct generator rated power.

3.4.3.4 Permanent magnet synchronous generator – Three stage gearbox (PMSG-3G) system costs

Figure 17 shows a scheme of a PMSG-3G system. In this system, the rotational speed of the low-speed shaft is stepped up using a three stage gearbox which consists of one planetary gear stage and two helical gear stages. The high-speed generator is connected to the grid through a full scale converter.

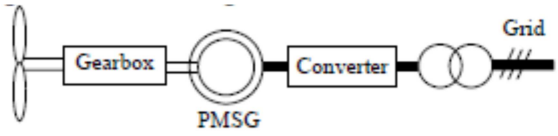

Figure 17: Scheme of a PMSG-3G system [42]

Although the size and cost of the gearbox are dependent on the rotational speed and required generator torque, the optimal gear ratio is not investigated. This is because the gearbox cost model does not account for the gear ratio used. Instead a gear ratio is assumed which makes the generator operate at a rated rotational speed of 1200 rpm. The results of the optimized system costs are shown in Figure 18. The exact results are given in Appendix A and interpolation will be done in order to find the costs for the investigated rated power.

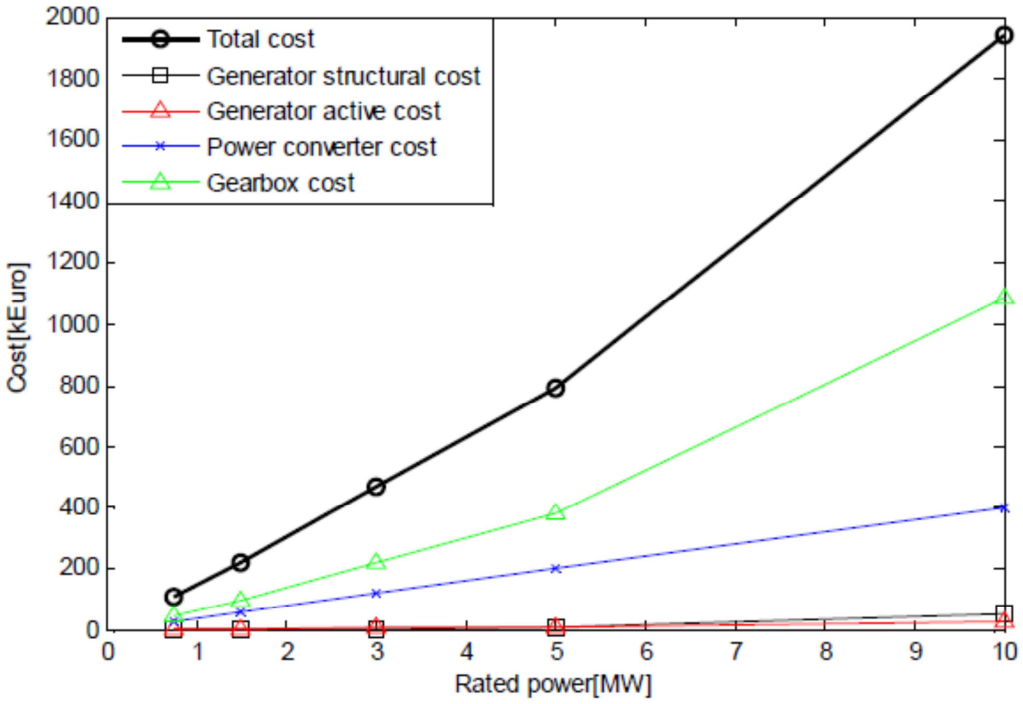

Figure 18: PMSG-3G system cost contributions as a function of rated power [9]

3.4.3.5 Electrically excited synchronous generator – Direct drive (EESG-DD) system costs

Figure 19 shows a scheme of a EESG-DD generator system. It can be seen that it is similar to the PMSG-DD system shown in Figure 11. The main difference is that the rotor winding carries a DC field and therefore this system requires slip rings and brushes. Figure 19 shows a converter connected to the rotor while in fact, this should be the rectifier that delivers this DC current to the rotor.

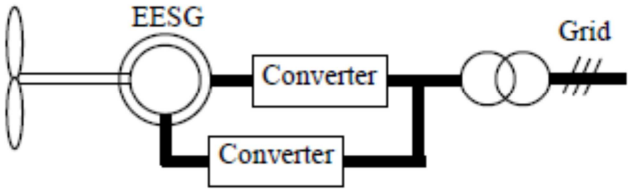

Figure 19: Scheme of a EESG-DD generator system [42]

The cost results of the optimization routine are shown in Figure 20. The detailed results can be found in Appendix A and interpolation will be done between these results in order to get the cost estimation for the desired power output.

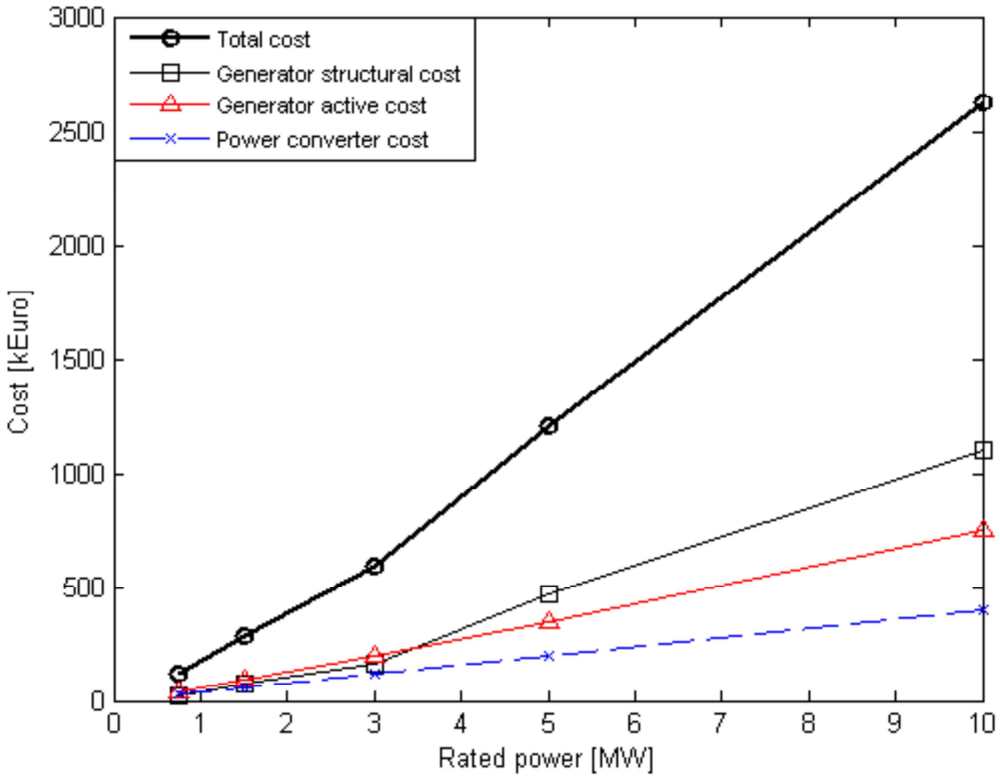

Figure 20: EESG-DD system component costs as a function fo rated power [9]

3.4.3.6 Doubly fed induction generator – Single stage gearbox (DFIG-1G) system costs

Figure 21 shows a scheme of a DFIG-1G generator-gearbox system. The most interesting feature of this system is that it only needs a partial power converter, which has a large impact on the system costs and system losses. This allows the system to have a variable speed range of ±30% around the synchronous speed.

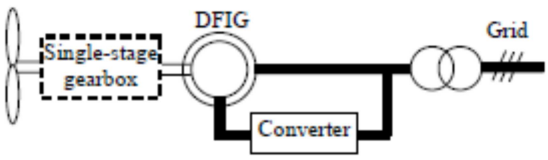

Figure 21: Scheme of a typical DFIG-1G system configuration [42]

The cost components as a function of the rated power are given in Figure 22. For this system, the same gear ratios were used as for the PMSG-1G configuration. The exact results can be found in Appendix A and interpolation will be used to find the cost estimation for the desired power level.

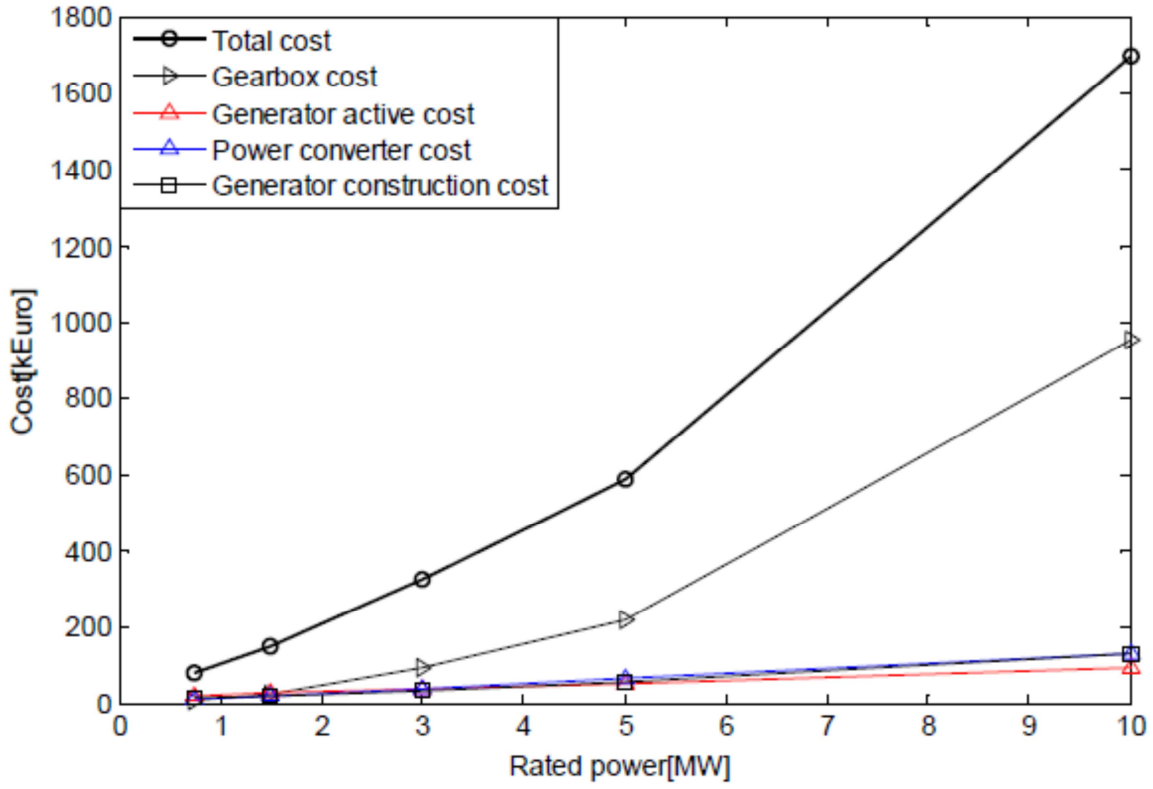

Figure 22: DFIG-1G system cost components as a function of rated power [9]

3.4.3.7 Doubly fed induction generator – Three stage gearbox (DFIG-3G) system costs

The DFIG-3G system is similar to the system shown in Figure 21 with the difference that a three-stage gearbox is used instead of a single-stage gearbox.

Figure 23 shows the cost contributions to the DFIG-3G system. The exact results are given in more detail in Appendix A and will be used to interpolate for the desired output power.

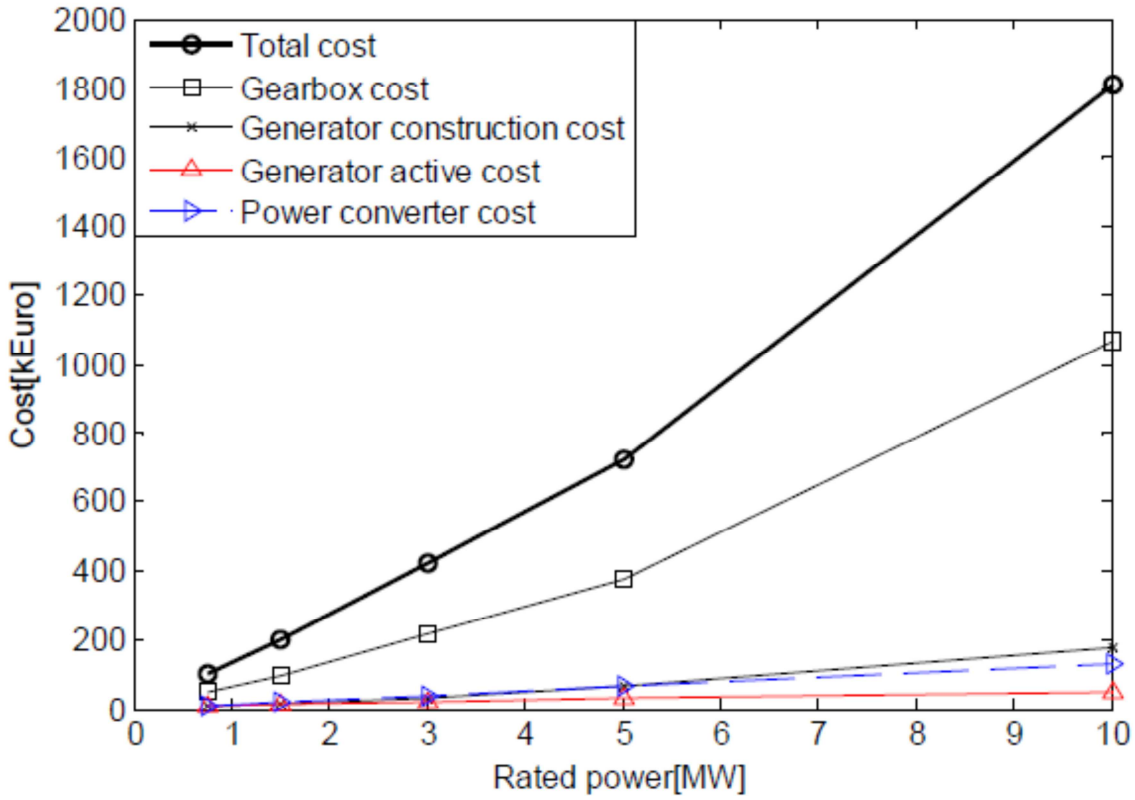

Figure 23: DFIG-3G system cost components as a function of rated power [9]

3.4.4 Costs of the electrical subsystem inside the nacelle

The electrical subsystem costs are the costs for all other electrical components present inside the nacelle apart from the generator and converter costs. The main contributions to the electrical subsystem costs are the transformer and the switchgear. The cost for the electrical subsystem is a function of the rated power. The system costs 38€ per kW rated power [9].

3.4.5 Tower costs

Current installed turbines and turbines under development all use tapered tubular steel towers. The cost of such a tower is a largely based on the necessary (steel) material needed. The amount of steel needed is determined by the tower length, base and top diameter and thickness distribution. The diameter and the thickness of the tower are determined by analysis of the natural frequency of the tower, the buckling stability and by fatigue analysis. Fully designing a turbine tower with these criteria in mind is beyond the scope of this project. The costs will be determined using the mass-based tower cost expression from the NREL cost model. The expression for tower mass, m_{tower} (kg), is given as [35]:

$$m_{tower} = 0.2694 H_{hub} (\pi R^2) + 1779$$

Where:

H_{hub}= Hub height (m)

In the WindPACT design studies, the tower height was assumed to be 1.3 times the rotor diameter [5]. For offshore wind turbines, the tower height is usually lower. Figure 24 shows the rotor diameter and hub height data presented in Table 1. A trend line was fitted to this data to give an estimate of the hub height, H_{hub} (m) as a function of rotor diameter D (m):

$$H_{hub} = 50 + 0.36D$$

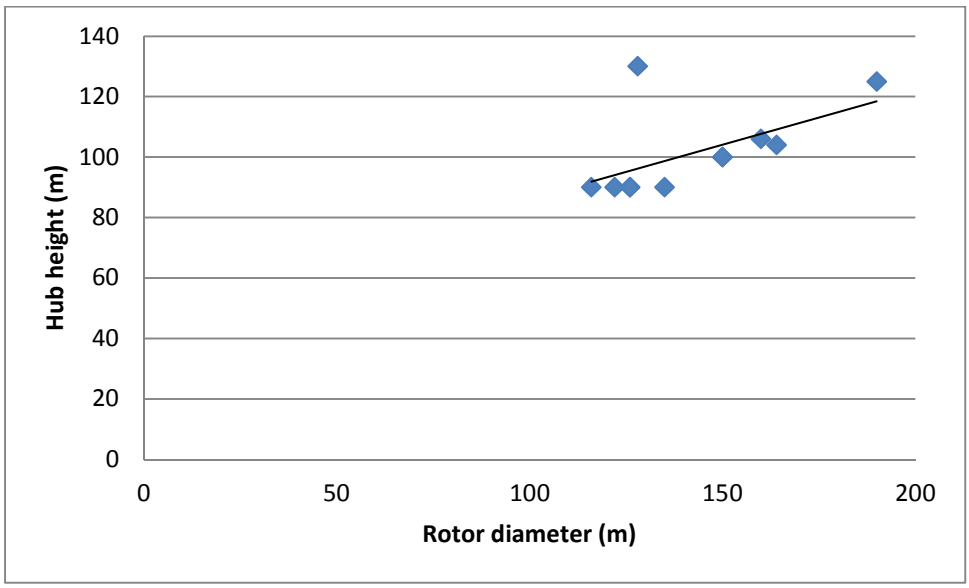

Figure 24: Hub height as a function of rotor diametet (based on data from Table 1)

Since part of the support structure up to hub height is covered by the transition piece, this number needs to be lowered to account for this. A platform height of 20 m, the height above mean sea level at which the transition piece ends and the tower is assumed to start, was assumed meaning that the first term in the expression for H_{hub} becomes 30 m instead of 50 m.

The cost of the tower is a direct function of the mass. It is assumed that the tower specific cost equals 2,5 €/kg. This number is based on the steel price with a mark-up for tower manufacturing [44].

3.4.6 Support structure cost model

The support structure of an offshore wind turbine is the component which connects the wind turbine tower to the seabed. It mostly consists of a foundation and a transition piece. The foundation is the part of the support structure which is below sea-level and fixes the turbine to its position on the seabed. Numerous configurations exist for the foundation and transition piece. The monopole is the most used support structure in recent projects, with almost 70% of the installed support structures being of this type up till 2011 [45]. In this configuration, a pile is driven into the seabed. On top of this foundation pile, a transition piece is placed in order to provide a good transition between the tower and the foundation and this transition piece holds a platform for easy access to the wind turbine. This model will only look at the monopile as an option for the support structure. Figure 25 shows a monopile support structure.

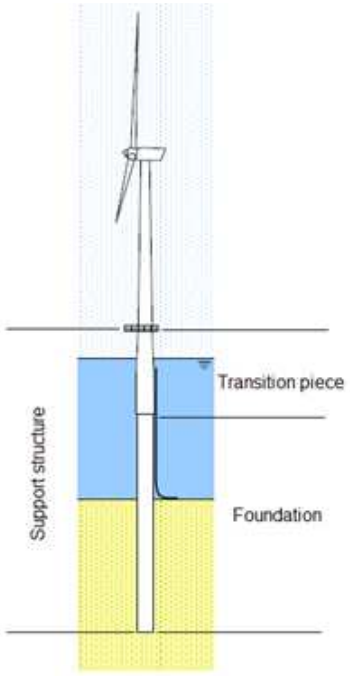

Figure 25: Monopile support structure [26]

The size of this support structure depends on the depth of the seabed, the soil composition of the seabed, the wave and tide climate present and the bending moments produced by the turbine itself. Accounting for all these factors is out of the scope of this conceptual design optimization for the drivetrain and instead, a rather simple cost expression was used for the cost of the support structure, $C_{\text{support structure}}$ (kEuro) [47]:

$$C_{\text{support structure}} = \left(8.171 D_{seabed} + 389.3\right) P_{rated}$$

Where:

D_{seabed}= the depth of the seabed (m)

P_{rated}= Rated power of the turbine (MW)

This cost expression only accounts for the costs of manufacturing the support structure. It does not account for transportation and installation of this component. This will be done in section 3.6.

3.4.7 Auxiliary turbine components

The following sections give costs estimations for all other main components and systems present inside the nacelle. The cost estimations are all taken from the NREL cost model [35]. It should be noted that almost all these cost models were determined by extrapolating existing turbine cost data. Most models therefore do not reflect the effects of changing the drive train configuration on the costs of these components.

3.4.7.1 Hub costs

The three-bladed configuration makes use of a rigid hub. The two-bladed configuration makes use of a teetering hub. The cost estimations are both dependent on the mass of the blades [35]:

$$m_{hub} = 0.954 m_{1blade} + 5680.3$$

Where m_{hub} is the hub mass in kg and m_{1blade} is the blade mass of a single blade in kg. A rigid hub costs 5.2 (€/kg) and a teetering hub costs 9,4 (€/kg) [48].

3.4.7.2 Pitch mechanism and bearing costs

The estimated costs of the pitch mechanism and the pitch bearing, $C_{pitch\ mechanism}$ ($), is a function of the rotor diameter D (m) [35]:

$$C_{\text{pitch mechanism}} = 2.28\left(0.2106 D^{2.6578}\right)$$

3.4.7.3 Nose cone costs

The hub cost estimation does not account for the nose cone. Therefore, it needs to be accounted for separately. The costs of the nose cone are again linearly dependent on the mass and the cone costs 5.57 ($/kg). The mass of the nose cone, m_{cone} (kg), is estimated as [35]:

$$m_{cone} = 18,5D - 520,5$$

3.4.7.4 Low-speed shaft costs

The cost of the low-speed shaft, $C_{ls-shaft}$ ($), is a function of the rotor diameter D (m) [35]:

$$C_{ls-shaft} = 0.01 D^{2.887}$$

3.4.7.5 Main bearings

The cost of the main bearings is a function of the mass of these bearings. The mass of the main bearings, $m_{\text{main bearings}}$ (kg), is estimated as a function of the rotor diameter D (m) [35]:

$$m_{\text{main bearings}} = 0.0092 D^{2.5}\left(\frac{8D}{600} - 0.033\right)$$

The cost of the main bearings, $C_{\text{main bearings}}$ ($), can now be estimated as [35]:

$$C_{\text{main bearings}} = 2 m_{\text{main bearings}} 17,6$$

3.4.7.6 Yaw drive and bearing

The costs of the yaw drive and bearing, $C_{\text{yaw drive}}$ ($), can be estimated as a function or rotor diameter D (m) [35]:

$$C_{\text{yaw drive}} = 0.0678 D^{2.964}$$

3.4.7.7 Main frame costs

The main frame is the frame which carries all the major nacelle components (gearbox, generator, transformer, etc.), fixes their position within the nacelle and transfers the loads by these components to the tower. The mass and costs of the mainframe are a function of the selected gearbox-generator configuration.

For a system with a three-stage gearbox and a high-speed generator, the main frame costs, $C_{\text{main frame}}$ ($), can be estimated as a function of rotor diameter D (m) [35]:

$$C_{\text{main frame}} = 9,486D^{1.953}$$

For a system with a single-stage gearbox and a medium-speed generator, the main frame costs, $C_{\text{main frame}}$ ($), can be estimated as a function of rotor diameter D (m) [35]:

$$C_{\text{main frame}} = 303.96D^{1.067}$$

For a system with a direct drive system with a low-speed generator, the main frame costs, $C_{\text{main frame}}$ ($), can be estimated as a function of rotor diameter D (m) [35]:

$$C_{\text{main frame}} = 627.28D^{0.85}$$

3.4.7.8 Hydraulics and cooling systems costs

The costs of the hydraulics and cooling systems, $C_{\text{hc systems}}$ ($), can be estimated as a function of the rated power P_{rated} (kW) [35]:

$$C_{\text{hc system}} = 12P_{rated}$$

3.4.7.9 Nacelle cover costs

The nacelle cover costs, C_{nacelle} ($), can be estimated as a function of P_{rated} (kW) [35]:

$$C_{\text{nacelle}} = 11.537P_{rated} + 3849.7$$

3.5 Wind Farm costs

When optimizing the cost of energy, not only the costs of the wind turbines have to be accounted for, but also the costs of other components and operations that are associated with an offshore wind farm. The costs considered here are the offshore electrical collection and transmission grid costs, transformer platform costs and installation costs of the turbines.

All these costs are dependent on the site for which the turbines are developed and on the size of the wind farm under investigation. The first step in evaluating the wind farm costs is thus to establish the 'wind farms' under investigation.

3.5.1 Wind farm layout

The size and layout of the wind farm determines the costs and the losses associated with wind turbines operating in a wind farm to a large extent.

The sizes of offshore wind farms under development have a very large range. But most projects under development are in the multiple hundreds of installed MW range. The target size for the wind farm in this report is assumed to be around 500 MW. This size was chosen as it also represents the size of the wind farm from which the operation and maintenance cost data was taken [3].

The optimization of the layout of a wind farm is an important subject because this layout determines:

- The wake losses in the wind farm
- The electrical losses in the power collection cables
- The costs of these power collection cables

The optimization thus needs to find a balance between wake losses and electrical losses and costs. This optimization requires extensive modeling and computations, which is out of the scope of this research. Instead a standard layout will be assumed that is independent on the selected configuration or on the input wind conditions. It is assumed that the turbines are placed in a square layout meaning that the number of rows and the number of turbines per row are equal.

The amount of turbines, $N_{turbines}$, with power $P_{turbine}$ (MW) necessary to reach 500 MW equals:

$$N_{turbines} = \frac{500}{P_{turbine}}$$

This number will be rounded to the nearest integer. The amount of rows, N_{rows}, and amount of turbines per row equals:

$$N_{rows} = \sqrt{N_{turbines}}$$

This number will also be rounded to the nearest integer. Since the amount of turbines, the amount of rows and the amount of turbines per turbine per row are rounded, this means that the actual total installed power will be slightly different than the 500MW target.

The optimal distance between rows and between the turbines in one row, called turbine spacing, is subject of debate. Although many studies show that the optimal spacing is around 7-8 times the rotor diameter, a recent study concluded that a spacing of 15 times the rotor diameter would be

more adequate [49]. However, a spacing of 7 times the rotor diameter will be used in this report as this is a conventional spacing for offshore wind farms.

3.5.2 Electrical collection and transmission costs

Several options exist for the connection of the turbines to the onshore grid. The wind farm in this report is assumed to have the following components in the connection to shore:

- The power collection cables: The turbines in one row are connected through a MVAC 33kV XLPE cable. There are N_{rows} number of such strings of cables.
- The offshore transformer substation: The power collection cables transport the power to an offshore transformer station which is located at one end of the rows of turbines. Here, the power is stepped up to 230 kV.
- The shore connection cable: From the offshore transformer station, the power is transported to the shore through a HVAC 230 kV XLPE cable (actually, these are usually three seperate cables each having only one conductor core).

3.5.2.1 Power collection cable costs

The costs of the submarine cables consists of the costs of the cables itself and of installation costs. Both cost components are a function of the length of these cables.

The length of each cable string, $L_{string,I}$ (m), equals:

$$L_{string,i} = (N_{rows} - 1)7D + L_{substation,i}$$

Where:

D is the rotor diameter (m)

$L_{substation,I}$ is the length of the cable section which connects the last turbine in one string to the offshore substation (m).

The specific cost of the cable itself, c_{cable} (€/m) is a function of the voltage and the maximal current [47]:

$$c_{cable} = \alpha + \beta e^{\left(\gamma I_n / 10^5\right)}$$

Where

α, β and γ are cost coefficients that depend on the operating voltage of the cable. For a 33kV cable, these coefficients equal 52.08 (€/m), 75.51 (€/m) and 234.34 (1/A) respectively [47].

$I_{n,MV}$ (A) is the maximal current in the medium voltage cable. The required current through each cable string equals:

$$I_{n,MV} = \frac{N_{rows} P_{turbine}}{\sqrt{3} U_{n,MV}}$$

Where $U_{n,MV}$ is the cable voltage (V).

The specific installation cost for MV submarine cables, $c_{MV,install}$ (€/m), is assumed to be 365 (€/m) [47].

The total costs for the power collection cables, C_{pcc} (€) can now be calculated as:

$$C_{pcc} = \sum_{i=1}^{N_{rows}} \left(c_{MV,cable} + c_{MV,install} \right) L_{string,i}$$

3.5.2.2 Offshore transformer substation

The components in the offshore transformer station are [47]:

- MV/HV transformer
- MV switchgear
- HV bus bar and switchgear
- A back-up diesel generator
- The platform and support structure
- A shunt reactor

The cost for the MV/HV transformer, $C_{MV/HV\ trans}$ (k€), equal [47]:

$$C_{MV/HV} = 42.688 P_{trans}^{0.7513}$$

Where P_{trans} is the transformer rating (MVA).

The cost for 33 kV switchgear, $C_{sg,MV}$, equals 67.3 k€ [47].

The cost for the 230 kV switchgear, $C_{sg,HV}$, equals 1250 k€ and the cost for a 230 kV single busbar equals 2900 k€ [47].

Inside the substation, a back-up generator is present. The function of this generator is to provide power to the turbines for essential equipment in case the wind farm is disconnected from the grid. The cost for such a back-up generator, $C_{bu\text{-}gen}$ (k€), equal [47]:

$$C_{bu-gen} = 21.242 + 2.069 N_{rows}^2 P_{target}$$

The costs for the substation platform and support structore, C_{SS} (k€), are equal to [47]:

$$C_{SS} = 2534 + 88.7 N_{rows}^2 P_{target}$$

Much reactive power builds up in long HVAC cables due to the capacitance between the conductor cores and the ground. This reactive power also limits the capacity of the cable for active power. In order to limit the capacity used by reactive power, half of the reactive power is already compensated for by a shunt reactor in the substation [50]. Since two submarine cables will be used for the connection to shore, there will be a total of four shunt reactors (two offshore and two onshore).

The cost of this shunt reactor, C_{SR} (k€), equals [47]:

$$C_{SR} = \frac{2}{3}\left(-153.05 + 131 P_{SR}^{0.4473} \right)$$

Where P_{SR} is the required size of the shunt reactor (MVAr). The size of this shunt reactor is determined as half the amount of reactive power that is created by this capacitance in the submarine cables:

$$P_{SR} = \frac{1}{2} P_{reactive} = \frac{1}{2} 2\pi f C U_n^2 10^{-6} L_{SCC}$$

Where

f is the grid frequency which equals 50 Hz.

C is the cable capacitance (µF/km)

L_{SCC} is the length of the shore connection cable (km)

Another shunt reactor is present onshore with the same size and same cost.

3.5.2.3 Shore connection cable

If it is assumed that the wind farm can be connected to the grid directly onshore, this means that the length of the shore connection cable is equal to the distance between the shore and the wind farm. The costs for the XLPE 230 kV can be calculated using the same formula as for the 33 kV cable but with different coefficients. For a 230 kV cable, α, β and γ equal 403.02 (€/m), 13.94 (€/m) and 462.1 (1/A) respectively [47].

The required current carrying capacity of the high voltage cables, $I_{n,HV}$ (A) equals:

$$I_{n,HV} = \frac{N_{rows}^2 P_{target}}{\sqrt{3} U_{n,HV}}$$

The specific installation costs for the HV cables, $C_{inst,HV}$, equal 720 (€/m) [47].

Since the current rating of this cable is really high if a single cable was used for a 500 MW wind farm, this would lead to an unrealistic high cost for the cable. Therefore, it is assumed that two parallel cables will be used, each transmitting half of the power from the wind farm.

3.5.3 Other wind farm costs

Two other components are accounted for in the wind farm costs. One is for the monitoring and control system of the turbines. The cost of such a SCADA system is assumed to be 75 k€ per turbine [47].

On top of all these costs, there is usually a mark-up for project development costs. The project development costs are estimated to be 47 k€ per MW of installed capacity [47].

3.5.4 Average wind farm costs

Since this report only looks at costs per turbine, all the wind farm costs are added together and this total number is divided by the amount of turbines in the wind farm to get a levelized wind farm cost per turbine.

3.6 Wind farm installation costs

The costs of transporting, erecting and installing the turbines are considerably larger for offshore projects than for onshore projects. This is due to the increased time needed for installation and the large costs for specialized installation vessels.

The main contribution to the installation costs is the cost to rent installation vessels. This cost can be calculated as the dayrate of the installation vessel times the amount of days required for installation of the wind farm [51].

3.6.1 Offshore installation vessel dayrate

Estimating the dayrate of offshore installation vessels is rather complicated. The price to rent such an installation vessel is determined by supply and demand for these vessels in the market. Since transportation of such vessels is time consuming and thus costly, the market for installation vessels is a rather local market with large price differences from region to region. The demand for these vessels is highly fluctuating and the amount of vessels available per region is usually very limited. This leads to largely fluctuating dayrates that are very location (or region) dependent [51]. Estimating the costs for installation based on such a heavily fluctuating parameter should thus be treated with care.

The costs of the installation vessels are largely dependent on the required hoisting height. Besides this, the required hoisting capacity is also important. Figure 26 shows a cost trend of the installation vessel dayrates as a function of hoisting height. It should be noted that this cost trend was established in 2001, at a time when special wind farm installation vessels were not yet designed for this purpose. Today, more of these vessels are available, which would reduce the costs. A very rough simplification is to assume that this decrease in vessel costs due to larger supply is counteracted by inflation effects, leading to an unchanged price relation. From Figure 26 the following relation for vessel dayrate costs, C_{vessel} (k€/day), as a function of the hoisting height, H_{hoist} (m), was assumed:

$$C_{vessel} = 50 + c_{hh} H_{hoist}$$

Where c_{hh} is a constant that determines the cost increase per meter of hoist height. From Figure 26 it is assumed to be 1 (k€/m).

The hoisting height is assumed to be equal to the hub height. In section 3.4.5, an empirical relation between hub height and rotor diameter was given which can be used for the hoisting height:

$$H_{hoist} = 50 + 0.36D$$

Besides the main installation vessel, additional smaller vessels are necessary such as tugboats, crew vessels, anchor handling vessels, etc. These additional vessels are called ‘vessel spread’ and account for an additional 20% of vessel costs [51].

Since different drive-train configurations will have different hub heights and hence hoisting heights, the cost of the vessel dayrate is variable for the different configurations under investigation.

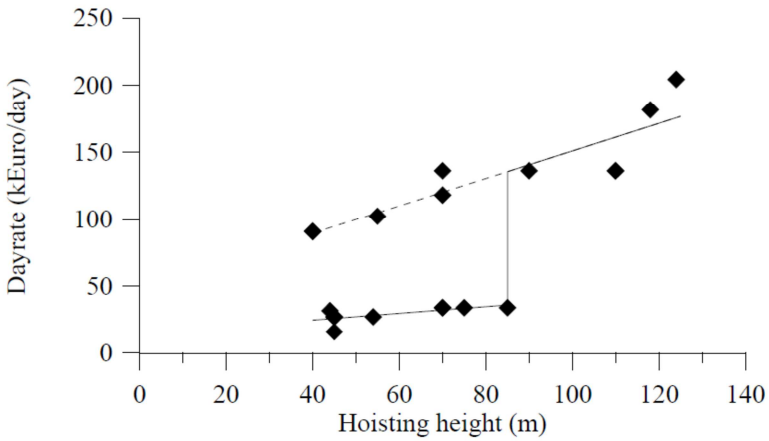

Figure 26: Installation vessel dayrate as a function of hoisting height [52]

3.6.2 Installation time

The installation of an offshore wind turbine consists of the following steps [51]:

- Foundation installation and placement of the transition piece
- Erection of the tower and turbine
- Installation of the electrical cables
- Installation of the transformer substation

Several installation methods exist for the installation of the foundation, transition piece, the tower, the nacelle and the rotor. The difference in these methods is in the amount of pre-assembly done onshore and amount of assembly required offshore. Since the foundation is a monopile, the pile driving is always the first step in the installation process and the installation of the monopile can not be done in combination with another component. After the monopile is driven in the seabed, the transition piece is placed on top of the monopile.

As was mentioned, for the tower, nacelle and rotor, several methods exist each with different amounts of sub-assemblies. Some of these methods are:

Method 1: - Installation of the tower in one lift

- Installation of the nacelle on top of the tower

- Installation of the rotor

Method 2: - Installation of the tower in one lift

- Installation of the nacelle and rotor assembly

Method 3: - Installation of the tower in two pieces and thus two lifts

- Installation of the nacelle and rotor assembly

Method 4: - Installation of the tower and nacelle assembly

- Installation of the rotor

Method 5: - Installation of the tower, nacelle and rotor in one assembly

A benefit of installing components separately is that multiple components can be placed on one vessel, reducing the amount of transportation time. However, this has the downside that more stock is required on shore and thus the storage cost is increased. Another benefit is that the weight of the sub-assemblies is much less, requiring less hoisting capacity and facilitating transport [53].

Pre-assembled components have the benefit that less lifts are necessary. Assembling the components requires high accuracy, which can be a problem offshore due to the wind and waves. Pre-assembling some (or all) components on shore will thus save time in this respect. Such pre-assemblies will be larger and therefore more difficult to handle and transport, increasing the transportation time [53].

It is rather difficult to give exact measure to the needed installation time as the installation time depends on the weather (wind and wave) conditions, the available installation vessels, distance to the shore.

Analysis of installation data of existing wind farms has shown that the average installation time for foundations (including transport, weather delays, transition piece placement) requires 2.6 days for wind farms with over 60 turbines. The average installation time for the turbines (consisting of the tower, nacelle and rotor) requires 2.1 days for wind farms with over 60 turbines [51].

These installation times are assumed to be independent of the selected rotor configuration since no more detailed information was found on the effects of changing the rotor configuration.

The cost for installation of the electrical cables and transformer substation were already accounted for in the cost formulas given in section 3.5.2.

3.6.3 Installation costs per wind turbine

The installation costs per wind turbine can now be estimated. The vessel dayrate is estimated by using the hub height as the required hoisting height. This number is then multiplied by 4.7, which is the combined number of days required for installation of the foundation, tower, nacelle and rotor.

3.7 Operation and maintenance (O&M) costs

As could be seen Figure 3, O&M costs take up a large share of the costs of an offshore wind project. A careful analysis of how these costs are built up and how the various configurations influence these costs is therefore needed.

The operation and maintenance costs for offshore wind farms are influenced by [54]:

- The failure rate (and failure behavior) of the turbine components and the complexity of replacement of these components
- The distance between the service buildings and the wind farm
- The accessibility of the wind turbines determined by the weather conditions at the site
- The loads due to wind, waves, wake effects which lead to wear and failure

Besides this, the chosen operation and maintenance strategy also has a large influence on the costs.

Because of these many influences on the costs, establishing estimates for O&M costs is very complex. Many estimates use probabilistic methods that take into account the stochastic nature of component failures and the accessibility of the wind turbines. Establishing such a method that can quantify for all the above mentioned influences is out of the scope of this project. Instead, a reference study from literature will be used upon which most of the estimates will be based. The reference costs are taken from the DOWEC project baseline and optimized O&M cost calculations [3] [55], in which the O&M costs were estimated for a wind farm consisting of 80 6MW turbines situated in the North Sea at 50km from the shore. The costs that are given in these reports are averaged costs over the lifetime of the turbine.

The costs for O&M consist of:

- The costs of spare parts and the costs of purchasing replacement components
- The labor costs for personnel
- The costs of the required equipment (such as vessels, cranes, etc.) that are either purchased or rented

The DOWEC studies also account for revenue losses as a cost component. In this report however, these reduced revenues are taken into consideration when the energy yield of the turbine is calculated. This is done by calculating the availability of the turbines.

The DOWEC studies only show the results for a 6MW, 3 bladed, 3-stage gearbox, DFIG configuration. The cost contributions of this configuration will first be given, after which a method to correct for the actual configuration is established.

3.7.1 O&M costs of the DOWEC 6MW configuration

The O&M costs can be split up into a part for preventive maintenance and a part for corrective maintenance.

3.7.1.1 Corrective maintenance

The components for which the O&M cost contributions are estimated in the DOWEC baseline report are [3]:

- Main shaft and bearing
- Brake
- Generator
- Parking brake
- Electrical subsystems
- Blades
- Yaw system
- Pitch mechanism
- Gearbox
- Power electronics
- Control system

For each of these components, the failure modes are categorized into 5 maintenance categories and the failure rates per category are estimated. Each of these categories has different equipment requirements and a different repair time.

Table 5 gives the cost contributions for each component that were estimated in the DOWEC baseline O&M study for one turbine.

Component	Material costs (€)	Labor costs (€)	Equipment costs (€)	Total Costs (€)
Shaft & Bearing	5.672	122	3.641	9.434
Brake	483	37	562	1.082
Generator	13.479	734	14.097	28.310
Parking Brake	420	17	363	800
Electrical Systems	2.991	251	3.766	7.008
Blade	14.061	736	14.448	29.245
Yaw System	3.691	208	3.921	7.820
Pitch Mechanism	3.268	165	3.095	6.527
Gearbox	8.735	550	9.733	19.018
Invertor	1.124	125	1.619	2.868
Control	4.575	231	4.333	9.138
Total:	**58.498**	**3.173**	**59.578**	**121.249**

Table 5: DOWEC 6 MW turbine component annual cost contributions baseline O&M. Reproduced from [3]

The maintenance strategy used in the DOWEC baseline report lead to an availability of only 91.6% resulting to unacceptable revenue losses. Therefore, an optimization study was done in which new strategies were used. The main improvement was the use of a permanent internal crane for external hoisting with a capacity of up to 50t. The use of such a permanent hoisting system reduces the required repair time which drastically reduces the waiting time. This leads to a much higher

availability and lower labor and equipment costs. However, in the optimized study, an extra 25.000 €/year is accounted for a supplier vessel, which is added to the equipment costs.

The new cost contributions per component are not given in such detail as in the baseline report. The material costs were unchanged, so these can be taken from the baseline report per component. The labor and equipment costs were somewhat lower. To account for the new values per component, the component labor and equipment costs are multiplied by the ratio of the optimized labor and equipment costs to the baseline labor and equipment costs. This gives the following component cost contributions in Table 6, which will be used as a reference case.

Component	Material costs (€)	Labour costs (€)	Equipment costs (€)	Total Costs (€)
Shaft & Bearing	5.672	107	3.318	9.097
Brake	483	33	512	1.027
Generator	13.479	647	12.845	26.972
Parking Brake	420	15	331	766
Electrical Systems	2.991	221	3.432	6.644
Blade	14.061	649	13.165	27.875
Yaw System	3.691	183	3.573	7.447
Pitch Mechanism	3.268	145	2.820	6.233
Gearbox	8.735	485	8.869	18.089
Invertor	1.124	110	1.475	2.709
Control	4.575	203	3.948	8.727
Total:	58.498	2.800	54.287	115.585

Table 6: DOWEC 6 MW turbine component annual cost contributions for optimized O&M.

3.7.1.2 Preventive maintenance costs

The turbines are visited once per year for preventive maintenance. During such a visit, inspection of components is done and some minor (preventive) replacements can be done.

The cost contributions to preventive maintenance are taken from the baseline DOWEC O&M report and given in Table 7 [3]. The overhead costs mentioned in this table are costs for a permanently manned control room. Every six years, the gearbox oil will be changed. One sixth of these costs is accounted for in the annual preventive maintenance cost.

Component	Cost (€)
Supply boat	4500
Labor	2800
Travel time	708
Parts	7350
Overhead	7665
Gearbox oil change	4550

Table 7: Preventive maintenance cost contributions [3]

These figures were multiplied by a factor to account for 'irregularities' such as bad weather [3].

3.7.2 Actual O&M costs for configuration under investigation

The O&M reference cost contributions mentioned in the previous paragraphs only apply to the turbine under consideration in the DOWEC studies. In this report however, a large number of turbine

configurations are possible, each with its specific effects on the O&M costs. In the following sections, a rough estimation on how the chosen configuration affects the O&M costs is given.

3.7.2.1 Corrective maintenance cost for the chosen configuration

The corrective maintenance costs will be different from the reference costs due to differences in size of the components or the omitting of some components. First, a correction is done for the difference in size of the components with respect to the 6MW reference turbine.

It is assumed that when changing the rated power of the turbine with respect to the 6MW reference turbine, the only effect on the corrective O&M costs will be in the material contributions to these costs. This implies that the labor costs and the equipment costs will stay the same for turbines of different sizes.

The material cost contributions to the O&M costs will vary with changing size of the turbine since the scaled parts will have a different cost. In this section, it is assumed that the turbine component costs vary linearly with changing rated power. In the previous sections, it was shown that this estimation is not entirely correct, but is gives a first estimate of the change in costs which is sufficient for the scaling of the O&M costs. The material O&M costs of all the components will thus be scaled linearly with rated power.

Next, a change in costs due to the different configuration needs to be estimated. The DOWEC 6MW turbine under consideration in the O&M studies is a three-bladed, three-stage gearbox, DFIG turbine.

When changing from a three-bladed to a two-bladed turbine, it could be expected that the costs due to blade failure would decrease. However, such two-bladed turbines use a more complex teethering hub. A. John Paul suggests that this eliminates the O&M cost difference between two-bladed and three-bladed turbines. For two-bladed rotors, the failure rate of the pitch system is assumed to be one third lower than for three-bladed rotors, leading to an O&M contribution of only two thirds of the reference case [48].

For the direct-drive configurations, there is no gearbox present, hence its associated O&M costs can be discarded. No estimate was found for the effect on O&M costs of the gearbox when changing from a three-stage gearbox to a single-stage gearbox. A rough estimate is made that a single-stage gearbox will have half of the O&M costs associated to this component.

Accounting for the change in generator system is also something that was not found in literature. It is assumed that the labor and equipment costs remain unchanged for the different generator systems. The O&M cost difference is only due to a change in material costs. The material O&M costs of the generator are assumed to vary with the costs of the generator system. The DFIG-3G generator cost is thus taken as a reference and the cost ratio between the DFIG-3G and the generator system under investigation is used to scale the material O&M costs.

Finally, a cost change due to the changed rotational speed of different configurations could be expected. However, it is unknown to the author whether for example a reduction in rotational speed will lead to lower O&M costs in the drive-train due to these lower speeds or will lead to an increase in O&M costs due to the higher torque encountered in the drive-train. Therefore, no effect due to the rotational speed was included.

3.7.2.2 Preventive maintenance costs for the configuration under consideration

Again, the change in maintenance costs for preventive maintenance is only due to a change in material costs (referred to as 'parts' in Table 7). The contributions to the costs of each component were not given for the preventive maintenance. Therefore, it is assumed that the total costs of preventive maintenance will scale with the rated power of the turbine.

Omitting the gearbox in the configuration will eliminate the contribution of the six-year gearbox oil-change to the preventive maintenance cost.

4 Wind turbine performance

In this chapter, the methods to determine the wind turbine performance will be explained. The first step in the analysis of the turbine performance is setting up the power curve of aerodynamic power delivered by each rotor design. Next, the losses in the power train components and in the power transmission are calculated. This gives a power curve for the turbine showing the power that could actually be delivered to the grid. This is linked to the wind speed distribution present at the site to give the energy yield for a turbine if it were to operate for one entire year. Finally, the availability of the turbine is estimated to correct the actual energy yield for times when the turbine is not running.

4.1 Aerodynamic power of the turbine

The power curve of a wind turbine shows the power that is delivered for each wind speed within the operational range of the turbine. The first step in setting up this power curve is to find the aerodynamic power which is delivered by the rotor for this wind speed range.

4.1.1 Aerodynamic power curve

A typical power curve is shown in Figure 27. It shows the power of the Areva Wind M5000 wind turbine versus the wind speed at hub height. Although this example shows a curve that already accounts for other losses in the power train (such as the generator losses), the shape of this curve closely resembles the shape of the aerodynamic power available from the rotor.

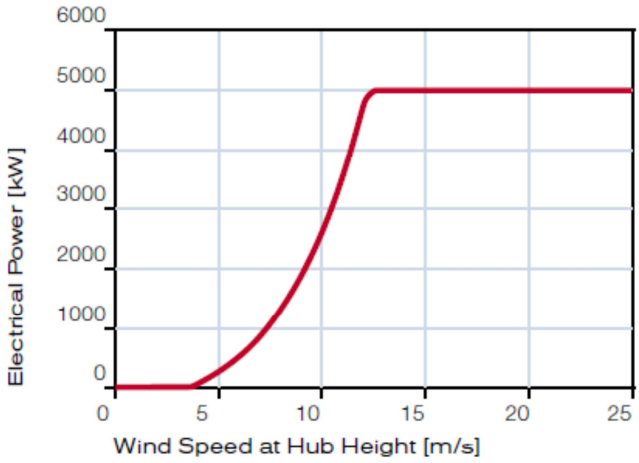

Figure 27: Power curve of the Areva Wind M5000 wind turbine [56]

The aerodynamic power that is available at a given wind speed V is often described as:

$$P(V) = \frac{1}{2}\rho C_{p,\lambda}\pi R^2 V^3$$

Where:

P(V)= Available rotor power at wind speed V (W)

R= Rotor radius (m)

V= Wind speed at hub height (m/s)

ρ= Air density at ISA conditions= 1.225 (kg/m³)

$C_{p,\lambda}$= Power coefficient of the rotor at tip speed ratio lambda (-)

The only unknown parameter in this equation is the power coefficient $C_{p,\lambda}$. Peter Jamieson describes this coefficient as the ratio of fraction of energy in the wind that is extracted by the rotor to the amount of energy in the wind that would pass through the rotor swept area with the rotor absent [57]. So this parameter gives measure to the aerodynamic performance of the rotor blades for the tip speed ratio at which it operates.

4.1.2 Aerodynamic power coefficient

The performance of the rotor is dependent on the design of the aerodynamic shape of the blades. Although the aerodynamic design of the blades is a key part of the wind turbine design, this report will not cover a full analysis of the different design options of the rotor blade. The only rotor design variables that will be evaluated are the number of blades and the design tip speed ratio. Other design variables such as the airfoil distribution along the blade span, the chord distribution and the twist distribution will not be subject of a parametric optimization. Instead, some assumptions concerning these parameters will be made which will result in a performance estimation that is good enough for the conceptual design optimization under consideration.

One very common and simple method to analyze the performance of wind turbine blades is with Blade Element Momentum (BEM) theory. In this method, the blade of a wind turbine is divided into several elements along the spanwise direction of the blade. The theory assumes that the flow of each element is independent of the flow at other elements. This allows each element to be analyzed separately in order to find the contribution to the rotor performance of this element. The thrust and torque contributions of each element are found by combining the momentum equations with blade element equations for each blade element, hence the name blade element momentum theory. And when adding up these contributions, the power coefficients are found and power curve can be established for the rotor. For a more detailed explanation on BEM theory, the interested reader is referred to some of the many books on wind turbine aerodynamics [2][32].

Although performing BEM analysis of one rotor design doesn't take up too much calculation time, it will be seen in chapter 5 that there are a very large number of rotor configurations which will be analyzed. This leads to considerable total calculation time if a BEM analysis of each rotor design was performed.

Instead, a simplified approach is taken. Wilson *et al.* performed a numerical analysis to find the maximal power coefficient for a number of blade designs with different number of blades, design tip speed ratios and lift-to-drag ratios of the airfoils used. The blades did not have exactly the same planform design as the planform design of the reference blade, but it does approximate the design close enough for the results to be used anyway. Wilson *et al.* calculated the maximal achievable power coefficient for rotors while taking into account the effects of the finite number of blades and the effects of drag on the blades performance. They found a relationship that fits to this data and is accurate to within 0.5% for tip speed ratios between 4 and 20, lift-over-drag ratios above 25 and one to three blades [2]. The relationship they found is [58]:

$$C_{p,\max} = \frac{16}{27}\lambda\left[\lambda + \frac{1.32 + \left(\frac{\lambda - 8}{20}\right)^2}{N^{\frac{2}{3}}}\right]^{-1} - \frac{0.57\lambda^2}{\frac{C_l}{C_d}\left(\lambda + \frac{1}{2N}\right)}$$

Where $C_{p,max}$ is the maximal achievable power coefficient for the blade design specified by design tip speed ratio λ (the tip speed ratio for which the blade is optimized), N number of blades and a maximal lift over drag ratio C_l/C_d. The results of this formula are shown for a number of cases in Figure 28. Jamieson suggests that an average equivalent lift to drag ratio of around 100 applies to current state of the art turbines [57].

The aerodynamic power curve will thus be established by using the above expression for maximal power coefficient. This coefficient is used to determine the power until rated power is reached. Once the rated power is reached, the power is constant until cut-out wind speed, after which the turbine stops producing power.

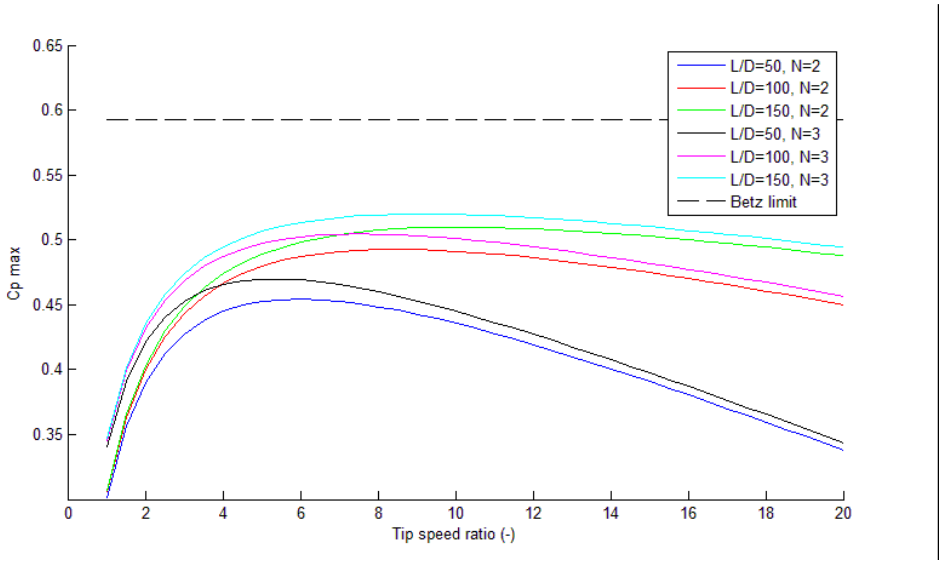

Figure 28: C_p max as a function of tip speed, N and L/D

4.2 Gearbox losses

The losses in a gearbox can be divided into two main categories [59]:

- The gear mesh losses, also called tooth friction losses. These losses are dependent on the transmitted power.
- The no-load losses. These losses are mainly caused by the bearings which are turning in the oil which is used as a lubricant. No-load losses are dependent on the rotational speed of the gears.

GL Garrad Hassan has developed a simplified empirical model of the gearbox efficiency. In this formula, the losses have a constant component which is dependent on the rated power and on the number of gearbox stages that are present. Another component of the losses is dependent on the power level at which the turbine is operating at that moment. The gearbox losses, $P_{loss,gearbox}$ (kW), are calculated as [57]:

$$P_{loss,gearbox} = \frac{\left[\left(\frac{10}{3} + 2N_{gear}\right)P_{rated} + 5N_{gear}P_i\right]}{1000}$$

Where

N_{gear} is the number of gearbox stages (-)

P_{rated} is the rated input power (kW) which equals P_{target}

P_i is the input power in the gearbox (kW)

The first term in this expression can be considered as the contribution of the no-load losses and the second term can be considered to represent the gear mesh losses.

4.3 Generator losses

To analyze the electrical losses inside a generator, very detailed information on the design of the complete generator has to be known. Since such a detailed analysis of each generator system is out of the scope of this report, a simplified approach will be taken.

The main contributions to the losses in the generator are [59]:

- The iron losses which consist of the hysteresis and eddy current losses.
- The copper losses. These are mainly resistive losses in the copper stator windings and in the rotor copper windings if rotor windings are present.

In the Upwind project, these losses were calculated over the operational wind speed range [Upwind 3]. The outcomes of this analysis are used in a simplified method to calculate the generator loss components as a function of the windspeed.

The iron losses are dependent on the generator frequency and since the generators under evaluation are variable speed generators, this frequency will therefore vary linearly with the wind speed (as the rotational speed varies linearly with the wind speed). The iron losses, $P_{loss,iron}$ (W) can now be estimated as:

$$P_{loss,iron} = p_{loss,iron}\sqrt[3]{\frac{P}{P_{rated}}}$$

Where

$p_{loss,iron}$ are the iron losses at rated wind speed (W). This value has to be found for each generator type and the value depends on the size of the generator. The values were found by interpolating between the results of the Upwind project for each generator type. The losses for all the generator types and sizes from the Upwind project can be found in Appendix B.

The above formula for the iron losses holds for wind speeds below rated wind speed. Above rated wind speed, the iron losses remain constant at the rated value.

The copper losses are assumed to vary with the square of the current in the rotor and stator. If the generator voltage is assumed to remain constant, this means that the generator current varies linearly with the power. The copper losses, $P_{loss,copper}$ (W), will therefore vary with the square of the power and can be calculated as:

$$P_{loss,copper} = p_{loss,copper}\left(\frac{P}{P_{rated}}\right)^2$$

Where $p_{loss,copper}$ are the copper losses at rated power (W). These values are determined using the same method as described above for the iron losses and the values from the Upwind report can also be found in Appendix B.

In the EESG and DFIG systems, there are both stator and rotor windings. For these systems $p_{loss,copper}$ is found by adding the rotor and stator copper losses at rated wind speed.

4.4 Converter losses

The converter losses can be divided into three parts according to their dependency on the load through the converter [Power electronics]. One part, which consists of dissipative power losses, is constant and independent of the load. Another part, which consists of the switching losses and conduction losses, is linearly dependent on the load. The final part varies with the square of the load and consists of conduction losses. A simplified method to calculate the losses in the converter, $P_{loss,converter}$ (W), can now be used [42]:

$$P_{loss,converter} = \frac{p_{conv,rated}}{31}\left(1 + 20\frac{p_{converter}}{P_{converter}} + 10\frac{p_{converter}^2}{P_{converter}^2}\right)$$

Where $p_{conv,rated}$ are the rated losses in the converter, which equal 3% of the rated load through the converter. $p_{converter}$ is the load through the converter (W) and $P_{converter}$ Is the rated load through the converter (W).

4.5 Additional losses

In this section, some additional losses are mentioned which do not occur in the drive train of the turbine. The main additional losses are the losses in the transmission system and the wake losses.

4.5.1 Transmission losses

The losses in the transmission system are all the electrical losses which occur between the converter and the onshore grid. The components in this transmission system are:

- A low to medium voltage transformer
- Medium voltage in field collection cables
- A medium to high voltage transformer substation
- A high voltage shore connection cable
- Reactive power compensation

Each of these losses varies over the operational range of the wind turbine. The cable losses are also dependent on the length of the cables. However, since modeling these losses is out of the scope of this report, a fixed value will be assumed for these losses. In a previous, unpublished, report made by

the author, the average transmission losses for the Princess Amalia wind farm were calculated to be 2,5% of the annual energy. Since this wind farm uses a similar transmission system to the one that was assumed for the offshore wind farm under consideration, the power levels over the operational wind speed range will therefore be multiplied by a value 0.975 to account for the transmission losses.

4.5.2 Wind farm wake losses

Inside the wind farm, the wind speed does not equal the free stream wind velocity. This is because the turbines are placed in rows behind each other and the turbines in the first row will receive higher wind speeds than the turbines behind this row. In literature, values between 5% to 15% of power losses were found caused by these wind farm wakes. In this model, a value of 10% wake losses was used.

4.6 Electrical power curve

When combining the results of sections 4.1 to 4.5, it is possible to set-up the power curve that represents the power that is actually delivered to the electrical grid. The aerodynamic power curve of section 4.1 is taken as a starting point and all the losses that were calculated in sections 4.2 to 4.5 are deducted from this power curve. The new power curve now represents the power that can be delivered to the onshore grid.

4.7 Annual energy yield

When the electrical power curve of the turbine is established, the annual energy yield can be calculated when the wind distribution for the specified site is known.

The annual energy yield, E_{year} (MWh), can be calculated as:

$$E_{year} = AT_{year}P_{avg}$$

Where:

A is the availability of the turbine. This will be calculated in section 4.7.1.

T_{year} is the amount of hours in one year, which equals 8760 hours.

P_{avg} is the average power output of the turbine at the specified site (MW). This average power output will be calculated in section 4.7.2.

4.7.1 Availability

The availability of the turbine is taken from the DOWEC O&M reports which were already mentioned in section 3.7. In these reports, the time between the occurrence of a failure in the turbine (which leads to stopping of the power production of this turbine) and the time when this failure is fully repaired is used taking into account the failure rate of these components and the type of failure occurring. The bulk of this time is ‘waiting time’ which is the time that the repair crew (and rented equipment) has to wait for acceptable weather conditions in order to perform the repair.

The baseline contributions to the unavailability (which equals the downtime of the turbine) of each component is given in Table 8 [3].

Component	Baseline downtime (hr)	Fraction of downtime (%)	Optimized downtime (hr)
Shaft & Bearing	6	0,82	0,87
Brake	2	0,27	0,29
Generator	235	32,31	33,93
Parking Brake	1	0,14	0,14
Electrical Systems	38	5,22	5,49
Blade	247	33,96	35,66
Yaw System	13	1,79	1,88
Pitch Mechanism	11	1,57	1,65
Gearbox	153	21,00	22,05
Invertor	5	0,71	0,75
Control	16	2,20	2,31
Total:	**727**	100,00	**105,00**

Table 8: Component contributions to the downtime of the DOWEC turbine using the baseline maintenance strategy [3]

Since the baseline maintenance strategy lead to a very low availability of only 91.7%, the maintenance strategy was optimized leading to an availability of 98.8% [55]. This corresponds to a total downtime of 105 hours. In the optimization report, the downtime contributions were not given in such detail as in the baseline report. Therefore, the optimized contributions to the downtime are assumed to equal the downtime contributions from the baseline O&M report times the ratio between total downtime of the optimized maintenance to the total downtime of the baseline maintenance.

For two-bladed configurations, the downtime caused by the pitch mechanism is assumed to be one third lower than for the reference case. For a direct-drive turbine, the gearbox downtime can be omitted and for a single-stage gearbox configuration, the downtime is assumed to be half of the downtime of the reference three-stage gearbox.

This gives the values for the availability of different drive train configurations shown in Table 9.

System	Availability (%)
2 Blades, PMSG-DD	99,2
3 Blades, PMSG-DD	99,1
2 Blades, PMSG-3G	98,9
3 Blades, PMSG-3G	98,8
2 Blades, PMSG-1G	99,1
3 Blades, PMSG-1G	98,9
2 Blades, EESG-DD	99,2
3 Blades, EESG-DD	99,1
2 Blades, DFIG-3G	98,9
3 Blades, DFIG-3G	98,8
2 Blades, DFIG-1G	99,1
3 Blades, DFIG-1G	98,9

Table 9: Turbine availability for different drive train configurations

4.7.2 Average power output

The average power output of a turbine at a specific site is dependent on the wind distribution at that site and on the hub height of the turbine. The average power P_{avg} (W) can be calculated as:

$$P_{avg} = \int_{V_{cut-in}}^{V_{cut-out}} P(V_{hub}) f(V_{hub}) dV_{hub}$$

Where

P(V) is the power as a function of the wind speed, which was established in section 4.6.

f(V) is the probability density function of the wind speed at the site.

The wind speed distribution is usually characterized by a Weibull distribution. The probability density function of the Weibull distribution equals:

$$f(V) = \frac{k}{c}\left(\frac{V}{c}\right)^{k-1} e^{\left[-\left(\frac{V}{c}\right)^{k}\right]}$$

Where k is shape parameter and c is the scale parameter that have been found for the wind distribution at the specified site.

The wind speed increases with increasing height. There are several methods to model this increase in wind speed with height. The relation used in this report is the relation that is given by GL regulations as this relation was also used in the cost scaling studies performed by NREL. This relation for the wind speed at hub height, V_{hub} (m/s), now becomes [61]:

$$V_{hub} = V_{ref}\left(\frac{H_{hub}}{H_{ref}}\right)^{\alpha_{shear}}$$

Where V_{ref} is the wind speed at reference height (m/s), H_{hub} is the hub height (m), H_{ref} is the reference height (m) and α_{shear} is the shear parameter which equals 0.11 [61].

5 Optimization procedure

In this chapter, the set-up of the optimization procedure will be described. In the previous chapters, the theoretical background which forms the basis of all the calculations is already given. This theory can now be applied to form a procedure which finds the optimal design of the drive train. More details on how this procedure was translated into a Matlab-code will be given in Appendix C.

5.1 Evaluation procedure

Instead of using a true optimization procedure, the procedure described below should be seen more as an evaluation procedure. Instead of finding the one optimal solution to the problem at hand using complex optimization procedures, the routine evaluates all possible configurations and calculates the levelized cost of energy for each configuration. After this is done, the best solution can be identified. The benefit of evaluating each design is that the different configurations can be compared in more detail to analyze the main drivers in this design procedure.

As input, the user needs to specify for which kind of project the turbine needs to be designed for. This project is described by giving three parameters:

- The desired rated aerodynamic power of one turbine
- The wind conditions at the selected site.
- Wind farm location and layout

5.1.1 Desired rated aerodynamic power

The desired aerodynamic power is the power that is harvested by the rotor and delivered to the main shaft at rated wind speed.

The optimal drive train configuration will be investigated for a range of desired rated aerodynamic power. The lower end of this range is determined as 4MW as the blade cost formula was based on cost estimations which are valid for rotors with a diameter above 100m [35]. The upper end of the range is 10MW as this corresponds to the highest power level of wind turbines under investigation and because the generator data from the Upwind reports only goes up to generators of 10MW rated power [9].

5.1.2 Wind conditions

Two different wind conditions will be evaluated in this report. These represent a low wind speed site and a high wind speed site.

The low speed wind site has a scale parameter A=6.5 m/s and a shape parameter k=2.2 at 10 m reference height.

The high speed wind site has a scale parameter A=9.5 m/s and a shape parameter k= 2.2 at 10 m reference height.

5.1.3 Wind farm location and layout

The distance between the wind farm and the shore only affects the costs of the submarine transmission cable in this model. Therefore, only one distance to the shore was considered and this distance equals 60km.

The seabed is assumed to be 20m below sea-level. This factor is needed to determine the costs of the support structure foundation.

The layout of the wind farm has been described in section 3.5. It is assumed that a total of around 500MW. The turbines will be placed in a square layout. The number of turbines of this wind farm is dependent on the desired power rating.

5.2 Design variables

The design variables were described in more detail in section 2.4. Three variables can be identified which determine the layout and performance of the rotor to a large extent. These variables are the tip speed ratio, the rotor diameter and the number of blades. As was already discussed, the 'range' of the number of blades is 2 and 3.

The range of the rotor diameter is set to be 30% above and below a default rotor diameter. The default rotor diameter $D_{default}$ is estimated to be:

$$D_{default} = \sqrt{\frac{8P_{target}}{\rho C_{p,est} V_{rated,est}^3 \pi}}$$

Where

P_{target} is the desired rated power (W)

$C_{p,est}$ is the estimated power coefficient = 0.5

$V_{rated,default}$ is the default rated wind speed = 12 (m/s)

ρ is the air density which equals 1.225 (kg/m³) at ISA conditions

The range of the rotor diameter D is thus $0.7D_{default} < D < 1.3D_{default}$

The range of the tip speed ratio is limited by two factors. On the lower end, the tip speed ratio is limited to 6, as the calculation of the power coefficient is only valid for tip speed ratios between 6 and 25 [57].

On the upper side, the tip speed ratio is limited by the maximal allowed tip speed. Although the maximal tip speed for offshore wind turbines is not limited by noise constraints, there is an upper limit to the tip speed. The power calculations assumed a constant air density in all conditions. Air flow is assumed to be incompressible up till a Mach number of 0.3 in ISA conditions. This corresponds to a tip speed of 100 m/s. However, in Table 1 was seen that some two-bladed rotors are being developed with a maximal tip speed of above 120 m/s. Therefore the maximal tip speed $V_{tip,max}$, is limited to 120 m/s

The tip speed, V_{tip} (m/s), is calculated as:

$$V_{tip} = \lambda V_{rated}$$

This means that the maximal tip speed ratio λ_{max} can be calculated as:

$$\lambda_{\max} = \frac{V_{tip,\max}}{V_{rated}}$$

In order to find the maximal tip speed ratio, the rated wind speed for each design needs to be estimated. The rated wind speed is a function of the rotor diameter D and is estimated as:

$$V_{rated} = \sqrt[3]{\frac{8P_{rated}}{\rho C_{p,est}\pi D^2}}$$

With these equations, the range of the tip speed ratio is determined for each rotor diameter as $6 < \lambda < \lambda_{max}$.

5.3 Rotor configurations

The user can specify the amount of rotor diameters, m, and amount of tip speed ratios, n, that will be evaluated between their minimal and maximal values. Each of these two design variables will be combined for two-bladed rotors and three-bladed rotors. This means that 2 x m x n rotor configurations will be evaluated. Table 10 gives an overview of the rotor configurations that are evaluated.

Now, the maximal power coefficient is determined for each rotor configuration. With this power coefficient, the power curve is set-up for each rotor configuration as explained in section 4.1.

Rotor configuration	Number of blades	Rotor diameter	Tip speed ratio
1	2	$D_1(=0.8D_{default})$	6
…			…
i			λ_i
…			…
n			$\lambda_{max,1}$
(j-1)n+1	2	D_j	6
…			…
(j-1)n+i			λ_i
…			…
jn			$\lambda_{max,j}$
(m-1)n+1	2	$D_m(=1.2D_{default})$	6
…			…
(m-1)n+i			λ_i
…			…
mn			$\lambda_{max,m}$
mn+1	3	$D_1(=0,8D_{default})$	6
…			…
mn+i			λ_i
…			…
mn+n			$\lambda_{max,1}$
mn+(j-1)n+1	3	D_j	6
…			…
mn+(j-1)n+i			λ_i
…			…
mn+jn			$\lambda_{max,j}$
mn+(m-1)n+1	3	$D_m(=1.2D_{default})$	6
…			…
mn+(m-1)n+i			λ_i
…			…
2mn			$\lambda_{max,m}$

Table 10: Overview of rotor configurations

5.4 Drive-train configurations

Now, each rotor configuration is linked with the six gearbox-generator configurations. In section 2.4, the gearbox-generator configurations were identified to be:

- PMSG with direct drive, single stage gearbox or three stage gearbox
- EESG with direct drive
- DFIG with single stage gearbox and three stage gearbox

Since each of the generator-gearbox configurations is linked with each rotor configuration, this means that the total number of drive-train configurations is equal to 12 x m x n drive-train configurations will be analyzed.

For each gearbox-generator configuration, the losses are calculated that occur in the gearbox, generator and converter at each power level that is encountered in the power curve. This is done for each power curve of the different rotor configurations.

The annual energy yield of the specified site can now be calculated when combining the wind speed distribution with each new power curve (accounting for all the loss components) while taking into account the availability that applies to each drive-train configuration.

5.5 Cost calculations

Next, all the cost calculations are done for each configuration. These calculations are done by using the cost models described in chapter 3. Most component costs are either dependent on the rotor diameter, the rated power or the maximal torque encountered.

The component costs are combined into a few subsystems:

- The rotor costs consisting of the costs for the blades, the hub, the pitch mechanism and the nose cone.
- The generator system costs consisting of the costs for the gearbox, the generator, the converter and the electrical subsystem.
- The auxiliary turbine costs consisting of all the components listed in section 3.3.8.
- The tower and support structure costs.
- The wind farm costs

The levelized investment cost is calculated by multiplying the costs of all these subsystems for each configuration with the fixed charge rate. This gives the annual cost contribution of all these subsystem for each configuration.

Next to this, the annual operation and maintenance costs are calculated per configuration.

Finally, the installation costs are accounted for and their levelized annual contributions are calculated.

When adding these three main costs and dividing by the annual energy yield, the levelized costs for each drive-train configuration are found.

5.6 Best configurations

Now that the COE of each drive-train configuration is known, the best configurations can be identified.

First, the best configurations are found per rotor size and per generator-gearbox configuration. Since this is done, it actually comes down to finding the best tip speed ratio per rotor size and per generator-gearbox configuration for two-bladed and three-bladed configurations.

Next, the best rotor size is selected out of these configurations with the optimal tip speed ratio. This gives one optimal configuration for all the generator-gearbox systems for two-bladed and three-bladed configurations. The cost contributions of these 12 optimal configurations are written into a table, which is exported to an excel-file. This can be used to compare the results of simulations with different input or to compare results of one model with the results of an altered model.

Finally, the optimal drive-train configuration is identified out of these results.

In chapter 6 and 8, extensive results of the simulations that were performed are given. It should be noted that not all the results that are shown in these chapters are automatically generated in the presented format.

6 Results of the first full model

The results are generated for two wind sites which both have a shape parameter k=2.2. One wind site represents a site with a rather low wind speeds and it is characterized by a Weibull scale parameter A=6.5. The second site represents a site with very high wind speeds and is characterized by a Weibull scale parameter A=9.5. For both these sites, the performance of the drivetrain configurations is investigated for wind turbines with a rated aerodynamic power of 4, 6, 8 and 10 MW. This chapter starts with an overview of the results at different power levels for both the low and high wind speed site. Next, a more detailed analysis of the results is done for one specific site and power level.

6.1 Rotor size range

As was described in section 5.2, the range of rotor sizes is first determined. The range of the rotor is between $0.7D_{default}$ and $1.3D_{default}$ where $D_{default}$ is the rotor size for which the desired rated aerodynamic power occurs at 12 m/s. The range of the rotor radius for each power level is shown in Table 11.

P_{aero} (MW)	R_{min} (m)	R_{max} (m)
4	34.3	63.8
6	42.1	78.1
8	48.6	90.2
10	54.3	100.8

Table 11: Rotor range under investigation per power level

6.2 Low speed wind site

In the following sections, the general results from the simulations for the low speed wind site are presented. The best configurations are first presented after which their performance and cost figures are analyzed.

6.2.1 Best configurations

Table 12 shows the configurations which have the lowest COE per power level.

Aerodynamic power	Generator system	Number of blades	Rotor radius (m)	Optimal tsr (-)	Tip Speed (m/s)	COE (€/MWh)
4	DFIG-1G	2	63,8	9,5	96	90,46
6	DFIG-1G	2	78,1	10,2	103	87,45
8	DFIG-1G	2	90,2	10,9	111	87,5
10	DFIG-1G	2	100,8	11,2	114	88,67

Table 12: Optimal drive train configurations per power level

It can be seen that the configuration with the lowest COE for each power level is the two-bladed rotor with a DFIG with a single stage gearbox. The rotor size of the optimal configurations is equal to the maximal rotor size under investigation for each power level. Although the optimal rotor size was not found (because this size lies outside of the rotor range), these results confirm that a large rotor size is preferred for low speed wind sites. A high rotational speed is preferred for each power level, but as can be seen from the optimal tip speeds at rated power, the tip speeds are still below the maximal 120 m/s and thus the rotational speed is below its upper limit.

The current model gives the lowest COE somewhere between 4MW and 8MW. However, since finding the optimal power level of a turbine was not the goal of this project (and because this model holds many rough estimates of component costs and performances), the exact level of power for the cheapest COE was not investigated.

Table 13 shows the best configurations with a different generator-gearbox combination than the optimal configurations of Table 12. The rotor sizes are exactly the same as for the optimal configuration. The generator-gearbox configuration which is the second best for each power level is the two-bladed PMSG with a single stage gearbox. The optimal tip speed ratios differ a little from the optimal configurations, but there is no real trend in the difference.

Aerodynamic power	Generator system	Number of blades	Rotor radius (m)	Optimal tsr (-)	Tip Speed (m/s)	COE (€/MWh)
4	PMSG-1G	2	63,8	9,5	96	91,79
6	PMSG-1G	2	78,1	9,9	100	89,24
8	PMSG-1G	2	90,2	10,7	109	89,51
10	PMSG-1G	2	100,8	11,4	116	90,82

Table 13: Second best drive train configurations per power level

Since both the best and second best configuration have a two-bladed rotor, it could be interesting to see which three-bladed configuration has the lowest COE. These configurations are listed in Table 14. It can be seen that the configurations are very similar to the ones in Table 12. The main differences (besides the rotors having three blades) are the somewhat lower tip speeds which can be attributed to the fact that the optimal power coefficient for three-bladed rotors occurs at a lower tip speed ratio than for two-bladed rotors. The rotor size equals the maximal rotor size for the power levels between 4-8MW, for the 10MW turbine however, the rotor size of the optimal configuration is slightly below the maximal value. At this point, a balance was reached between the benefits of having a larger rotor, increased energy yield, and the drawback of the larger rotor, the increased costs.

Aerodynamic power	Generator system	Number of blades	Rotor radius (m)	Optimal tsr (-)	Tip Speed (m/s)	COE (€/MWh)
4	DFIG-1G	3	63,8	9	90	93,9
6	DFIG-1G	3	78,1	9,4	95	91,74
8	DFIG-1G	3	90,2	10,2	103	92,41
10	DFIG-1G	3	98,9	10,6	108	94,09

Table 14: Best three bladed drive train configurations

6.2.2 Performance of the optimal configurations

Table 15 shows some performance characteristics of the optimal turbine configurations. The rated efficiency represents the ratio between the power delivered to the grid at rated wind speed and the aerodynamic power at this wind speed. It can be seen that this rated efficiency is always around 82% and increases slightly for increasing power levels. The capacity factor represents the ratio of energy yield that would have been delivered if the turbine operated at maximal (electrical) power for an entire year to the actual energy yield. The capacity factor also has an increasing trend for increasing power levels. The average efficiency represents the ratio of the actual energy produced over the energy captured by the rotor. The average efficiency increases for increasing power levels and is slightly higher than the rated efficiency indicating that the point of maximal efficiency is not located

at rated power. Both the increasing rated efficiency and increasing capacity factor contribute to the increasing annual energy yield per unit of rated aerodynamic power. The cost over power ratio represents the ratio of the levelized annual costs per unit of installed aerodynamic power. This ratio reaches a minimum around 6MW. This lower cost per unit of installed power and the increased efficiency at higher power levels causes the COE to be minimal around 6MW as was shown in Table 12.

Aero-dynamic power	Electrical power (MW)	Rated efficiency (%)	Annual yield (MWh)	Capacity factor	Energy loss (MWh)	Average efficiency (%)	Total cost (€/year)	Cost/Power (€/MW*yr)
4	3,27	81,75	12961	0,452	2805	82,21	1172435	358543
6	4,94	82,33	19842	0,459	4175	82,62	1735257	351267
8	6,61	82,63	26833	0,463	5566	82,82	2347970	355215
10	8,28	82,80	33904	0,467	6971	82,95	3006449	363098

Table 15: Turbine performance and costs for the optimal configurations at low wind speeds

6.2.3 Cost contributions of the optimal configurations

Table 16 shows the cost contributions for the optimal configurations. Both the installation costs and O&M costs reduce drastically for increasing power levels. This is caused by the very rough estimates in their cost models. Both the contributions of the labour costs and equipment cost to the O&M cost fractions are independent of the turbine size. This causes the cost contribution of the O&M cost to drop drastically with increasing power level. It can also be seen that the support structure and electrical connection take up the majority of the costs. The shares of the rotor costs and of the generator system costs (consisting of the generator, gearbox and converter costs) increase with increasing power level.

When these cost contributions are compared to the cost contributions presented in Figure 3, it can be seen that there are a number of large variations. The cost contribution of the O&M costs is much lower than expected (especially at higher power levels), the share of the support structure is a little higher and the costs of the electrical connection are much larger than expected. The costs of what is indicated in Figure 3 as the 'turbine' costs (consisting of the rotor, generator system and auxiliary component costs) are lower for the model than the values from literature.

From these figures can be seen that around 65-70% of the cost contributions are from the auxiliary nacelle component costs, the support structure costs and the electrical connection costs. These are all components which are only influenced by the drive train configuration for a small part. The fact that this is such a large share of the costs explains why the COE of all the configurations is still within a rather small range of each other.

Aerodynamic power (MW)	Rotor cost	Generator system cost	Auxilliary nacelle component cost	Support structure cost	Electrical connection cost	Installation cost	O&M cost
4	11,3%	4,7%	4,5%	29,3%	29,7%	5,9%	14,7%
6	13,6%	5,4%	4,9%	30,6%	30,2%	4,3%	11,2%
8	15,1%	5,9%	5,2%	30,9%	30,5%	3,4%	9,2%
10	16,1%	6,4%	5,4%	30,8%	30,6%	2,8%	7,9%

Table 16: Cost contributions for the optimal configurations at low wind speed

6.3 High speed wind site

6.3.1 Best configurations

The best configurations for the high speed wind site are presented in Table 17. Just like for the low speed wind site, the two-bladed DFIG with single stage gearbox configuration has the lowest COE. The rotor sizes are still at the higher part of the range, but are already considerably lower than for the low speed wind site. The tip speed of the optimal configuration is high and for the higher power levels, the tip speed reaches its maximal allowable level (the fact that it is 121 m/s instead of the maximal 120 m/s is due to estimating and rounding errors). As expected, the COE is much lower than for the low speed wind site. It reaches a minimum around 8MW aerodynamic power.

Aerodynamic power	Generator system	Number of blades	Rotor radius (m)	Optimal tsr (-)	Tip Speed (m/s)	COE (€/MWh)
4	DFIG-1G	2	58,9	9,8	105	59,03
6	DFIG-1G	2	67,6	10,8	121	56,78
8	DFIG-1G	2	76,3	10,7	121	56,38
10	DFIG-1G	2	83,4	10,5	121	56,78

Table 17: Best configurations per power level for the high speed wind site

Table 18 shows the second best configurations with a different generator system than the optimal configurations. For the low power levels, the second best configuration is the two-bladed PMSG with a single stage gearbox. However, for the 10MW simulation, the second best generator system was found to be the two-bladed DFIG with a three stage gearbox. The rotor sizes are similar to the rotor sizes for the optimal configurations. The tip speeds also differ slightly, but remain on the high end of the range.

Aerodynamic power	Generator system	Number of blades	Rotor radius (m)	Optimal tsr (-)	Tip Speed (m/s)	COE (€/MWh)
4	PMSG-1G	2	58,9	10	107	59,73
6	PMSG-1G	2	69,1	10,6	117	57,85
8	PMSG-1G	2	76,3	10,5	119	57,64
10	DFIG-3G	2	83,4	10,5	121	57,96

Table 18: Second best configurations per power level for the high speed wind site

Table 19 shows the best three bladed configurations per power level. Again, the DFIG with a single stage gearbox is the best generator-gearbox configuration. The rotor sizes are smaller than the optimal two-bladed configurations due to the increased price for a three-bladed rotor. The optimal tip speed ratio is also lower.

Aerodynamic power	Generator system	Number of blades	Rotor radius (m)	Optimal tsr (-)	Tip Speed (m/s)	COE (€/MWh)
4	DFIG-1G	3	56,4	9,5	104	60,99
6	DFIG-1G	3	64,6	9,6	110	58,9
8	DFIG-1G	3	72,8	10,1	117	58,57
10	DFIG-1G	3	79,5	10,2	120	59,04

Table 19: Best three-bladed configurations for the high speed wind site

6.3.2 Performance of the optimal configurations

Table 20 shows some performance characteristics of the optimal configurations for the high speed wind site. The rated efficiency is the same as for the low speed wind sites. This is because the rated aerodynamic power is independent of the design wind speed and because the rated losses are also the same since the gearbox, generator and converter will have the same size independent of the design wind speed. The performance and cost characteristics show the same trends as for the low speed wind site. One difference is that the lowest cost per unit of installed power occurs at a higher power level than for the low speed wind site.

Aero-dynamic power	Electrical power (MW)	Rated efficiency (%)	Yield (MWh)	Capacity factor	Energy loss (MWh)	Average efficiency (%)	Total cost (€/year)	Cost/Power (€/MW*yr)
4	3,27	81,75	18818	0,657	4111	82,07	1110916	339730
6	4,94	82,33	27429	0,634	5798	82,55	1557563	315296
8	6,61	82,63	36375	0,628	7565	82,78	2050795	310256
10	8,28	82,80	45113	0,622	9290	82,92	2561405	309348

Table 20: Turbine performance and costs for the optimal configurations at high wind speeds

6.3.3 Cost contributions to the optimal configurations

Table 21 summarizes the cost contributions for the optimal configurations. The rotor cost contributes less to the total costs than for the low wind speed site. On the other hand, the relative contribution of the support structure and electrical connection has also increased. The installation and O&M costs are slightly more important for this site than for the low speed wind site. They do show the same decreasing trend for increasing power level.

Aerodynamic power (MW)	Rotor cost	Generator system cost	Auxilliary nacelle component cost	Support structure cost	Electrical connection cost	Installation cost	O&M cost
4	9,4%	4,7%	4,2%	29,6%	30,6%	6,1%	15,5%
6	10,0%	5,3%	4,1%	31,4%	32,2%	4,5%	12,4%
8	10,7%	6,0%	4,2%	31,9%	33,0%	3,6%	10,5%
10	11,1%	6,7%	4,2%	32,0%	33,8%	3,0%	9,3%

Table 21: Cost contributions for the optimal configurations at the high wind speed site

6.4 Detailed analysis of the results for one simulation

The previous sections gave a general overview of the results and trends for different power levels and wind conditions. In this chapter, the results will be analyzed in more depth for one simulation. The simulation under investigation is for the high speed wind site as for these conditions, the rotor size was not at its maximal value. When investigating the effects of changing different parameters, this gives the possibility to also see the effect on the rotor size, which would have been more difficult if the low speed wind site was selected. For this wind site, the lowest COE is found around 8MW, so this simulation was chosen for a more in depth analysis.

6.4.1 Rotor sizes and tip speeds

Table 22 shows the optimal rotor size and tip speed ratio for each generator-gearbox system and for both two-bladed and three-bladed rotors. It can be seen that the rotors of the direct-drive systems are a bit larger than for the other systems. The two-bladed rotors are slightly larger than the three-bladed rotors due to the lower total blade costs. The optimal tip speed ratio is also much lower for

direct-drive systems. This is because for a direct-drive system, the tip speed ratio only influences the performance of the turbine, but not the costs. Therefore, the tip speed ratio with the highest C_p gives the lowest COE for direct-drive systems. The rest of the configurations operate near the maximal allowable tip speed ratio as this decreases the gearbox cost.

Generator system	Number of blades	Rotor radius (m)	Optimal tsr (-)	Tip Speed (m/s)
PMSG-DD	2	78	8	89
PMSG-3G	2	76,3	10,7	121
PMSG-1G	2	76,3	10,5	119
EESG-DD	2	78	8,2	91
DFIG-3G	2	76,3	10,7	121
DFIG-1G	2	76,3	10,7	121
PMSG-DD	3	74,6	7,1	81
PMSG-3G	3	72,8	10,3	120
PMSG-1G	3	72,8	10,3	120
EESG-DD	3	74,6	7,3	83
DFIG-3G	3	72,8	10,3	120
DFIG-1G	3	72,8	10,1	117

Table 22: Rotor sizes and tip speed ratios for each generator-gearbox system

6.4.2 Performance of each configuration

Table 23 shows the performance of the abovementioned optimal configurations. Although one might expect the direct drive systems to be more efficient, it can be seen that this is not the case. In fact, the worst efficiency is seen for the EESG-DD systems. This is due to the high losses in the generator. All rated efficiencies are within a 5.5% range of each other. It can be seen that the energy yield is the highest for the two-bladed rotors and this is attributed to the larger rotor sizes for these configurations. The energy yield of all the different configurations is within a 5.4% range of each other. A remarkable observation is that the average efficiencies for two- and three-bladed rotors with the same gearbox-generator combinations are equal. When placing the COE next to the average efficiency and looking at the configurations with the same number of blades, it can be seen that the configurations with a higher efficiency generally lead to a lower COE although there are some exceptions. For these exceptions, the increase in efficiency is not enough to counteract the higher investment costs.

Generator system	Number of blades	Rated power	Rated efficiency	Energy yield (MWh)	Energy loss (MWh)	Average efficiency	COE (€/MWh)
PMSG-DD	2	6,53	81,6	36672	8057	82,0	59,01
PMSG-3G	2	6,49	81,1	35445	8406	80,8	59,42
PMSG-1G	2	6,57	82,1	36051	7901	82,0	57,64
EESG-DD	2	6,28	78,5	35495	9237	79,4	61,55
DFIG-3G	2	6,64	83,0	36265	7586	82,7	57,72
DFIG-1G	2	6,61	82,6	36375	7565	82,8	56,38
PMSG-DD	3	6,53	81,6	35813	7857	82,0	61,19
PMSG-3G	3	6,49	81,1	34475	8189	80,8	61,62
PMSG-1G	3	6,57	82,1	35027	7681	82,0	59,87
EESG-DD	3	6,28	78,5	34674	8999	79,4	63,8
DFIG-3G	3	6,64	83,0	35275	7390	82,7	59,86
DFIG-1G	3	6,61	82,6	35371	7353	82,8	58,57

Table 23: Performance comparison of different configurations

Table 24 shows the (levelized) cost contributions of all the different components for each configuration. Again, it can be seen that the costs per component are within a small range for different configurations. The only exception is the generator system cost, which shows large variations. The support structure and electrical connection cost are quasi constant showing only 3.4% and 2.1% variation respectively. Since they take up such a large share of the costs, the total levelized costs will also be close together. The range of total costs is 7.9% and it can be seen that the differences in total costs can almost entirely be attributed to the differences in number of blades and in generator system costs. The COE for the best and worst configuration shown below are within a 9.3% range of each other. This might seem high, but since there are so many assumptions in this model, the level of inaccuracy of the model is also high. Given this high level of inaccuracy and the small difference between the COE of all the different configurations, the user should treat the results of the simulation as an indication of the range wherein the optimal configuration should be found.

Gene-rator system	Rotor cost (€/year)	Generator system cost (€/year)	Auxilliary nacelle component cost (€/year)	Support structure cost (€/year)	Electrical connection cost (€/year)	Installation cost (€/year)	O&M cost (€/year)	Total cost (€/year)	COE (€/MWh)
PMSG-DD	234652	226479	87014	662407	681752	74874	196947	2164126	59,01
PMSG-3G	220432	152732	98357	654880	677080	74201	228464	2106147	59,42
PMSG-1G	220432	150310	85740	654880	677080	74201	215512	2078156	57,64
EESG-DD	234652	247245	87014	662407	681752	74874	196947	2184892	61,55
DFIG-3G	220432	139837	98357	654880	677080	74201	228464	2093252	57,72
DFIG-1G	220432	122949	85740	654880	677080	74201	215512	2050795	56,38
PMSG-DD	291451	226479	80039	647639	672407	73528	199958	2191502	61,19
PMSG-3G	271680	150630	89972	640276	667459	72816	231475	2124308	61,62
PMSG-1G	271680	147702	78751	640276	667459	72816	218523	2097207	59,87
EESG-DD	291451	247245	80039	647639	672407	73528	199958	2212268	63,8
DFIG-3G	271680	137733	89972	640276	667459	72816	231475	2111411	59,86
DFIG-1G	271680	122304	78751	640276	667459	72816	218523	2071809	58,57

Table 24: Levelized cost contributions for each configuration

6.4.3 Effect of changing the rotor size

As was mentioned in the previous chapter, the results of the model should be interpreted as a range of configurations which give the best results. Table 25 shows the COE for configurations with a different rotor size than for the optimal configuration, but with the same TSR (= 10.7) and the same gearbox-generator combination (DFIG-1G). It can be seen that the difference in COE is within a large range of rotor sizes. A change in rotor size of 15% only yields a change in COE of 3%. This means that a large range of rotor sizes could be feasible.

Rotor radius (m)	**% change**	**COE (€/MWh)**	**% change**
53,8	-29,5	63,89	13,3
60,7	-20,4	59,49	5,5
64,2	-15,9	58,12	3,1
69,4	-9,0	56,89	0,9
72,8	-4,6	56,5	0,2
76,3	0,0	56,38	0,0
79,8	4,6	56,52	0,2
83,2	9,0	56,87	0,9
88,4	15,9	57,78	2,5

Table 25: COE for different rotor sizes for a two-bladed DFIF-1G configuration with TSR=10.7

6.4.4 Effect of changing the tip speed ratio

Table 26 shows the effects of changing the tip speed ratio for turbines with a two-bladed, DFIG-1G configuration and a rotor radius of 76.3m. It can be seen that the variation of tip speed ratio yields almost no difference in COE.

TSR	**% change**	**COE (€/MWh)**	**% change**
6	-43,9	57,53	2,0
7	-34,6	57,05	1,2
7,9	-26,2	56,76	0,7
9,1	-14,9	56,52	0,2
9,9	-7,5	56,43	0,1
10,7	0	56,38	0

Table 26: COE for different tip speed ratios for a two-bladed DFIG-1G configuration with rotor radius 76.3m

6.4.5 Lowest COE per rotor size

In section 6.4.3, the change in COE was shown for the DFIG-1G configuration for a changing rotor size, but while keeping the tip speed ratio fixed at its optimal number. In this section, the lowest COE will be shown per configuration and per rotor size. Unlike in section 6.4.3, the tip speed ratio is not fixed. Figure 29 shows the lowest COE per configuration and per rotor size for two-bladed rotors. It can be seen that the lowest COE occurs around a radius of 76m for each configuration. In this region just below and just above 76m, the change in COE is not large, but changes get larger the further away from the ideal blade size.

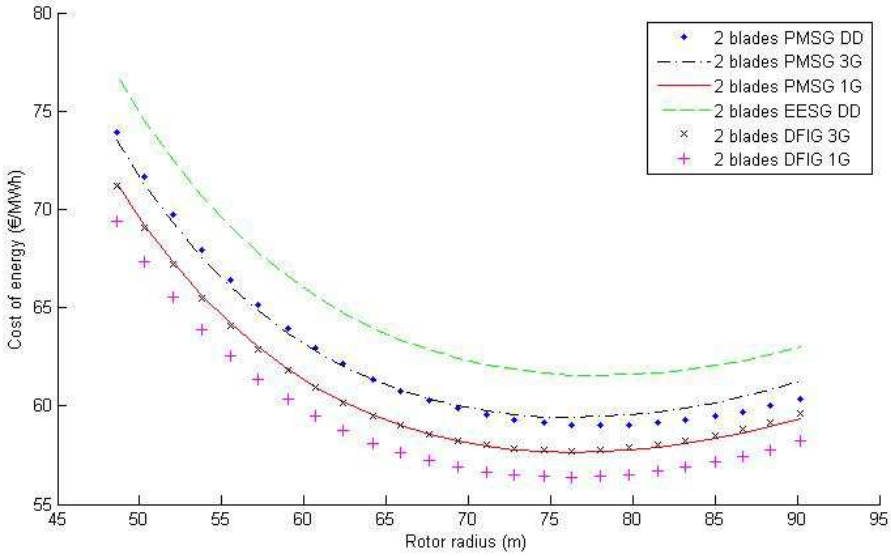

Figure 29: Lowest COE per rotor size for two-bladed rotors

Figure 30 shows the lowest COE per configuration and per rotor size for three-bladed rotors. The optimal rotor size is slightly less than for two-bladed rotors and is around 73m. It is lower since a rotor with three blades obviously is more expensive than a two-bladed rotor and therefore the point at which the increase in rotor costs outweighs the increase in energy yield is at a smaller rotor size. It can also be seen that when changing the costs are more sensitive to changes in rotor size, again due to the fact that the rotor cost is higher for a three-bladed rotor than for a two-bladed rotor.

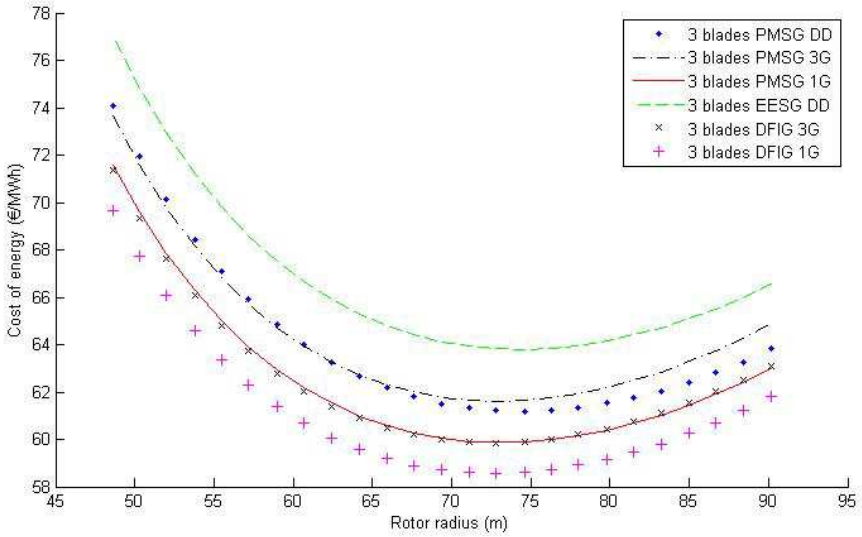

Figure 30: Lowest COE per rotor size for three-bladed rotors

6.4.6 Range of COE for all analyzed configurations

Table 27 shows the ranges of the minimal and maximal COE for all the configurations under investigation. The least favorable configuration has a COE that is 37% higher than for the optimal configuration.

Cost of energy (€/MWh)				
Configuration	Two-bladed		Three-bladed	
	min	max	min	max
PMSG DD	59,01	74,4	61,19	74,26
PMSG 3G	59,42	74,52	61,62	74,4
PMSG 1G	57,64	72,23	59,87	72,2
EESG DD	61,55	77,32	63,8	77,18
DFIG 3G	57,72	72,19	59,86	72,08
DFIG 1G	56,38	70,25	58,57	70,25

Table 27: Range of cost of energy of all the configurations

6.5 Conclusions of the first model

In the previous sections, it was shown that varying the design parameters does not yield large differences in COE. Because of the large uncertainties in the model and because of the small variations in COE for different configurations, the current model should not be used to draw large conclusions concerning the optimal configuration. In the next chapter, some suggestions are made to improve the model and therefore reduce the uncertainties and possibly give a better indication of the optimal configuration.

7 Model limitations and improvements

Since cost and performance data is very hard to find for many components, the cost and performance estimations were all done based on many assumptions and simplifications. In this chapter, real cost and performance drivers are determined and the limitations of the used models listed. Improvements to the used models are then suggested. Three of these improvements will implemented in order to have an improved design tool. The results of this improved model will be given in Chapter 8.

7.1 Real cost

In this section, the design parameters which affect the costs and performance in a major way are first identified. Next, they are linked to the design variables and input parameters in order to see which design and input choices should have an impact on the cost and performance models.

The design variables are, as listed in section 2.4:

- Tip speed ratio
- Rotor diameter
- Number of blades
- Choice of gearbox technology
- Choice of generator technology

Besides this, there are the following input parameters:

- Rated aerodynamic power
- Wind speed distribution

In the following sections, the cost drivers are analyzed per component and linked to the design variables and input parameters.

7.1.1 Blade costs

The blade costs drivers are the blade planform design and the loads to which the blade is subjected.

The blade planform parameters are:

- The chord distribution
- The twist distribution
- The airfoil distribution
- The thickness distribution

All these blade planform parameters are designed keeping in mind the tip speed ratio, the number of blades, the rotor radios and the wind speed distribution.

A large portion of the loads is dependent on:

- Fatigue loads: The fatigue loads are dependent on the rotational speed of the blades, the number of blades, the wind conditions and the blade planform design.
- Extreme loads: The extreme loads are dependent on the blade planform design and on the wind conditions.

7.1.2 Single-stage gearbox costs

The single stage gearbox costs are determined as a function of:

- The maximal input torque it encounters: This maximal input torque could be considered to be linked to the rated rotor torque. The rated rotor torque is a function of rated aerodynamic power, tip speed ratio and rotor diameter.
- The gearbox ratio: The gearbox ratio in a single-stage gearbox is a design choice and this choice is dependent on the input torque.

7.1.3 Three-stage gearbox costs

The three-stage gearbox costs are a function of:

- The maximal torque just like for the single-stage gearbox.
- The gearbox ratio: For a three-stage gearbox, the gearbox ratio is not a design choice but determined as the ratio required to reach 1200 rpm nominal generator torque. It is therefore dependent on the tip speed ratio and rotor diameter.

7.1.4 Generator costs

The generator costs are a function of:

- The generator type, which in itself is a design variable
- The generator torque which is determined by the maximal rotor torque and the gearbox ratio.

7.1.5 Converter costs

The converter costs are a function of the required converter size, which is a function of the target aerodynamic power.

7.1.6 Tower costs

The tower cost is a function of the:

- Tower height: The tower height is actually a design choice. But in general, it can be assumed that it is dependent on the rotor diameter as a larger rotor is usually combined with a larger tower.
- Tower loads: The main tower load is the aerodynamic bending moment created by the rotor. It is therefore a function of the rotor thrust, which is a function of the target aerodynamic power and the rotor diameter.
- Tower eigenfrequency: The tower eigenfrequency is dependent on the tower height, the rotational speed of the rotor and the tower top mass. This tower top mass is determined as the weight of all the rotor and nacelle components and therefore a function of all the variables mentioned in sections 7.1.1 to 7.1.5.

7.1.7 Support structure costs

The support structure costs are a function of:

- The selected support structure type
- Soil type
- Tower loads

7.1.8 Wind farm costs

The wind farm costs are a function of:

- The wind farm layout. This can be considered as a design choice. The most important factor in this choice is the inter turbine distance, which is a function of the rotor diameter.
- Distance to shore.
- Type of shore connection selected.

7.1.9 Installation costs

The installation costs are dependent on:

- The weight of the tower, nacelle and rotor
- The lifting height, which can be seen as a function of the nacelle height and thus tower height.
- The installation strategy which is used.

7.1.10 O&M costs

The O&M costs are the most difficult to predict as they have a large stochastic nature and there are many failure modes. It is assumed that the failure rate of the components is the main driver in the O&M costs. This failure rate is dependent on:

- Complexity of the components: This is linked to the generator and gearbox type that was selected. The number of degrees of freedom also determine the failure rate as moving parts have a higher tendency to fail.
- The loads which all the components encounter: This is linked to all the design variables and input parameters.

7.2 Cost model limitations and improvements

In the previous chapter, the main cost drivers were identified and linked to the design and input parameters. Table 28 summarizes the assumptions that were made in the cost models that are used up till now.

When comparing these assumptions to the real design drivers given in section 7.1, it can be seen that the cost models for most components are largely simplified. Only the wind farm cost model and the converter cost model are thought to be accurate enough. The single-stage gearbox cost model is also accurate enough, although it can be improved when the gearbox ratio is also implemented as a design variable.

A more detailed analysis of the model limitations for some components is now performed and where possible, improvements were already suggested.

Cost component	Assumption
Blades	The blade costs are a function of the blade radius. The blade is designed for a rated wind speed of 12 m/s and an extreme gust of 70 m/s. The blade planform design is shown in Figure 8 and Table 3.
Single-stage gearbox	The cost of the single stage gearbox is both a function of the gear ratio and the torque the gearbox has to withstand. The gear ratios are taken from the Upwind report and are not varied to find the optimal gear ratio,
Three-stage gearbox	The cost of the three stage gearbox is solely dependent on the input torque. The gearbox ratio is not taken into consideration.
Generator	The cost models are based on the rated output power of the generator.
Converter	The cost for the converter is based on the power transmitted through this converter.
Tower	The cost of the tower is dependent on the length of the tower. The tower starts at 20m above MSL and goes up to hub height, which is equal to 50+0,36D
Support structure	The support structure cost model is for a monopile foundation with a transition piece. The cost is dependent on the depth of the seabed (which is assumed to be 20m) and on the power of the rotor.
Auxilliary nacelle components	The costs for most auxilliary components are assumed to be dependent on the rotor radius. The hydraulics, cooling system and nacelle cover costs are assumed to be a function of rated power. The cost of the SCADA system is constant.
Wind farm	The wind farm is assumed to be a 500MW wind farm. The turbines are in a square formation with 7D inter turbine distance. The collection cables operate at a 33kV voltage and the transmission cables are XPLE HVAC cables which operate at 230kV. The distance to the shore is assumed to be 60km.
Installation	The installation costs are a function of the vessel which is required for installing the turbine. The vessel dayrate is a function of the required hoisting height. The required time for installation is fixed and is assumed to be 4,7 days in total for the support structure and turbine installation
O&M	The DOWEC O&M cost studies are used to establish a reference O&M cost. This reference O&M cost was based on an 80 x 6MW wind farm with 3-bladed DFIG-3G turbines. Their is a correction for the different possible configurations.

Table 28: Cost model assumptions

7.2.1 Blade scaling while taking the blade shape and loads into account

In section 3.3.1 of the report, the blade cost scaling relation was given. A major part of the blade costs are the material costs. The cost scaling relation was found to be:

$$C_{blade} = \left(0.4019R^3 - 21051 + 2.7445R^{2.5025}\right)\frac{1.8}{0.72*1.1}$$

The first two terms between the brackets are the costs for the blade material. As can be seen, this relationship is entirely dependent on the radius of the blade.

The blade material consists of two contributions:

- A structural element, usually a box-beam, which takes up most of the loads.
- Blade skin material used to give the blade the desired aerodynamic shape and prevent buckling of the blade.

The amount of blade material thus depends on the loads that the blade has to withstand, which determines the material needed for the structural element, and on the blade planform design, which determines the blade skin material. The above scaling relation only holds for one type of blade planform design and a fixed value for the rated wind speed, 12 m/s. The rated wind speed plays a role in the determination of the maximal forces which the blade is subjected to and on the fatigue loading.

However, in the model under consideration, the planform design should be dependent on the number of blades and design tip speed ratio and the rated wind speed is not fixed for a given blade radius. The necessary blade material and associated costs therefore need to be determined with a more detailed method. Although a detailed determination of the loads which the blade is subjected to in all conditions is still too complex for this design stage, some simple calculations can be done to have a first differentiation in blade costs for each design.

In the following sections, the blade specified in section 3.4.1 is used as a reference blade after which corrections are applied for the loads and planform of the blade under investigation.

7.2.1.1 Spar cap material

Figure 31 shows a typical layout of a cross section of a wind turbine blade.

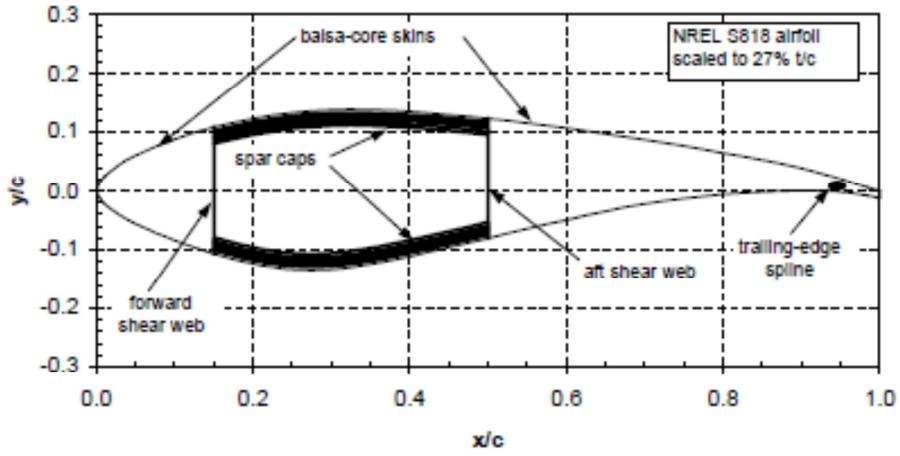

Figure 31: Typical cross section of a wind turbine blade [20]

The main structural element consists of two spar caps and two shear webs. It is assumed that the spar caps are the component which take up all the out of plane bending loads. In a real blade, part of the loads will be carried by the blade skin material (and shear webs), but in this section, this contribution will be ignored. This material therefore needs to be sufficient to:

- Withstand the extreme out of plane bending moment
- Withstand the out of plane fatigue loads
- Limit the out of plane tip deflection

In order to find the necessary spar cap material, the critical design driver needs to be identified. The reference blade reaches its extreme load during a 70m/s gust [38]. However, when upscaling a blade, the extreme loads will no longer be the critical design driver, but instead, fatigue loading will become more critical [63]. Calculation of fatigue damage without requires a full analysis of the load spectrum and is therefore not possible in this design stage. It is assumed that when the stresses due to the out-

of-plane bending moment at rated wind speed are kept constant to the stresses in the reference blade at rated wind speed, the blade will not fail due to fatigue.

The stresses in a blade due to the bending moment equal:

$$\sigma = \frac{My}{I}$$

Where M is the bending moment (Nm), y is half the thickness of the blade (m) and I is the second moment of area of the blade section (m^4).

The out-of-plane bending moment M varies along the blade span (x=r/R):

$$M(x) = C_m(x) 0.5 \rho V^2 \pi R^3$$

The moment coefficient C_m is dependent on the number of blades and the tip speed ratio. It can be approximated as [57]:

$$C_M(x) = \frac{16}{27B} G(B,\lambda) f(x)$$

Where

$$G(B,\lambda) = 5.5744\times10^{-7} B^3\lambda^3 - 8.2871\times10^{-5} B^2\lambda^2 + 4.4085\times10^{-3} B\lambda + 2.3245\times10^{-1}$$

B is the number of blades and λ is the tip speed ratio.

$$f(x) = \frac{(x-1)^2 (x+2)}{2}$$

The main structural element can be approximated as a rectangular structure consisting of two shear webs and two spar caps as shown in Figure 32.

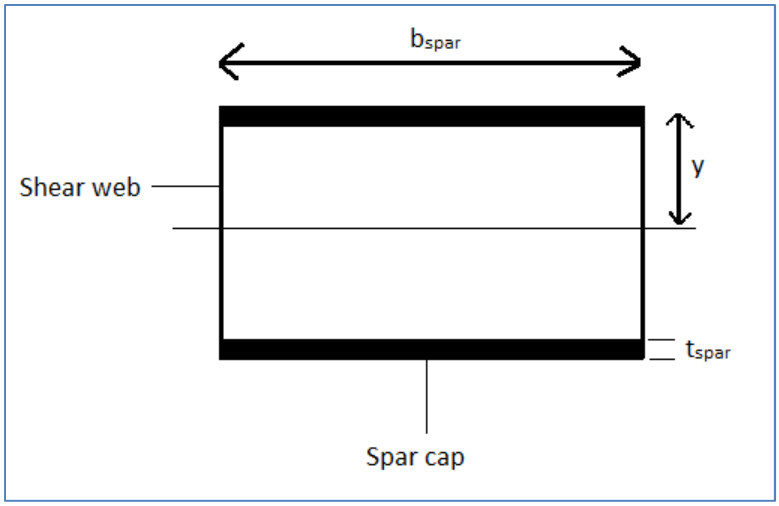

Figure 32: Dimensions of the box-beam inside the blade

The second moment of inertia of the spar caps can now be approximated as:

$$I = 2\left[\frac{b_{spar}t_{spar}^3}{12} + b_{spar}t_{spar}\left(y - \frac{t_{spar}}{2}\right)^2\right]$$

Where

b_{spar} is the width of the spar cap. The spar cap for the reference blade is located between 15% and 50% chord length and thus has a width of 0.35 times the chord length.

t_{spar} is the thickness of the spar cap.

Since $b_{spar} >> t_{spar}$, the expression for the second moment of inertia can be simplified to:

$$I = 2b_{spar}t_{spar}y^2$$

In order to keep the bending stress constant, the second moment of inertia needs to be scaled as:

$$\frac{I_{new}}{I_{ref}} = \frac{\frac{M_{new}y_{new}}{\sigma_{ref}}}{\frac{M_{ref}y_{ref}}{\sigma_{ref}}} = \frac{M_{new}y_{new}}{M_{ref}y_{ref}}$$

Where the subscript *ref* refers to the variables of the reference blade and *new* refers to the variables of the blade design that is analyzed.

Using $I = 2b_{spar}t_{spar}y^2$ this can be rewritten as:

$$\frac{b_{spar,new}t_{spar,new}}{b_{spar,ref}t_{spar,ref}} = \frac{M_{new}y_{ref}}{M_{ref}y_{new}}$$

The mass of the spar cap material, m_{spar} (kg), can be estimated as:

$$m_{spar} = 2\rho_{spar}b_{spar}t_{spar}L_{spar}$$

Where ρ_{spar} is the density of the spar cap material (kg/m³) and L_{spar} is the length of the structural element (m). The blade under analysis has the same length as the reference blade and therefore, the length of both structural elements is the same.

The ratio of the spar cap mass under evaluation to the spar cap material of the reference blade can now be calculated as:

$$\frac{m_{spar,new}}{m_{spar,ref}} = \frac{2\rho_{new}b_{spar,new}t_{spar,new}L_{spar,new}}{2\rho_{ref}b_{spar,ref}t_{spar,ref}L_{spar,ref}}$$

The density terms now disappear as the material does not change and the spar length terms also disappear as the new blade is compared to a reference blade of the same length. The ratio can now be expressed as:

$$\frac{m_{spar,new}}{m_{spar,ref}} = \frac{b_{spar,new}t_{spar,new}}{b_{spar,ref}t_{spar,ref}} = \frac{M_{new}y_{ref}}{M_{ref}y_{new}}$$

Since the airfoils are not subject of the optimization procedure, the thickness distribution along the blade remains constant. The thickness at a certain location is usually expressed as a function of the chord length. The chord distribution for an 'ideal blade' is proportional to:

$$c \sim \frac{1}{B\lambda^2}$$

Although the ideal chord distribution is not implemented in practice, it is assumed that the chord distribution will still be proportional to the above expression.

Using this and filling in the expression for out of plane bending moment at rated wind speed, the expression for the ratio of spar cap mass can now be simplified to:

$$\frac{m_{spar,new}}{m_{spar,ref}} = \frac{M_{new}c_{ref}}{M_{ref}c_{new}} = \frac{C_{m,new}0.5\rho V_{rated,new}^2 \pi R^3}{C_{m,ref}0.5\rho V_{rated,ref}^2 \pi R^3}\frac{B_{new}\lambda_{new}^2}{B_{ref}\lambda_{ref}^2} = \frac{C_{m,new}V_{rated,new}^2 B_{new}\lambda_{new}^2}{C_{m,ref}V_{rated,ref}^2 B_{ref}\lambda_{ref}^2}$$

The reference blade has a maximal chord length of 0.08R, a design tip speed ratio of 7 and a rated wind speed of 12 m/s.

7.2.1.2 Skin material

It can be assumed that the blade skin mass is proportional to the blade surface area and the skin thickness [57]. Both are proportional to the chord, so the skin mass is proportional to the square of the chord length. The mass of the skin material, m_{skin} (kg), can be estimated as [57]:

$$m_{skin} = kc^2L$$

Where

L is the length of the blade and k is a constant that depends on the thickness of the skin and material used for the skin.

The ratio of the skin mass of the blade design under consideration to the reference blade skin mass can be estimated as:

$$\frac{m_{skin,new}}{m_{skin,ref}} = \frac{c_{new}^2}{c_{ref}^2} = \frac{B_{new}^2\lambda_{new}^4}{B_{ref}^2\lambda_{ref}^4}$$

7.2.1.3 Shear web material

Although the shear webs were not considered in the calculation of the required material to withstand the loads, the shear webs still contribute to the blade weight. The size of the shear webs is proportional to the thickness of the shear webs times the height of the shear webs. The thickness is assumed to be independent of the design. The height of the shear webs is proportional to the thickness of the blade and thus proportional to the chord length. The mass of the shear web material, m_{web} (kg), thus scales as:

$$\frac{m_{webs,new}}{m_{webs,ref}} = \frac{c_{new}}{c_{ref}} = \frac{B_{ref}\lambda_{ref}^2}{B_{new}\lambda_{new}^2}$$

7.2.1.4 Improved calculation of the blade mass and costs

The previous sections gave scaling relations for different components of the wind turbine blades. In order to scale the total blade mass, the relative contributions of each component to the total weight must be known. The exact values for the reference blade were not found. Therefore, data was used of a similar blade from the NREL 5MW turbine for which the mass contributions are shown in Table 29.

Component	Relative contribution
Spar caps	42,8%
Shear webs	16,9%
Skin material	40,3%

Table 29: Blade weight contributions for the NREL 5MW blade [44]

The total blade weight can now be calculated as:

$$\frac{m_{blade,total,new}}{m_{blade,total,ref}} = 0.428\frac{m_{spar,new}}{m_{spar,ref}} + 0.169\frac{m_{webs,new}}{m_{webs,ref}} + 0.403\frac{m_{skin,new}}{m_{skin,ref}}$$

It is assumed that the blade material costs are proportional to the mass of the blades. As was explained in section 3.4.1, the total blade costs also consist of labor and overhead costs. It is rather complicated to estimate the impact of the change in blade material and the change in planform design on these costs. It is assumed that these costs scale proportional to the change in material costs and therefore:

$$\frac{C_{blade,new}}{C_{blade,ref}} = \frac{m_{blade,new}}{m_{blade,ref}}$$

7.2.2 Generator cost model

For now, the costs per generator system are purely a function of the rated power of the turbine. Since the rotational speed of the generators and hence the torque can differ for a given rated power, this assumption is not entirely correct. The size and costs of the generator actually scale with the maximal torque of the generator [57]. This trend is confirmed when the costs of the different generator systems are plotted as a function of the maximal torque. An example of such a plot is shown in Figure 33 and the plots for the different generator systems under evaluation show the same trend.

The generator input torque, T_{gen} (Nm), is simply calculated as:

$$T_{gen} = \frac{T_{aero}}{n_{gearbox}}$$

Where $n_{gearbox}$ is the gear ratio of the gearbox (if present) and T_{aero} (Nm) is the aerodynamic torque which is calculated as:

$$T_{aero}(V) = \frac{P_{aero}(V)}{\Omega(V)}$$

Here P_{aero} (W) is the aerodynamic power and Ω (rad/s) is the rotational speed of the rotor as a function of the wind speed which is calculated as:

$$\Omega = \frac{\lambda V}{R}$$

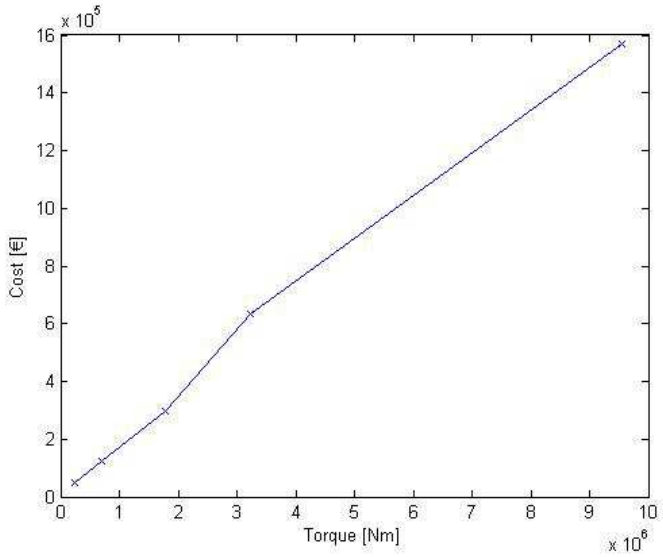

Figure 33: Torque-cost relation for a PMSG DD generator (reproduced from data in [9])

7.2.3 Gearbox costs

The single stage gearbox cost model incorporates the effects of input torque and gear ratio to find the costs per configuration. But the gear ratios are not treated as a variable in the model. However, the gear ratio should also be subject of optimization as the gearbox cost tends to go down with decreasing gear ratio, but the generator cost tends to go up with decreasing gear ratio (since this means an increasing generator input torque).

The high speed generators that are linked with a three stage gearbox all operate at a rotational speed of 1200 rpm [9]. This means that for a given rated power, the gear ratio of the three stage gearbox will have to vary as the input rotational speed at the gearbox varies per rotor configuration. However, the three stage gearbox cost was only a function of the input torque. The gearbox cost relation thus needs to be extended to include the effect of varying gear ratio to achieve the 1200 rpm rotational speed for each rotor configuration.

7.2.4 Tower cost

The tower costs are a function of the tower length and the swept area of the rotor. This is because the tower has to withstand a bending moment which is determined by the length of the tower and the rotor thrust at the tower top. In the scaling study, the rated wind speed was 12 m/s and thus, the rotor thrust at the tower top was a function of the swept area of the rotor.

In this study however, the maximal thrust will vary depending on each configuration, so the thickness of the tower could be scaled to account for the bending moment encountered by the tower.

But the natural frequency of the tower is also an important issue. Most towers are usually soft-stiff towers, meaning that their natural frequency is in between the 1P and NP (where N is the blade number) rotational frequency. Since the number of blades varies and the rotational speed varies per configuration, this will also have impact on the design of the tower. For example, it is possible that a soft-stiff tower is impossible for 2-bladed rotors in combination with variable speed as the 1P and 2P region could overlap in such a configuration.

Scaling the tower thus proves to be rather complex and finding the natural frequencies for the tower in each configuration requires information on the masses of the nacelle components too.

7.2.5 Installation costs

The installation costs were calculated to be a function of the hub height of the turbine. However, the vessel dayrates are also a function of the mass that needs to be lifted up to this height and on the installation method. A more extensive research on the effects of different conceptual designs could lead to a more realistic cost estimate. However, as will be seen in chapter 7, the installation costs only account for a small percentage of the total costs, meaning that it will not largely affect the optimized configuration.

7.2.6 O&M costs

The O&M cost model is also somewhat limited. For example, omitting the gearbox removes the O&M cost contribution for the gearbox. However, the generator will become far more expensive and the forces encountered by this generator are higher too, possibly leading to higher failure rates. Both these effects could lead to an increased O&M cost, which is not accounted for in the current model.

A more extensive research is needed to account for all the design interactions which have an effect on the O&M costs.

One small alteration to the O&M cost model is already done. In section 3.7, it was assumed that the equipment costs are constant per turbine and independent of the (target) rated power of the turbine. This is not exactly correct. When the size of the windfarm is assumed to remain constant, a higher/lower rated power of a single turbine means that less/more turbines are necessary to reach a certain combined power level in a windfarm. The total costs to rent or buy the necessary transportation and lifting equipment will remain approximately constant for the given windfarm, independent of the amount of turbines present. This means that when there are less/more turbines in the windfarm, this total equipment cost per turbine will increase/decrease as a function of the amount of turbines in the windfarm. It is therefore assumed that equipment costs need to be scaled as a function of the rated electrical power.

7.3 Performance drivers

Just like for the cost models, the main drivers that determine the performance of the turbine components will be analyzed.

7.3.1 Aerodynamic performance

The aerodynamic performance is determined by:

- The blade planform design
- The tip speed ratio at which the blade is operating

7.3.2 Gearbox performance

The gearbox performance is already described in section 4.3.

7.3.3 Generator performance

The generator performance is largely dependent on:

- The selected generator type
- The rotational speed of the generator
- The generated power

7.3.4 Converter performance

The converter performance is already described in section 4.4.

7.3.5 Wake and transmission losses

The wake and transmission losses are dependent on the layout of the wind farm and therefore on:

- The inter-turbine distance, which is dependent on the rotor diameter
- The wind conditions
- The distance to shore

7.4 Performance model limitations and improvements

Now that the performance drivers are analyzed, they can be compared to the performance assumptions shown in Table 30.

Component	Assumption
Rotor	The rotor aerodynamic power is calculated by using the maximal power coefficient for each configuration and using this value up to rated wind speed. This maximal power coefficient is determined using an emperical relation.
Gearbox	The gearbox losses are found as a function of power transmitted by the gearbox, rated power and the number of stages in the gearbox.
Generator	The generator losses are taken from the Upwind reference turbines and interpolation is done for the correct power rating. The losses are dependent on the rated power of the turbine and on the selected generator configuration.
Converter	The converter losses are a function of the converter size.
Wind farm	The fact that the wind turbines are placed in a wind farm causes wake losses and losses in the submarine power cables. These losses are assumed to be independent of turbine configuration. They are a function of the power output of the wind turbines.

Table 30: Performance model assumptions

The gearbox and converter performance models are already accurate enough. The generator performance model is not so accurate, but improvements to this model are very complex and the author lacks sufficient knowledge concerning electrical machines to go further into detail on improvements to this model.

Some improvements to the other models are suggested in the following sections.

7.4.1 Decreased performance due to rotational speed limitations

In section 4.1, it was assumed that from cut-in to rated wind speed, the rotor operates at maximal power coefficient. The power curve of a real rotor will diverge slightly from this optimal power curve in the region just above cut-in wind speed. Since the rotational speed of the rotor and hence the rotational speed of the generator's rotor varies linearly with wind speed, the rotor will operate at very low rotational speeds in low wind conditions. Such low rotational speeds would lead to very unfavorable operational conditions of the generator and a DFIG can't even operate at these conditions due to the limited variable speed. So at low wind speeds, the rotor operates at a fixed minimal rotational speed that is higher than the rotational speed at design tip speed ratio.

Figure 34 shows a typical C_p-λ-curve of a wind turbine blade. From this curve can be seen that when operating at a higher or lower tip speed ratio than the design tip speed ratio, the power coefficient will be below the maximal power coefficient that was used so far. At low wind speeds, when the turbine operates at a fixed rotational speed, the tip speed ratio will be above the design tip speed ratio and the power coefficient will thus be below its maximal value. The power at low wind speeds is therefore lower than was assumed so far. The effect of these lower power levels at low wind speeds differs for each design. But since this only happens at the low power levels, which usually don't contribute much to the total annual energy yield, it is thought that the effects of this error is rather limited. On top of this, analyzing the effects of the fixed rotational speed at low wind speeds requires e.g. a BEM analysis of each design which requires a lot of computational time.

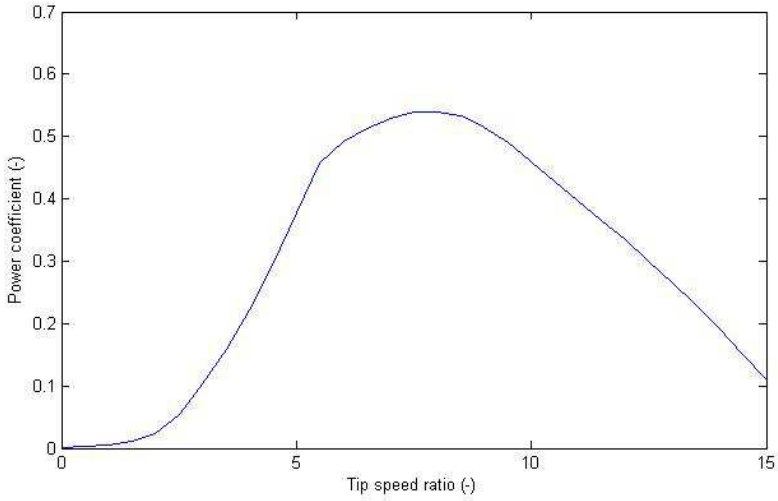

Figure 34: Power coefficient as a function of tip speed ratio for the reference blade planform design

7.4.2 Wind farm wake losses and transmission losses

The wake losses were accounted for as a fixed percentage of the total energy yield independent of the drive train configuration. The wake losses are dependent on the size of the rotors and on the amount of energy each rotor takes out of the wind. Since this varies for each configuration, the wake losses should be calculated for each configuration. However, this is out of the scope of this report.

Another problem is that the wind farm layout is fixed and far from optimized. However, finding the optimal wind farm layout is not a goal of this report.

The transmission losses are variable over the operational range of the wind turbine. At low wind speeds, the relative losses are high due to the no-load losses. At high wind speeds, the relative losses will rise due to the high ohmic losses in the components. In between these regions, the relative losses will be lower. This thus means that the relative losses in the transmission system are far from constant over the operational range of the turbine. It is uncertain what effect this will have on the optimal drive train configuration.

7.4.3 High availability

The results from the reference O&M reports show a theoretical availability of almost 99%. This value is higher than the values that are encountered in operational wind farms. Even if components are optimized for offshore conditions, this value is still very high.

Besides this, the availability of direct drive configurations is higher than for geared systems following the assumptions made in section 4.7.1. Figure 35 shows the estimates of the failure frequency of different drive train configurations that were investigated for the OWEC project [62]. In this figure, the 'advanced' configuration corresponds to a 3 bladed, variable-speed, DFIG-3G configuration. It can be seen that the reliability of this concept is thought to be higher than for a direct drive configuration, which is the opposite of what is assumed in this report.

A better analysis of the reliability is thus needed to find an improved availability estimate for each configuration.

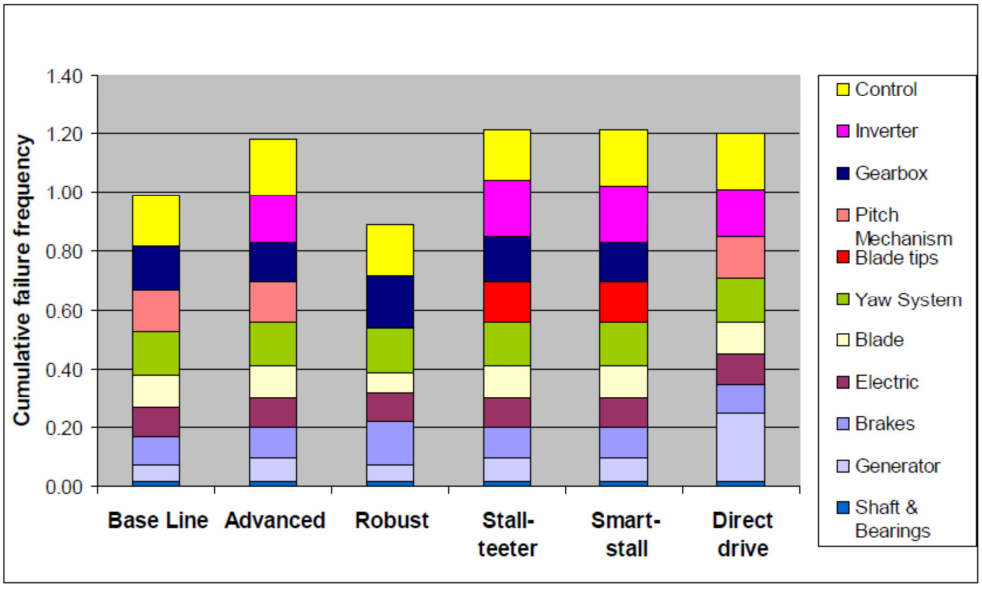

Figure 35: Yearly cummulative failure frequencies for different drive train configurations

7.5 Implemented improvements

As was mentioned before, some of the suggested improvements will be implemented. To see which improvements are the most necessary, a table is presented which shows the expected impact on the model results and the complexity of the improvements. Based on these criteria, the improvements will be implemented. The evaluation of both criteria are shown in Table 31 for the cost models. From this table can be seen that most improvements are very complex. The gearbox improvements should not be too difficult to implement, but are not expected to have a large impact in the results. The generator improvements could have a large impact and are relatively easy to implement. Therefore, these improvements will be implemented. Improving the converter cost model is not necessary. Improving the support structure model is rather complex and is not expected to give much different results concerning the drive train configuration and will not be done. Improving the wind farm model is complex and not worthwhile for this project. The installation cost model now gives a very rough estimate of the installation costs. Improvement to this model requires much effort and the effects of this improvement will remain small as the installation costs take up only a small fraction of the costs. The remaining three improvements are all very complex, but are thought to give significant improvements to the model. But since they are such large improvements, it is thought that they are out of the scope of this project. They could be suitable options for a follow-up project.

However, in the previous sections, some further improvements were suggested to the blade model and the O&M model and as these cost models are thought to be very important, it could be interesting to already implement these improvements. Therefore, the improvements from sections 7.2.1, 7.2.2 and 7.2.6 will be done and the results of these improvements are shown in the following chapter.

Cost model	Impact on results	Difficulty to fully implement
Blades	5	5
1 G Gearbox	1	3
3G Gearbox	2	3
Generator	4	1
Converter	0	/
Tower	5	5
Support structure	2	4
Windfarm	1	4
Installation	2	5
O&M	4	5

Table 31: Impact and complexity of improvements to the cost models

A similar analysis was done for the possible improvements to the performance models. This analysis is summarized in Table 32. From this analysis can be seen that again, most improvements are rather difficult. The gearbox, converter and wake and transmission models are thought to be sufficient for this project. Improving the generator and availability models are far too complex, but could also be very interesting to implement. A follow-up study on these subjects could thus be very interesting. Some improvements could be done to the aerodynamic model, but it the impact of these improvements is thought to be limited and the large effort for this improvement makes it not interesting to do.

Performance model	Impact on results	Difficulty to fully implement
Aerodynamic	3	4
Gearbox	1	4
Generator	3	5
Converter	1	4
Wake and transmission	1	5
Availability	4	5

Table 32: Impact and complexity of improvements to the performance models

8 Results of the improved model

In the previous chapter, various suggestions for improvements to the model were given and a selection of such improvements was done. The sections below show the results after implementing these improvements.

8.1 Improved results for the low speed wind site

In this section, the improved results will be shown for a site with Weibull parameters A=6.5m/s and k=2 at 10m reference height.

8.1.1 Best configurations

The optimal configurations for turbines with a rated aerodynamic power of 4 to 10MW are shown in Table 33. When comparing these results to the results from section 7.1, it can be seen that not much changes have taken place. The optimal generator system, number of blades and rotor radius remain the same. The rotational speed shifts to a slightly lower value for power levels above 4MW. The COE values change slightly, but no clear trend can be seen in these values.

Aerodynamic power (MW)	Generator system	Number of blades	Rotor radius (m)	Optimal tsr (-)	Tip Speed (m/s)	COE (€/MWh)
4	DFIG-1G	2	63,8	9,5	96	88,77
6	DFIG-1G	2	78,1	9,4	95	87,35
8	DFIG-1G	2	90,2	9,4	95	88,19
10	DFIG-1G	2	100,8	10,2	103	90,08

Table 33: Best configurations for the low speed wind site

Table 34 shows the second best configurations. One remarkable result is that at 10MW, the second best configuration becomes the DFIG-3G system. This is probably caused by the fact that the DFIG system has a lower generator cost at high torque levels. The number of blades and rotor radius remain the same as in section 7.1. Just like for the best configurations, the optimal tip speed ratio lowers for higher power levels.

Aerodynamic Power (MW)	Generator system	Number of blades	Rotor radius (m)	Optimal tsr	Tip Speed (m/s)	COE (€/MWh)
4	PMSG-1G	2	63,8	9,5	96	90,08
6	PMSG-1G	2	78,1	9,4	95	89,11
8	PMSG-1G	2	90,2	9,4	95	90,17
10	DFIG-3G	2	100,8	9,4	95	92,27

Table 34: Second best configurations at the low speed wind site

Table 35 shows the best results for three-bladed rotors. Two large differences can be seen compared to the results from the first model. At 10MW, the DFIG-3G system becomes the most interesting due to the lower generator costs at high torque levels. The second difference is that a much lower tip speed ratio is used, which appears to be constant around 8 for all power levels.

Aerodynamic Power (MW)	Generator system	Number of blades	Rotor radius (m)	Optimal tsr	Tip Speed (m/s)	COE (€/MWh)
4	DFIG-1G	3	63,8	8	80	90,72
6	DFIG-1G	3	78,1	8	80	89,88
8	DFIG-1G	3	90,2	8	80	91,18
10	DFIG-3G	3	100,8	8,2	82	95,49

Table 35: Best three bladed configurations for the low speed wind site

8.1.2 Turbine performance for improved model

Table 36 shows the turbine performance of the optimal configurations at the low speed wind site. The results are nearly all the same except for some very minor changes to the energy yield due to the change in rotational speed and the total costs due to the cost model changes.

Aerodynamic Power (MW)	Electrical Power (MW)	Rated efficiency	Yield (MWh)	Capacity factor	Energy loss (MWh)	Average efficiency	Total costs (€/year)	Cost/Power (€/MWyr)
4	3,27	81,8%	12961	0,452	2805	82,2%	1150588	351861,8
6	4,94	82,3%	19869	0,459	4181	82,6%	1735597	351335,4
8	6,61	82,6%	26912	0,465	5582	82,8%	2373277	359043,4
10	8,28	82,8%	33986	0,469	6988	82,9%	3061508	369747,3

Table 36: Performance of optimal turbines at low speed wind site

8.1.3 Cost contributions to the optimal configurations

The cost contributions for the optimal configurations at the low speed wind site are shown in Table 37. The rotor and generator costs have decreased slightly in the new cost model. The O&M costs have also changed as the cost contribution of the equipment became dependent on the size of the turbine. For the 4MW turbine, the costs lowered, for 6MW they remained quasi the same and for higher power levels, they increased.

Aerodynamic Power (MW)	Rotor cost	Generator system cost	Auxilliary nacelle component cost	Support structure cost	Electrical connection cost	Installation cost	O&M cost
4	11,2%	4,9%	4,6%	29,8%	30,2%	6,0%	13,2%
6	13,3%	5,7%	4,9%	30,6%	30,2%	4,3%	11,2%
8	14,6%	6,4%	5,1%	30,6%	30,1%	3,4%	9,9%
10	15,9%	6,7%	5,3%	30,2%	30,1%	2,7%	9,1%

Table 37: Offshore wind cost contributions for the low speed wind site

8.2 Improved results for the high speed wind site

In this section, the improved results will be shown for a site with Weibull parameters A=9.5m/s and k=2 at 10m reference height.

8.2.1 Best configurations

The optimal configurations for the high speed wind site have been shown in Table 38. The generator system remains the same as for the first model, just like the number of blades. The optimal rotor radius increases slightly for the 4 and 6MW turbines. The tip speed ratio decreases, especially at the

higher power levels. At 4MW, the COE is lower for the improved model than for the first model. At higher power levels, the COE is higher than for the first model.

Aerodynamic power (MW)	Generator system	Number of blades	Rotor radius (m)	Optimal tsr (-)	Tip Speed (m/s)	COE (€/MWh)
4	DFIG-1G	2	60,1	9,4	99	58,07
6	DFIG-1G	2	69,1	9,3	102	57,1
8	DFIG-1G	2	76,3	9,3	105	57,42
10	DFIG-1G	2	83,4	9,2	106	58,28

Table 38: Best configurations for the high speed wind site

Table 39 shows the second best configurations. Just like for the low speed wind site, the best configuration at 10MW becomes the DFIG-3G system due to its lower generator costs. The rotor radius remains the same, with some minor variations at 4 and 8MW. The tip speeds are lower than before and show an increasing trend with increasing power levels. This is due to the increasing rotor radius at increasing power levels. The COE is lower at 4MW, but higher for the higher power levels when compared to the first model.

Aerodynamic Power (MW)	Generator system	Number of blades	Rotor radius (m)	Optimal tsr	Tip Speed (m/s)	COE (€/MWh)
4	PMSG-1G	2	60,1	9,2	97	58,76
6	PMSG-1G	2	69,1	9,3	102	58,17
8	PMSG-1G	2	78	9,2	103	58,67
10	DFIG-3G	2	85,3	9,3	105	59,65

Table 39: Second best configurations for the high speed wind site

The best three-bladed configurations are shown in Table 41. The gearbox systems are the same as before. The rotor size increased a little and the optimal tip speed ratio decreased significantly. Just as for the low speed wind site, the optimal tip speed ratio is around 8. The COE have decreased for 4 and 6 MW, but increased for 8 and 10MW.

Aerodynamic Power (MW)	Generator system	Number of blades	Rotor radius (m)	Optimal tsr	Tip Speed (m/s)	COE (€/MWh)
4	DFIG-1G	3	57,6	7,9	85	59,43
6	DFIG-1G	3	67,6	7,8	86	58,64
8	DFIG-1G	3	74,6	7,9	90	59,08
10	DFIG-1G	3	81,4	7,8	90	60,08

Table 40: Best three-bladed configuration for the high speed wind site

8.2.2 Performance of the best configurations

The performance of the optimal configurations is shown in Table 41. The results are practically the same as for the first model since no changes were made to the performance models. The total costs have gone down a bit for the 4MW turbine, but increased for the higher power levels.

Aerodynamic Power (MW)	Electrical Power (MW)	Rated efficiency	Yield (MWh)	Capacity factor	Energy loss (MWh)	Average efficiency	Total costs (€/year)	Cost/Power (€/Mwyr)
4	3,27	81,8%	19058	0,665	4165	82,1%	1106787	338467
6	4,94	82,3%	27880	0,644	5895	82,5%	1591994	322266
8	6,61	82,6%	36433	0,629	7577	82,8%	2091945	316482
10	8,28	82,8%	45177	0,623	9303	82,9%	2632748	317965

Table 41: Performance of the best configurations for the high speed wind site

8.2.3 Cost contributions

From the cost contributions in Table 42 can be seen that the rotor costs have increased when compared to the first model. This is partly due to the larger optimal rotor size and due to the changed rotor costs. The generator system costs have increased slightly. Just like for the low speed wind site, the O&M costs have decreased for the lower power levels and increased for the higher power levels.

Aerodynamic Power (MW)	Rotor cost	Generator system cost	Auxilliary nacelle component cost	Support structure cost	Electrical connection cost	Installation cost	O&M cost
4	10,1%	4,8%	4,3%	30,0%	30,9%	6,1%	13,7%
6	10,9%	5,6%	4,2%	31,0%	31,7%	4,5%	12,2%
8	11,3%	6,1%	4,1%	31,3%	32,4%	3,5%	11,3%
10	11,7%	6,8%	4,1%	31,2%	32,9%	2,9%	10,5%

Table 42: Cost contribution for the optimal configurations at the high speed wind site

8.3 Detailed analysis of the 8MW turbine for high speed wind sites

A detailed analysis of the improved results for the 8MW turbine at the high speed wind site is done in this section.

8.3.1 Rotor sized and tip speed ratio

Below, in Table 43, the rotor radius, optimal tip speed ratio and tip speed have been given per generator system and per number of blades. A small increase in rotor size can be seen for most configurations when compared to the first model. The optimal radius is 74.6m for three-bladed rotors and 76.3-78m for two-bladed configurations. The tip speed and tip speed ratios have decrease for all configurations with the exception of the direct drive configurations for which the tip speed ratio has increased. For these configurations, the optimal point in the first model was purely determined by the tip speed ratio with optimal power coefficient, while in the improved model, the tip speed ratio affects the blade and generator cost.

Generator system	Number of blades	Rotor radius (m)	Optimal tsr	Tip speed (m/s)
PMSG-DD	2	76,3	9,5	108
PMSG-3G	2	78	9,2	103
PMSG-1G	2	78	9,2	103
EESG-DD	2	76,3	9,5	108
DFIG-3G	2	78	9,4	105
DFIG-1G	2	76,3	9,3	105
PMSG-DD	3	74,6	8,1	92
PMSG-3G	3	74,6	7,9	90
PMSG-1G	3	74,6	7,9	90
EESG-DD	3	74,6	8,1	92
DFIG-3G	3	74,6	7,9	90
DFIG-1G	3	74,6	7,9	90

Table 43: Optimal configuration per generator system and number of blades for the 8MW turbine

8.3.2 Performance of the optimal configurations

Table 44 shows the performance of the optimal configurations. It should be noted that the order of the configurations has changed when comparing to the previous section and it is now ordered according to COE. The rated efficiency has remained the same as the performance model was not changed. The energy yield increased somewhat due to the increased rotor sizes. The average efficiency has remained almost the same. The COE has increased for all the configurations. Since the performance of the configurations has remained unchanged, the increase in COE is attributed to the increased total levelized costs.

Generator system	Number of blades	Rated power	Rated efficiency	Energy yield (MWh)	Energy loss (MWh)	Average efficiency	COE (€/MWh)
DFIG-1G	2	6,61	82,6%	36433	7577	82,8%	57,42
PMSG-1G	2	6,57	82,1%	36647	8029	82,0%	58,67
DFIG-3G	2	6,64	83,0%	36873	7707	82,7%	58,92
DFIG-1G	3	6,61	82,6%	36080	7503	82,8%	59,08
PMSG-DD	2	6,53	81,6%	36120	7928	82,0%	59,43
PMSG-1G	3	6,57	82,1%	35748	7836	82,0%	60,37
DFIG-3G	3	6,64	83,0%	36005	7534	82,7%	60,54
PMSG-3G	2	6,49	81,1%	36047	8539	80,8%	60,64
PMSG-DD	3	6,53	81,6%	35811	7856	82,0%	61,19
EESG-DD	2	6,28	78,5%	34965	9083	79,4%	62,02
PMSG-3G	3	6,49	81,1%	35191	8348	80,8%	62,31
EESG-DD	3	6,28	78,5%	34670	8998	79,4%	63,86

Table 44: Turbine performance of the optimal configurations

The cost contributions are shown in Table 45. Again, the configurations are sorted according to their COE. The rotor costs have increased for each configuration even if the rotor radius remained unchanged. The generator system costs have increased, with the exception of the direct-drive

systems. This is because the tip speed ratios have decreased, which increased the gearbox costs. Although the generator costs have gone down, this was not enough to counteract the increase of the gearbox costs. For the direct drive systems, there is no gearbox, hence the cost decrease. The rest of the costs have remained approximately the same, except for the O&M costs. These costs have increased due to the changed O&M cost model.

Gene-rator system	Number of blades	Rotor cost (€/year)	Generator system cost (€/year)	Auxilliary nacelle component cost (€/year)	Support structure cost (€/year)	Electrical connection cost (€/year)	Installation cost (€/year)	O&M cost (€/year)	Total cost (€/year)	COE (€/MWh)
DFIG-1G	2	236167	128252	85740	654880	677080	74201	235623	2091945	57,42
PMSG-1G	2	247647	158492	89392	662407	681752	74874	235623	2150189	58,67
DFIG-3G	2	248951	151622	102715	662407	681752	74874	250399	2172721	58,92
DFIG-1G	3	277998	138762	82258	647639	672407	73528	239021	2131612	59,08
PMSG-DD	2	237864	204010	83442	654880	677080	74201	215236	2146713	59,43
PMSG-1G	3	277998	165244	82258	647639	672407	73528	239021	2158095	60,37
DFIG-3G	3	277998	160305	94187	647639	672407	73528	253796	2179861	60,54
PMSG-3G	2	247647	166181	102715	662407	681752	74874	250399	2185976	60,64
PMSG-DD	3	280593	218545	80039	647639	672407	73528	218633	2191383	61,19
EESG-DD	2	237864	225848	83442	654880	677080	74201	215236	2168551	62,02
PMSG-3G	3	277998	173191	94187	647639	672407	73528	253796	2192747	62,31
EESG-DD	3	280593	241288	80039	647639	672407	73528	218633	2214126	63,86

Table 45: Cost contributions to the improved optimal results for the 8MW turbine

8.3.3 Effect of changing the rotor size or the tip speed ratio

A sensitivity analysis was done to see the changes in COE as a function of changing the rotor size or tip speed ratio away from its optimal value. This was done to see if the results presented above show are certain enough to determine an optimal configuration or not certain enough and only indicate a range in which the optimal rotor size and tip speed ratio has to be looked for.

Table 46 shows the changes in COE for the two-bladed DFIG-1G configuration when the rotor radius is changed, but the tip speed ratio remains fixed at 9.3. It is seen that the COE shows very little variation for a changing rotor size. This means that since there is a large uncertainty in the rotor cost model, the optimal rotor size should be treated with caution.

Rotor radius (m)	TSR change %	COE (€/MWh)	COE change %
60,7	-20,4	60,74	5,8
64,2	-15,9	59,35	3,4
69,4	-9,0	58,06	1,1
72,8	-4,6	57,61	0,3
76,3	0,0	57,42	0,0
79,8	4,6	57,47	0,1
83,2	9,0	57,72	0,5
88,4	15,9	58,45	1,8

Table 46: Changes in COE when the rotor radius changes

The change in COE as a function of rotor radius has been shown in Figure 36 for two-bladed configurations and in Figure 37 for three-bladed configurations. In these figures, the tip speed ratio

was allowed to change per rotor size. This confirms that the optimal radius is found at 76.3m for two-bladed configurations, but that there is a large range of rotor sizes for which the COE doesn't change very much. For three-bladed rotors, the optimal radius is at 74.6m. This lower value is caused by the increased rotor cost when three blades are present. The increased blade number also causes the change in COE to increase for varying rotor sizes.

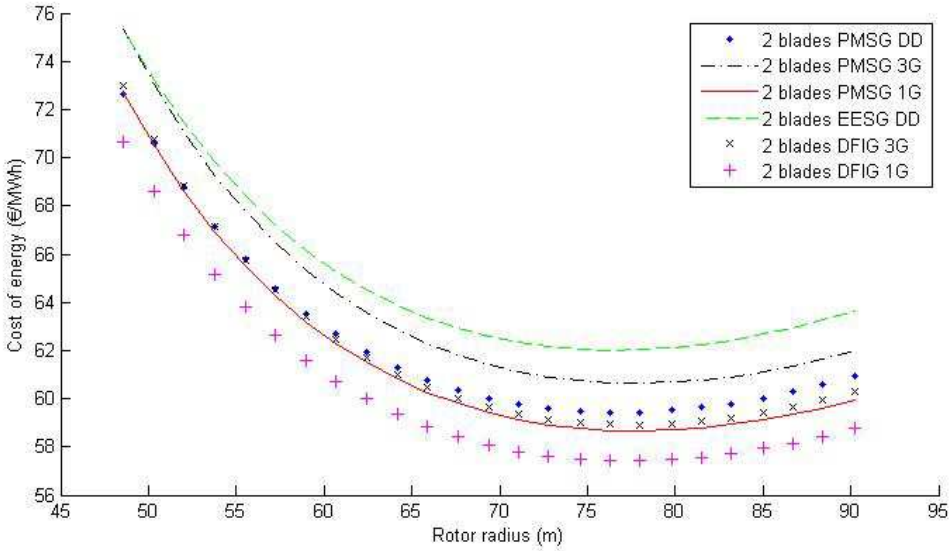

Figure 36: COE as a function of rotor radius for two-bladed configurations

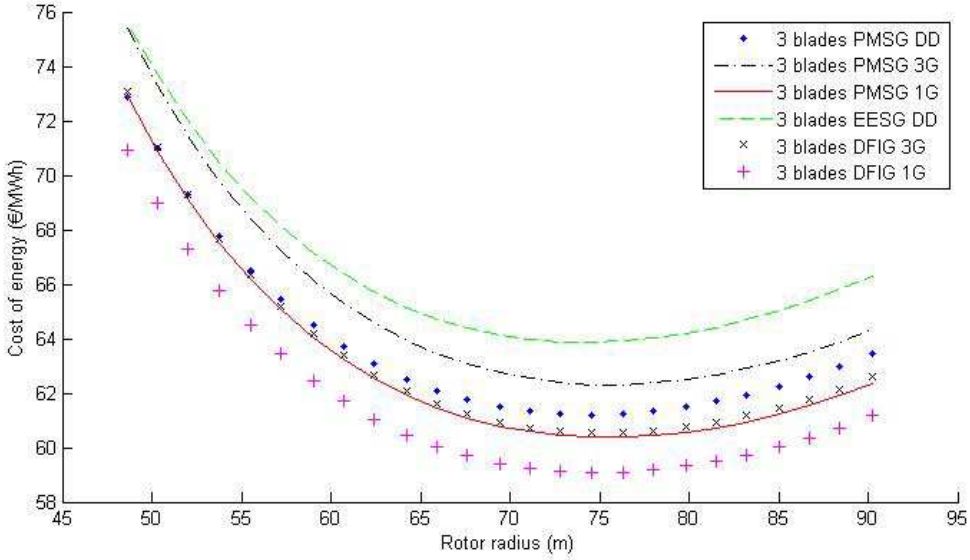

Figure 37: COE as a function of rotor radius for three-bladed configurations

Table 47 shows the changes in COE for the two-bladed DFIG-1G configuration when the tip speed ratio is changed, while the rotor radius remains at 76.3m. The changes in COE for changing tip speed ratio have increased when comparing to the previous model and optimal tip speed ratio therefore is thought to be more accurate. But the results show that a small change in tip speed ratio can be done with only a minor change in COE. Since the model still has such a large inaccuracy, the selection of an optimal tip speed ratio should thus still be treated with caution.

TSR	TSR change %	COE (€/MWh)	COE change %
6	-35,5	63,16	10,0
7	-24,7	59,5	3,6
8,1	-12,9	57,86	0,8
9,3	0,0	57,42	0,0
10,7	15,1	57,88	0,8

Table 47: COE sensitivity to changes in tip speed ratio

8.4 Optimal configuration: two-bladed DFIG-1G

The optimal configuration was determined to be the two-bladed DFIG-1G system with a rotor that has a radius of 76.3m and operates at a tip speed ratio of 9.3. The power curve is shown for this configuration in Figure 38. Cut-in wind speed equals 2 m/s and rated wind speed is 11.4 m/s where the rated electrical power of 6.61 MW is reached. Figure 39 shows the efficiency of the turbine as a function of wind speed. Below 2 m/s, the no-load losses are higher than the aerodynamic power and therefore, the rotor does not operate. Above 2 m/s, the efficiency starts to rise rapidly and already reaches 80% around 5 m/s. The efficiency reaches its maximal value at 8.3 m/s and drops slightly after this point. From Figure 40 can be seen that efficiency rises even more rapidly when it is shown as a function of electrical power output. 80% efficiency is already reached below 1 MW and the highest efficiency is reached at 2.64 MW. This high efficiency as a function of power output is the reason why the average efficiency is above 80%.

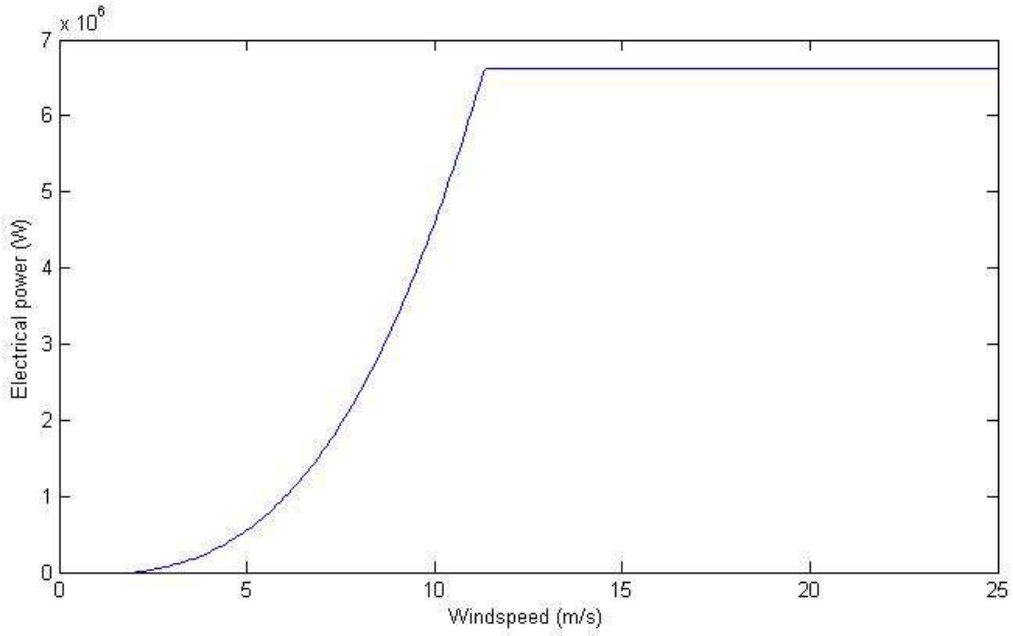

Figure 38: Power curve for the optimal configuration

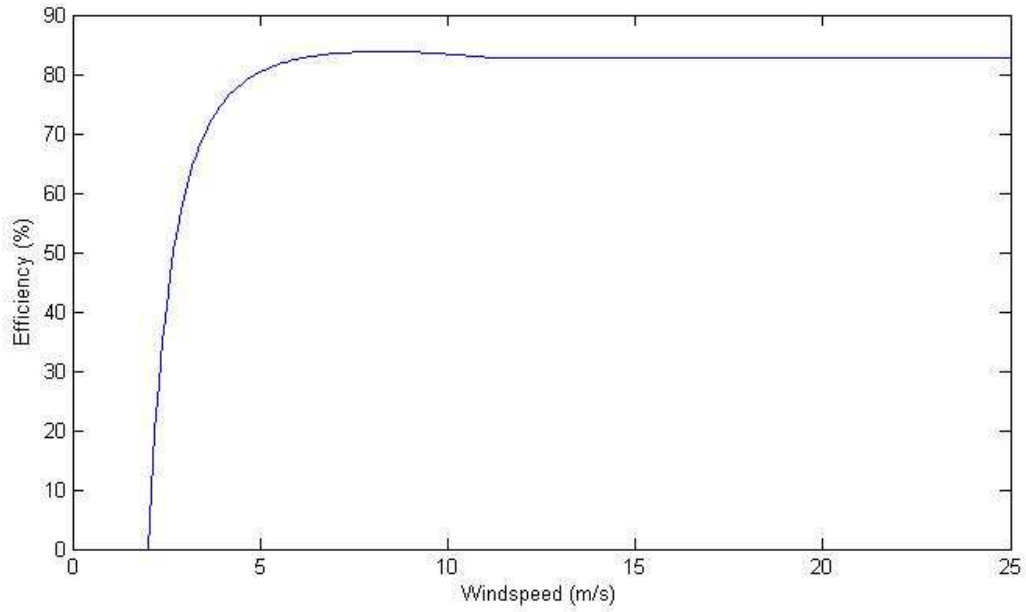

Figure 39: Drive-train efficiency as a function of wind speed

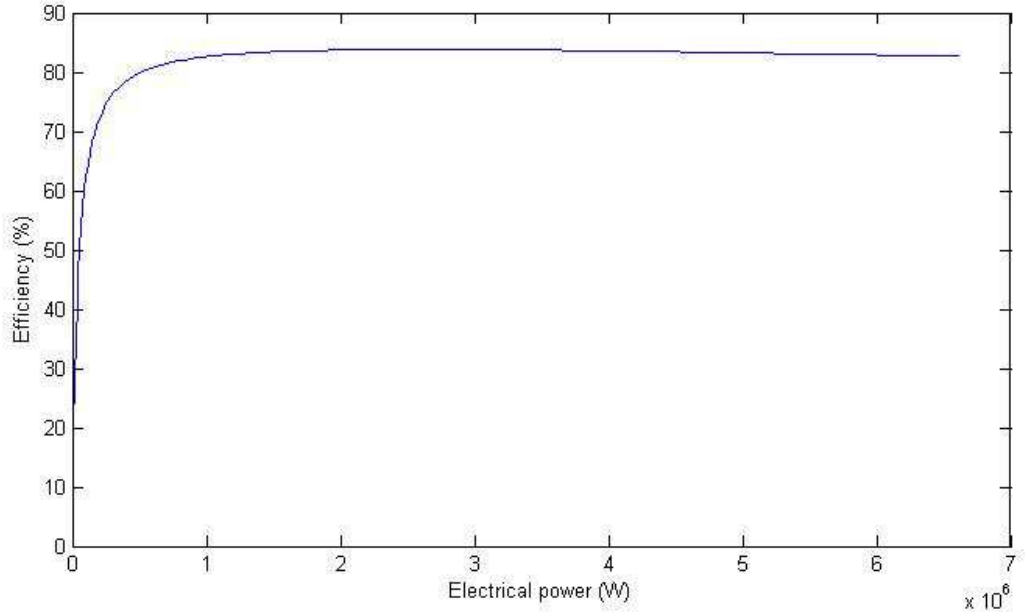

Figure 40: Drive-train efficiency as a function of electrical power

8.5 Optimal configurations when only turbine is considered in optimization

In the introduction, it was mentioned that to find the optimal turbine configuration, not only the turbine itself and its components should be considered, but also the other contributions to the cost such as O&M cost, installation cost and wind farm cost should be considered. To prove this assumption, the optimization results were calculated when only the turbine components are considered in the cost contributions. These results are shown in Table 42. The rotor radius is around 15% smaller when a single turbine is considered. The tip speed ratio generally lower for a single turbine. The last column shows the change in COE and this clearly shows that the configurations

which have the lowest COE when only the turbine is considered are more expensive when the contributions of the installation cost, O&M cost and wind farm cost are added.

Configuration	Number of blades	Rotor radius (m)	Radius change	TSR	TSR change	COE (€/MWh)	COE change
PMSG-DD	2	65,9	-13,6%	9,1	-2,2%	60,79	3,0%
PMSG-3G	2	65,9	-15,5%	8,9	-3,3%	62,3	4,8%
PMSG-1G	2	65,9	-15,5%	9,1	-3,2%	60,26	4,5%
EESG-DD	2	65,9	-11,7%	9,2	16,5%	63,36	2,9%
DFIG-3G	2	65,9	-13,6%	9,1	-4,2%	60,47	4,8%
DFIG-1G	2	65,9	-11,7%	8,9	12,7%	58,84	4,4%
PMSG-DD	3	64,2	-13,9%	7,9	0,0%	62,5	2,1%
PMSG-3G	3	64,2	-17,7%	7,7	-16,3%	63,94	3,8%
PMSG-1G	3	64,2	-13,9%	7,6	-6,2%	61,93	3,4%
EESG-DD	3	64,2	-15,9%	7,9	-16,8%	65,15	2,1%
DFIG-3G	3	64,2	-13,9%	7,7	-2,5%	62,07	3,7%
DFIG-1G	3	64,2	-13,9%	7,7	-4,9%	60,47	3,2%

Table 48: Results of the optimization when only the turbine components are considered

8.6 Sensitivity analysis to changes in availability estimation

In this section, a sensitivity analysis will be done to changes in the model. As was mentioned in chapter 7, there are still a number of improvements and follow up studies possible. Intuitive claims were made on what could influence parts of the model and claims about the importance of these improvements were made. To check these claims, a sensitivity analysis was done to see the effects of changing the model on the results. For this sensitivity analysis, changes were done to the availability model.

It was stated in section 7.4.3 that a much deeper study was necessary to determine the availability of the turbines with different drive train configurations. In this section, some 'wild' assumptions will be made just to check how the results react to such changes. It is not the goal to make claims on whether the changed availability model is better than before.

Three assumptions will be made now:

1. It was stated in section 7.4.3 that the availability used so far seems rather high with all values being around 99%. It will be assumed that the unavailability of each configuration will at least be 3 times higher than before.
2. To include a differentiation depending on other input variables rather than blade number, gearbox configuration and generator configuration, a differentiation will be added with respect to the rotational speed of several components of the drive train. It is assumed that components rotating at a higher speed will be more likely to fail and thus have a lower availability. The second model has rotational speeds of the rotor between 6,4 to 23,7 rpm. Rotational speeds below 12 rpm are assumed to have 10% lower unavailability (relative to the original values) and rotational speeds above 18 rpm are assumed to have 10% higher unavailability.

3. In Figure 35, the failure rate of PMSG systems appears to be 3 times the failure rate of other generator systems. Since 32% of the downtime is due to generator failure in the original availability model, the unavailability of PMSG systems will be 1,6 times higher than for the other systems.

The new availability values are shown in Table 49.

Rotational speed	**<12 rpm**	**12-18 rpm**	**>18 rpm**
System	**Availability**		
2 Blades, PMSG-DD	96,5	96,2	95,8
3 Blades, PMSG-DD	96,1	95,7	95,2
2 Blades, PMSG-3G	95,2	94,7	94,2
3 Blades, PMSG-3G	94,8	94,2	93,7
2 Blades, PMSG-1G	96,1	95,7	95,2
3 Blades, PMSG-1G	95,2	94,7	94,2
2 Blades, EESG-DD	97,8	97,6	97,4
3 Blades, EESG-DD	97,6	97,3	97,0
2 Blades, DFIG-3G	97,0	96,7	96,4
3 Blades, DFIG-3G	96,8	96,4	96,0
2 Blades, DFIG-1G	97,6	97,3	97,0
3 Blades, DFIG-1G	97,0	96,7	96,4

Table 49: Update drive train availability for different configurations

The model was altered with these changes and new results made. Table 50 shows the effects of these changes in the model. It can be seen that there are both changes in optimal rotor radius and optimal tip speed ratio. For most systems, the rotor radius increases due to the changed availability. The optimal tip speed ratio tends to decrease for most systems. In Table 51, the ranking of the generator-gearbox systems is shown. It can be seen that the DFIG-1G system remains the best. After this, the ranking changes due because the lower availability makes PMSG systems less attractive.

Generator system	**Number of blades**	**Rotor radius (m)**	**Change in radius**	**Optimal tsr**	**Change in tsr**	**COE (€/MWh)**	**Change in COE**
PMSG-DD	2	76,3	0,0%	9,5	0,0%	58,6	3,1%
PMSG-3G	2	79,8	4,6%	9,1	-2,2%	60,5	4,0%
PMSG-1G	2	79,8	4,6%	9,1	0,0%	58,0	3,2%
EESG-DD	2	76,3	0,0%	9,5	0,0%	60,2	1,6%
DFIG-3G	2	79,8	4,6%	9,1	-2,2%	57,5	2,1%
DFIG-1G	2	79,8	4,6%	9,1	-2,2%	55,7	1,8%
PMSG-DD	3	74,6	2,5%	7,9	-1,3%	60,4	3,1%
PMSG-3G	3	74,6	0,0%	7,9	0,0%	62,3	4,2%
PMSG-1G	3	74,6	0,0%	7,9	0,0%	60,1	3,9%
EESG-DD	3	74,6	2,5%	8,1	1,3%	62,0	1,6%
DFIG-3G	3	74,6	0,0%	7,9	0,0%	59,1	2,1%
DFIG-1G	3	74,6	0,0%	7,9	0,0%	57,5	2,0%

Table 50: New results with altered availability model

	Before		Now	
Ranking	System	Blades	System	Blades
1	DFIG-1G	2	DFIG-1G	2
2	PMSG-1G	2	DFIG-3G	2
3	DFIG-3G	2	DFIG-1G	3
4	DFIG-1G	3	PMSG-1G	2
5	PMSG-DD	2	PMSG-DD	2
6	PMSG-1G	3	DFIG-3G	3
7	DFIG-3G	3	PMSG-1G	3
8	PMSG-3G	2	EESG-DD	2
9	PMSG-DD	3	PMSG-DD	3
10	EESG-DD	2	PMSG-3G	2
11	PMSG-3G	3	EESG-DD	3
12	EESG-DD	3	PMSG-3G	3

Table 51: Original and new ranking of drive train configurations

From the above results, it can be concluded that the availability has a significant effect on the results.

8.7 Conclusions of the second model

In the second model, several improvements were made to the cost models. This showed to change the optimal configuration. The rotor radius changed slightly and the optimal tip speed ratio changed considerably. However, the order of best to worst gearbox-generator configurations did not change for most rotor sizes.

The sensitivity analysis to changes in rotor radius and tip speed ratio showed that the change in COE is rather small when these variables were changed. This means that the results from the model should still be treated with caution. Especially since Chapter 8 still mentions many improvements which could be added to the model to decrease the uncertainty in the results.

A sensitivity analysis was done in order to see the results of a possible change to the availability model to support the claim that it can have an important effect on the results. The results showed that indeed, the availability model has the potential to give new, interesting results if is implemented. It should be noted however, that the suggestions made in this chapter are not based on scientific research.

9 Conclusions and recommendations

The goal of this project was to produce a tool which is capable of finding the optimal drive train configuration for a specified offshore wind project. Five variables were selected which were subject of optimization: the rotor radius, the tip speed ratio, the number of blades, the gearbox type and the generator type. For each combination of variables, the COE was determined.

The determination of the COE was split up into two large tasks: determining the costs of the turbine and determining the performance of the turbine. This last task proved to be the easier of the two as the performance of different drive train concepts and the performance of the various components is widely documented. It was therefore possible to find a relatively easy method to determine a good estimate of the performance of each drive train configuration. The most difficult part of the performance calculation proved to be the estimation of the availability of the turbine. Only one project was found which elaborated on the determination of the availability of a turbine in detail. Unfortunately, this project only covered the availability of one drive train configuration and size.

The more difficult task was to determine the costs of all the components. There are only a very limited amount of reports and books that elaborate on cost models for wind turbines. And the cost models that were found all had two sources of inaccuracy:

- Many cost models are several years old. In a relatively young industry such as the wind industry, this means that large changes have taken place since the writing of these models. Technology has changed, labour and material prices have changed, … . The older a cost model gets, the more inaccurate the give cost becomes.
- Cost models are subject to large simplifications. The cost models are often based on parameters that do not accurately reflect the cost drivers of components.

Therefore, very simple cost models were used to calculate the costs of the different turbines.

The two-bladed DFIG-1G configuration proved to be the best configuration for all wind conditions and turbine sizes. For this configuration, the COE showed large sensitivity to changes in rotor radius or tip speed ratio.
Since the COE for different configurations showed to be very close together and since the cost model is thought to be rather inaccurate, it can be concluded that many improvements need to be added to the model in order for the results to be really reliable. A number of recommended improvements are:

- Improved blade cost models. The cost model used was only based on one planform design and the blade was designed to withstand an extreme wind gust. The improved model should be able to account for different planform designs and its effects on the required skin material and the required structural material to withstand the loads. An analysis of the cricital loads is therefore also required per blade configuration.
- The tower costs are now purely a function of the hub height. An improved tower model should make sure that the tower is capable of withstanding the bending loads to which it is subject. Besides the loads, the natural frequency of the tower is also a large issue which for now has been completely overlooked. The mass of the drive train determines the natural frequency of the tower and the number of blades and rotational speed of the rotor determine the range of natural frequencies which should be avoided by the tower. It is therefore not something which should just be overlooked.
- The O&M costs now show very little variations for different drive train concepts. A more detailed study should focus more on the effects of different drive train concepts to the O&M

costs. The result of such a study could also help estimate the impact of the drive-train configuration on the availability per configuration.
- Installation procedures for various configurations should be determined and the required time (and vessel costs) for each procedure should be determined.

Each of these recommended improvements could be subject of an extensive study and it was therefore not possible to add one of the abovementioned improvements to the model within this project.

References

[1] European Wind Energy Association, *The European offshore wind industry key 2011 trends and statistics,* 2012

[2] J.F. Manwell, J.G.McGowan, A.L.Rogers, *Wind energy explained: Theory, design and application*, John Wiley & Sons Ltd, 2002

[3] H. Braam, L.W.M.M. Rademakers, *O&M aspects of the 500MW offshore wind farm at NL7: Baseline configuration*, DOWEC, 2002

[4] E. de Vries, *Technology of the sea – Offshore wind turbines*, Wind Power Monthly, 2011, www.windpowermonthly.com last visited may 2012

[5] D.J. Malcolm, A.C. Hansen, *WindPACT turbine rotor design study*, National Renewable Energy Laboratory, 2006

[6] P. Fuglsang, K. Thomsen, *Site-specific design optimization of 1.5-2.0MW wind turbines*, Journal of Solar Energy Engineering, Vol. 123, pp. 296-303, 2001

[7] K. Martin, *Site-specific optimization of rotor/generator sizing of wind turbines*, Master thesis, Georgia Institute of Technology, 2006

[8] M. Schmidt, *The economic optimization of wind turbine design*, Master thesis, Georgia Institute of Technology, 2007

[9] H. Li, Z. Chen, H. Polinder, *Research report on numerical evaluation of various variable speed wind generator systems*, Project UpWind, 2007

[10] G.J.W. van Bussel, M.B. Zaaijer, *Integrated analysis of wind turbine and wind farm*, Gigawind Symposium, Hannover, 2002

[11]A. Derks, *Development of a wind turbine drive train engineering model*, Master thesis, TU Delft, 2008

[12]Areva, *M5000 Technical data*, www.areva-wind.com/1/m5000/technical-data last visited may 2012

[13]Bard, *Concepts*, http://www.bard-offshore.de last visited may 2012

[14]Repower Systems, *The 5-megawatt power plant with 126m diameter*, www.repower.de last visited may 2012

[15]Repower Systems, *The Next Step: The REpower 6M Offshore Wind Power Plant*, www.repower.de last visited may 2012

[16]Alstom, *Haliade 150 – 6MW Offshore wind turbine*, www.alstom.com last visited may 2012

[17]AMSC, *SeaTitan 10MW wind turbine,* www.amsc.com last visited may 2012

[18]BARD, *Bard is testing new enhanced offshore wind converters – Two prototypes of the 6.5 megawatt class at the Rysumer Nacken*, www.bard-offshore.de last visited may 2012

[19]CONDOR Wind Energy, *5MW two-bladed wind turbine - technical data*, www.condorwind.com/condorfive.html last visited may 2012

[20]DSME, Offshore Wind Generator - DSME 7.0MW, www.dsme.co.kr last visited may 2012

[21]GamesaCorp, *Gamesa 5.0MW Offshore – Cutting edge offshore technology,* www.gamesacorp.com

[22]The WindPower, *Gamesa G14X/7000*, www.thewindpower.net last visited may 2012

[23]GE Energy, *4.1-113 Wind turbine*, www.ge-energy.com last visited may 2012

[24]Mitsubishi Power Systems Europe, *Sea Angel – The future of offshore wind*, www.mhips.com last visited may 2012

[25]Nordex, *N150/6000: The most economical solution for offshore projects,* www.nordex-online.com last visited may 2012

[26]SCD Technology, *SCD 6MW,* www.scd-technology.com last visited may 2012

[27]Siemens, *Siemens 6.0 MW Offshore wind turbine,* www.energy.siemens.com last visited may 2012

[28]The WindPower, *Vestas V164/7000*, www.thewindpower.net last visited may 2012

[29]Darwind, *Commercial and business planning overview for XEMC,* www.clingendael.nl last visited may 2012

[30]4C Offshore, *2B6,* www.4coffshore.com last visited may 2012

[31]H. Polinder, D. Bang, H. Li, Z. Chen, *Concept report on generator topologies, mechanical and electromagnetic optimization*, Project UpWind, 2007

[32]T. Burton, D. Sharpe, N. Jenkins, E. Bossanyi, *Wind energy handbook*, Wiley, 2001

[33]S. Thomas, M. Fischedick, *Levelized cost of energy (LCOE) and GHG abatement costs*, Budget allocation charts workshop, Beirut, 2009

[34]R. Poore, T. Lettenmaier, *Alternative design study report: WindPACT advanced wind turbine drive train designs study,* National Renewable Energy Laboratory, 2003

[35]L. Fingerish, M. Hand, A. Laxson, *Wind turbine design cost and scaling model*, National Renewable Energy Laboratory, 2006

[36]S. Butterfield et al., *Engineering challenges for floating offshore turbines*, National Renewable Energy Laboratory, 2007

[37]M.I.Blanco, *The economics of wind energy*, Renewable and Sustainable Energy Reviews, Vol. 13, pp. 1372-1382, 2009

[38]TPI Composites Inc., *Cost study for large wind turbine blades: WindPACT blade system design studies,* Sandia National Laboratories, 2003

[39]D.A. Griffin, *WindPACT turbine design scaling studies technical area 1 – Composite blades for 80- to 120 meter rotor*, National Renewable Energy Laboratory, 2001

[40]TPI Composites Inc., *Parametric study for large wind turbine blades*, Sandia National Laboratories, 2002

[41]TPI Composites Inc., *Innovative design approaches for large wind turbine blades,* Sandia National Laboratories, 2003

[42]H. Li, Z. Chen, H. Polinder, *Research report on models for numerical evaluation of variable speed different wind generator systems*, Project UpWind

[43]R. Harrison, E. Hau, H. Snel, *Large wind turbines: Design and economics*, John Wiley & Sons Ltd, 2000

[44]O. Barten, *What is the ideal power curve? Optimizing the power curve above rated wind speed for large offshore wind turbines*, Master thesis, TU Delft, 2012

[45]LORC Knowledge, *The monopile – Close to a monopole*, 2011, www.lorc.dk last visited may 2012

[46]W.E. de Vries, *Assessment of bottom-mounted support structure types with conventional design stiffness and installation techniques for typical deep water sites*, Project UpWind, 2007

[47]M. Dicorato et al., *Guidelines for assessment of investment cost for offshore wind generation*, Renewable Energy, Vol. 36, pp 2043-2051, 2011

[48]J.P. Anish, *A comparative analysis of the two-bladed and three-bladed wind turbines for offshore wind farms,* Master thesis, TU Delft, 2010

[49]J. Meyers, C. Meneveau, *Optimal turbine spacing in fully developed wind farm boundary layers*, Wind Energy, Vol. 15., Issue 2, pp 305-317, 2012

[50]National Grid, *Transmission networks: Offshore development information statement*, 2009 www.nationalgrid.com last visited august 2012

[51]M.J. Kaiser, B.F. Snyder, *Offshore wind cost modeling: Installation and decommissioning*, Springer-Verlag, 2012

[52]M.B. Zaayer, W. van den Broek, G.J.W. van Bussel, *Toward selection of concepts for offshore support structures for large scale wind turbines*, DOWEC, 2001

[53]S.A. Herman, *Offshore wind farms: Analysis of transport and installation costs*, ECN, 2002

[54]A. Curvers, L. Rademakers, *WP6: Operation and maintenance. Task 3: Optimization of the O&M costs to lower energy costs*, RECOFF Project, ECN, 2004

[55]H. Braam, L.W.M.M. Rademakers, *O&M aspects of the 500MW offshore wind farm at NL7: Optimization study*, DOWEC, 2003

[56]*M5000 Technical data*, AREVA Wind GmbH, 2010, www.areva-wind.com last visited august 2012

[57]P. Jamieson, *Innovation in wind turbine design*, John Wiley & Sons Ltd, 2011

[58]R.E. Wilson et al., *Aerodynamic performance of wind turbines*, Energy Research and Development Administration, 1976

[59]A. Grauers, *Efficiency of three wind energy generator systems*, IEEE Transactions on Wind Energy Conversion, Vol. 11, No. 3, pp. 650-657, 1996

[60]N. Mohan, T.M. Undeland, W.P. Robbins, *Power electronics: Converters, applications and designs*, Wiley, 2003

[61]GL, *Regulations for the certification of offshore wind energy conversion systems*, Germanischer Lloyd, 1999

[62]G.J.W. van Bussel, M.B. Zaayer, *'Reliability, availability and maintenance aspects of large scale offshore wind farms, a concept study',* DOWEC, 2001

[63]*Scale-up of wind turbine blades – Changes in failure type*, Bladena, bladena.rosell.dk last visited January 2012

[64]J. Jonkman et al., *Defenition of a 5MW reference wind turbine for offshore system development*, National Renewable Energy Laboratory, 2009

Appendix A: Detailed generator system specifications

The following appendices hold some specifications for the generator-gearbox systems that were optimized in the Upwind study [9].

A.1 PMSG DD system specifications

Rotor Specifications					
Rated power (MW)	0,75	1,5	3	5	10
Diameter (m)	50	70	90	115	170
V_{rated} (m/s)	11,3	11,3	12	12	11,7
Rated rpm	28,6	20,5	16	14,8	10
Weight (ton)					
Active material	2,93	5,82	14,85	21,48	51,46
Iron	2,04	3,95	9,79	14,85	34,31
Copper	0,67	1,16	3,21	4,65	10,96
Permanent magnets	0,22	0,71	1,85	1,98	6,19
Generator construction	4,37	13,5	29,22	88,15	211,22
Total Generator	7,3	19,32	44,07	109,63	262,68
Costs (kEuro)					
Active material	25,1	57,7	151,4	193,7	515,1
Construction material	21,9	67,5	146,1	440,7	1056
Power Electronics	30	60	120	200	400
Electrical subsystem	28,4	56,7	113	189	378
Total system costs	105,4	241,9	530,5	1023,4	2349,1

Table 52: Detailed PMSG DD system specifications [9].

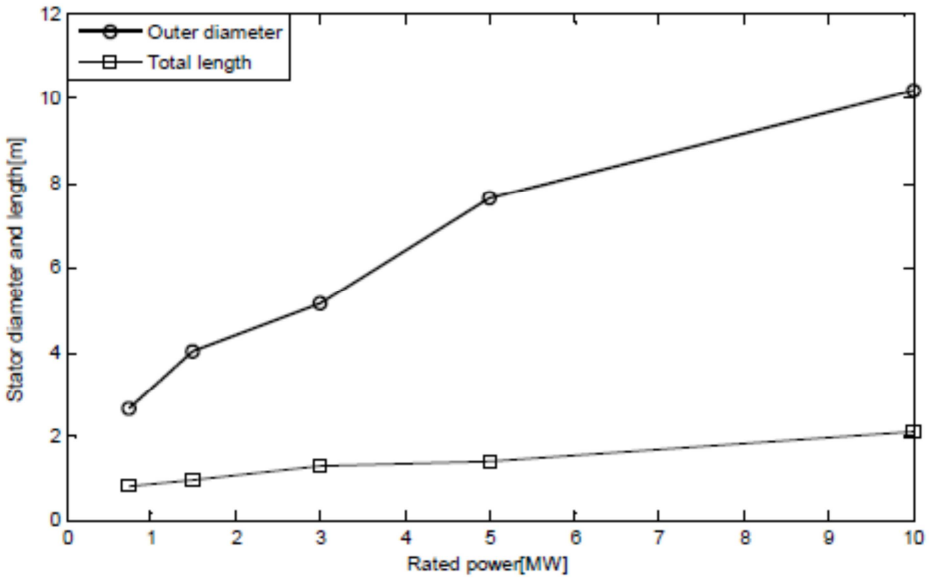

Figure 41: PMSG outer dimensions as a function of rated power [9].

A.2 PMSG -1G system specifications

Rotor Specifications					
Rated power (MW)	0,75	1,5	3	5	10
Diameter (m)	50	70	90	115	170
V_{rated} (m/s)	11,3	11,3	12	12	11,7
Rated rpm	28,6	20,5	16	14,8	10
Gearbox specifications					
Gear ratio (-)	4,68	5,17	6,27	7,25	9,02
Output rated rpm	133,8	106,0	100,3	107,3	90,2
Weight (ton)					
Active material	1,28	2,46	4,35	5,39	8,23
Iron	0,98	1,66	2,97	3,72	5,55
Copper	0,23	0,55	1,01	1,25	1,95
Permanent magnets	0,07	0,25	0,37	0,42	0,73
Generator construction	0,97	2,58	6,07	10,68	24,05
Gearbox	1,28	4,25	15,5	36,4	159
Total Generator	3,53	9,29	25,92	52,47	191,28
Costs (kEuro)					
Active material	9,15	23,14	38,31	46,9	75,34
Construction material	4,85	12,88	30,35	53,42	120,24
Gearbox	7,7	25,51	93,03	218,2	957
Power Electronics	30	60	120	200	400
Electrical subsystem	28,4	56,7	113	189	378
Total system costs	80,1	178,23	394,69	707,52	1930,58

Table 53: Detailed PMSG 1G system specifications [9].

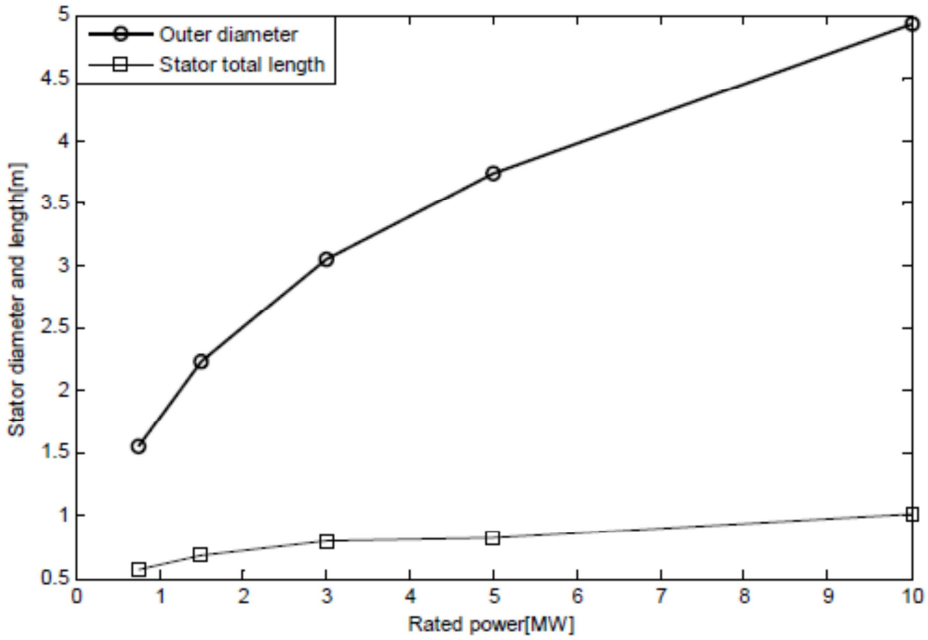

Figure 42: PMSG outer dimensions as a function of rated power [9].

A.3 PMSG 3G system specifications

Rotor Specifications					
Rated power (MW)	0,75	1,5	3	5	10
Diameter (m)	50	70	90	115	170
V_{rated} (m/s)	11,3	11,3	12	12	11,7
Rated rpm	28,6	20,5	16	14,8	10
Gearbox specifications					
Gear ratio (-)	42,0	58,5	75,0	81,1	120,0
Output rated rpm	1200,0	1200,0	1200,0	1200,0	1200,0
Weight (ton)					
Active material	0,379	0,634	1,118	1,54	4,22
Iron	0,29	0,49	0,88	1,19	3,35
Copper	0,074	0,11	0,17	0,24	0,6
Permanent magnets	0,015	0,034	0,068	0,11	0,27
Generator construction	0,17	0,4	0,98	1,89	10,09
Gearbox	4,77	9,77	21,98	38,24	108
Total system weight	5,319	10,804	24,078	41,67	122,31
Costs (kEuro)					
Active material	2,56	4,5	7,96	11,51	29,94
Construction material	0,84	2,02	4,9	9,44	50,46
Gearbox	47,67	97,68	219,84	382,44	1082,44
Power Electronics	30	60	120	200	400
Electrical subsystem	28,4	56,7	113	189	378
Total system costs	109,47	220,9	465,7	792,39	1940,84

Table 54: Detailed PMSG system specifications [9].

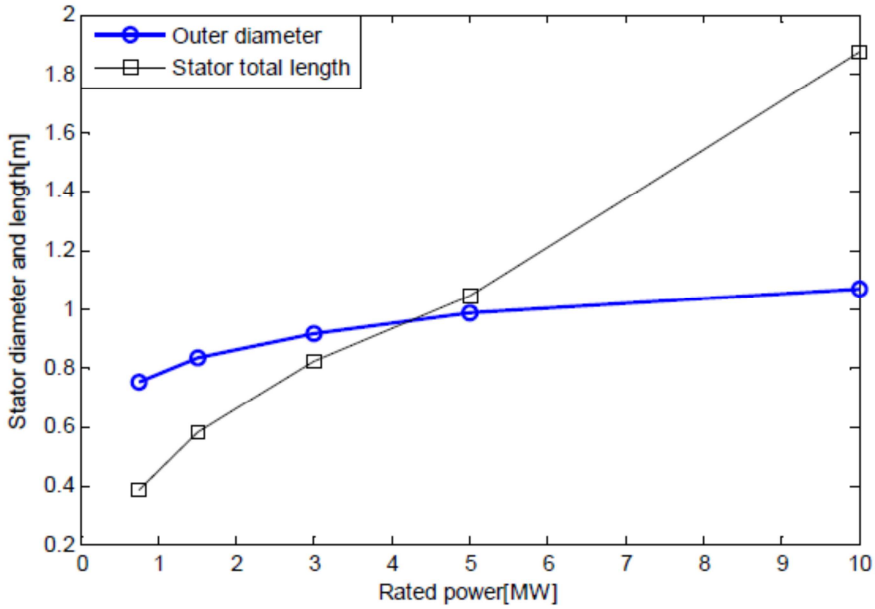

Figure 43: PMSG outer dimensions as a function of rated power [9].

A.4 DFIG-1G system specifications

Rotor Specifications					
Rated power (MW)	0,75	1,5	3	5	10
Diameter (m)	50	70	90	115	170
V_{rated} (m/s)	11,3	11,3	12	12	11,7
Rated rpm	28,6	20,5	16	14,8	10
Gearbox specifications					
Gear ratio (-)	4,68	5,17	6,27	7,25	9,02
Output rated rpm	133,8	106,0	100,3	107,3	90,2
Weight (ton)					
Active material	3,84	4,74	7,12	9,86	18
Iron	3,04	3,59	5,5	7,87	14,45
Stator copper	0,44	0,6	0,83	1,02	1,81
Rotor copper	0,36	0,55	0,79	0,97	1,74
Generator construction	2,79	3,72	6,99	11,86	26,65
Gearbox	1,38	4,37	15,76	36,37	158,65
Total system weight	8,01	12,83	29,87	58,09	203,3
Costs (kEuro)					
Active material	21,16	28,13	40,81	53,58	96,62
Construction material	13,94	18,62	34,96	59,29	133,23
Gearbox	8,14	26,21	94,54	218,2	951,9
Power Electronics	10	20	40	67	133
Electrical subsystem	28,4	56,7	113	189	378
Total system costs	81,64	149,66	323,31	587,07	1692,75

Table 55: Detailed DFIG-1G system specifications [9].

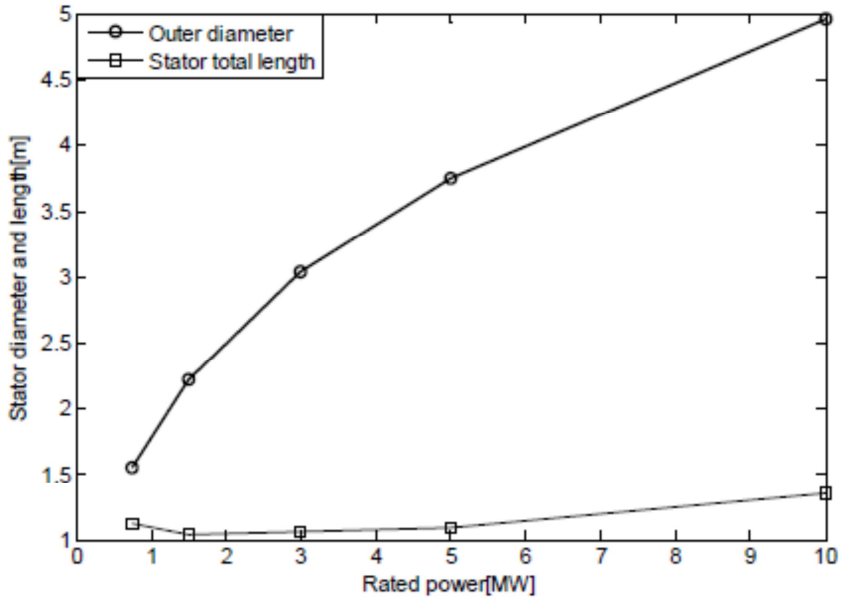

Figure 44: DFIG outer dimensions as a function of rated power [9].

A.5 DFIG-3G system specifications

Rotor Specifications					
Rated power (MW)	0,75	1,5	3	5	10
Diameter (m)	50	70	90	115	170
V_{rated} (m/s)	11,3	11,3	12	12	11,7
Rated rpm	28,6	20,5	16	14,8	10
Gearbox specifications					
Gear ratio (-)	42,0	58,5	75,0	81,1	120,0
Output rated rpm	1200,0	1200,0	1200,0	1200,0	1200,0
Weight (ton)					
Active material	1,29	2,27	4,13	6,85	12,62
Iron	1,04	1,86	3,56	6,06	11,43
Stator copper	0,15	0,24	0,33	0,45	0,68
Rotor copper	0,1	0,17	0,24	0,34	0,51
Generator construction	1,65	3,04	6,32	12,85	35,74
Gearbox	4,77	9,73	21,66	37,28	106,54
Total system weight	7,71	15,04	32,11	56,98	154,9
Costs (kEuro)					
Active material	6,82	11,69	19,26	29,93	52,14
Construction material	8,29	15,22	31,55	64,29	178,73
Gearbox	47,67	97,26	216,64	372,84	1065,38
Power Electronics	10	20	40	67	133
Electrical subsystem	28,4	56,7	113	189	378
Total system costs	101,18	200,87	420,45	723,06	1807,25

Table 56: Detailed DFIG-3G system specifications [9].

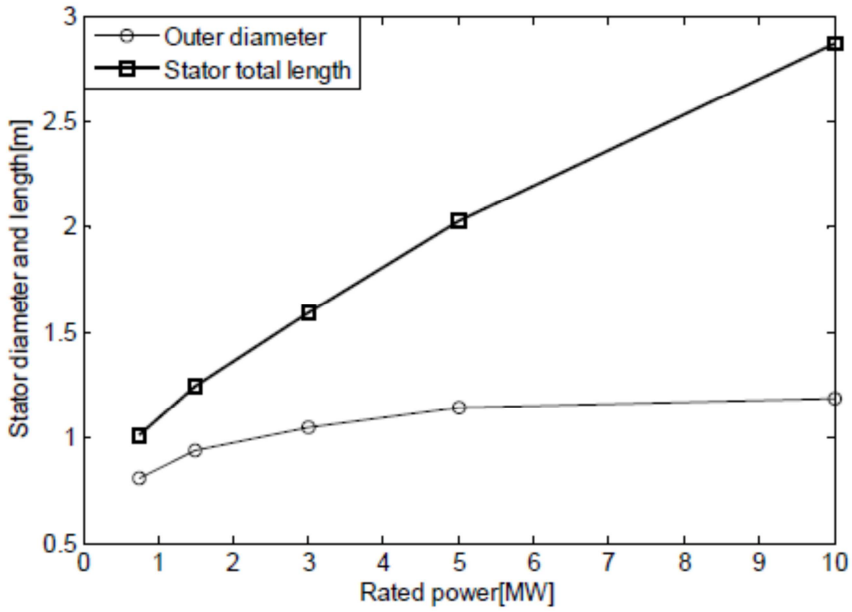

Figure 45: DFIG outer dimensions as a function of rated power [9].

A.6 EESG-DD system specifications

Rotor Specifications					
Rated power (MW)	0,75	1,5	3	5	10
Diameter (m)	50	70	90	115	170
V_{rated} (m/s)	11,3	11,3	12	12	11,7
Rated rpm	28,6	20,5	16	14,8	10
Weight (ton)					
Active material	6,3	14,5	32,3	53,8	119,5
Iron	4,6	10,6	24,1	38,5	87,2
Copper	1,7	3,9	8,2	15,3	32,3
Generator construction	4,8	14,9	32,3	93,9	211,22
Total Generator	11,1	29,4	64,6	147,7	330,72
Costs (kEuro)					
Active material	38,9	90,8	195	344	746
Construction material	24,1	74,4	162	470	1102
Power Electronics	30	60	120	200	400
Electrical subsystem	28,4	56,7	113	189	378
Total system costs	121,4	281,9	590	1203	2626

Table 57: Detailed EESG-DD system specifications [9].

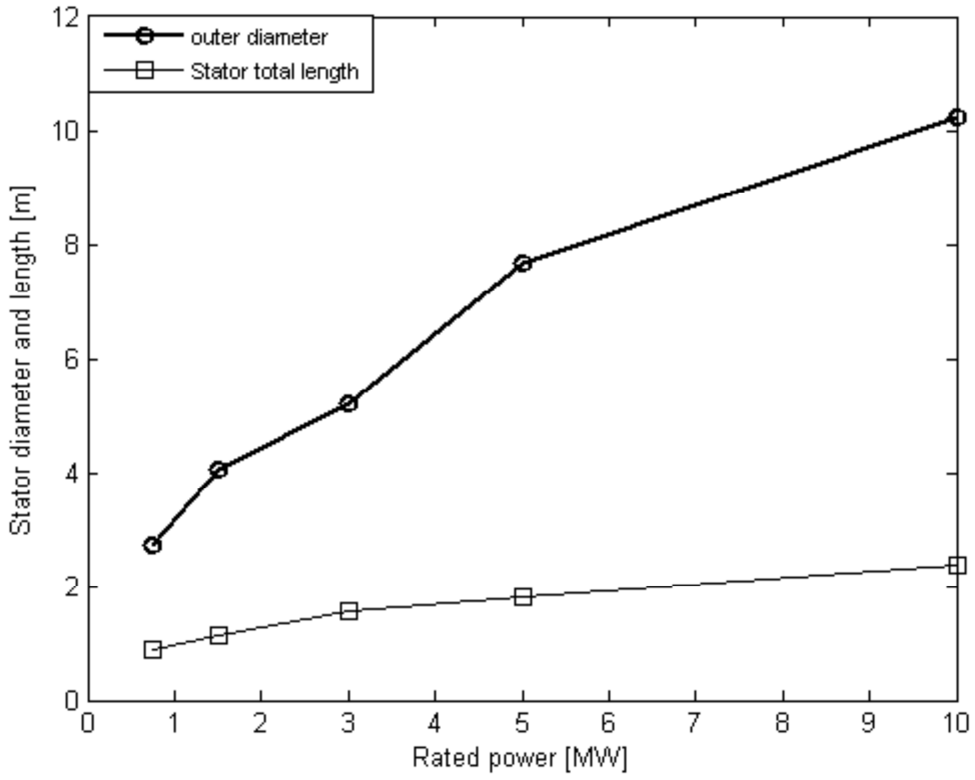

Figure 46: EESG outer dimensions as a function of rated power [9].

Appendix B: Generator losses

The generator losses were derived from the losses that are presented the Upwind project [9]. The loss results were given only in the form of figures, so the exact results were derived using a geometrical method. These results are summarized in Table 58 which shows the generator losses at rated power for each generator system under consideration.

Turbine size(MW)	0,75	3	10
PMSG DD			
Copper loss (kW)	53	110	321
Iron loss (kW)	8	26	63
PMSG 1G			
Copper loss (kW)	22	42	97
Iron loss (kW)	9	24	133
PMSG 3G			
Copper loss (kW)	6	22	32
Iron loss (kW)	18	64	160
EESG DD			
Stator loss (kW)	50	104	395
Rotor loss (kW)	51	103	322
Iron loss (kW)	5	13	39
DFIG 1G			
Stator loss (kW)	36	82	174
Rotor loss (kW)	40	64	150
Iron loss (kW)	8	13	32
DFIG 3G			
Stator loss (kW)	15	33	68
Rotor loss (kW)	21	44	89
Iron loss (kW)	3	12	32

Table 58: Generator losses at rated power per system [9].

Appendix C: Optimization routine in Matlab

In Chapter 5, the general set-up of the optimization procedure was already described. In this chapter, the procedure will be described in more detail and details on how it was implemented in Matlab will be given. Matlab was chosen as the programming language due to past experience of the author with this language and because it has many built-in statistical, graphical, … functions.

C.1 Initialization of variables

The first step in the routine is the initialization of the variables. In order to do this, the user has to specify the following things:

- Target aerodynamic power
- The size of the windfarm (which is used to calculate the windfarm costs and O&M costs)
- The wind distribution: Weibull shape and scale parameter for a certain reference height and the wind shear exponent at the site.
- The range of rotor sizes which will be evaluated.
- The amount of rotor sizes evaluated
- The amount of tip speed ratios evaluated
- The lower value of the tip speed ratio
- The maximal allowed tip speed

Using this information, the subfunction `'Initialize_rotor_variables'` will form sets of parameters which represent all the rotor configurations under evaluation. A vector of rotor sizes under consideration is specified (using the average rotor size and rotor range) and a vector of tip speed ratios is specified (using the minimal value and the maximal allowed tip speed). Now, each rotor size and tip speed ratio is combined for both a two-bladed and a three-bladed rotor to have a matrix which holds the rotor design variables for each rotor configuration.

C.2 Set-up of aerodynamic power curve

For each rotor configuration, the power curve will be set-up. An estimated power coefficient for each configuration is calculated in the subfunction `'calc_Cp'`. In this subfunction, the coefficient is estimated based on the number of blades, tip speed ratio and average lift over drag ratio of the blade.
Now that the power coefficient is known for each rotor configuration, the aerodynamic power curve for these configurations is set-up. The turbine operates at the maximal power coefficient from 0 m/s up to the wind speed for which the target aerodynamic power is reached. Above this wind speed, the aerodynamic power remains fixed at the target power until 25 m/s (which is considered to be cut-out wind speed). For each step in the power curve, the rotational speed is also determined and the tip speed.
After this, the aerodynamic torque is calculated by dividing the aerodynamic power through the rotational speed.

C.3 Real power curve

Now that the aerodynamic power curve is known for each rotor configuration, the real power curve, including losses, will be set-up for each rotor and generator-gearbox configuration.

To do this, the gearbox losses are calculated for two types of gearboxes: the three-stage and single-stage gearbox. A new power curve is then set-up for the two gearbox configurations combined with each rotor configuration.

After this, the generator power curve is set-up for each gearbox-generator configuration using the subfunction ‘calculate_generator_losses‘. Now, the generator power curve is set-up for each rotor configuration and for six generator-gearbox configurations. Using the subfunction ‘calculate_converter_losses‘ the power curve after the converter is now calculated for each configuration. Finally, the transmission and wake losses are accounted for to find the real power curve for each generator-gearbox configuration and rotor configuration.

C.4 Energy yield

Now that the power curves are known, the energy yield can be calculated. The wind speed distribution is calculated at the hub height of each configuration. This wind speed distribution is then linked to the power curve to find the annual energy yield of all the configurations. The same is done for the losses to find the total annual energy losses for each configuration.

Finally, the found energy yield is corrected for the availability of the turbines.

C.5 Component costs

As a first step in the component cost calculation, the inflation rates for different years and the exchange rate from US Dollar to Euro is defined.

Next, a number of component cost factors are defined. These factors can be used to change costs of certain components in case they show different price trends than general inflation. They could also be used to see the effects of e.g. a projected decrease in costs for a certain component.

Now, all the components costs will be calculated. Most component costs are calculated in the main function, but some are calculated using subfunctions.

- The costs (and mass)of the blades are calculated in the subfunction ‘calculate_blade_cost’.
- The gearbox, generator and converter costs are calculated in the subfunction ‘calc_generatorsystem_cost’. This subfunction calls several lower functions too: ‘gear_1’ for the gear-ratio and cost calculation for a single-stage gearbox. ‘gear_3’ for the gear-ratio and cost calculation for a three-stage gearbox. ‘generatur_cost_calculation’ for the generator and converter costs.
- ‘calculate_cable_costs’is used to calculate the costs of all the transmission cables for the entire windfarm. For this calculation, the amount of turbines necessary to reach the total wind farm size is estimated. Next, the amount of rows and turbines per row is estimated to form a square wind farm. Now, the total cable length is calculated for in-field cables(from the turbines to the transformer). Next, the required current rating for these cables is calculated to estimate the cable cost per unit of length. The total cost of the in-field cables is now calculated.
  The shore connection cable costs are calculated by calculating the required current rating per cable to calculate the specific cost of the cable. The length of these cables is specified by the user.
- The substation costs are calculated in the subfunction ‘calculate_substation_cost ‘.

After the total cable and substation costs are known, the costs per turbine are calculated.

The installation costs are the final capital costs which have to be added. This cost is calculated for each rotor configuration (since it is solely dependent on the height of the configuration, which is a function of the rotor diameter).

Now that all the capital costs are known, the levelized capital costs are calculated.

The final cost component are the O&M costs. These costs are calculated in the subfunction ‘operation_and_maintenance_cost’.

C.6 Minimal COE

Now that the energy yield and levelized cost for each configuration is known, the COE is calculated. To find the optimal configuration, the minimal COE has to be found. It could easily be found by just taking the minimum value of the entire COE matrix. However, this would make it difficult to compare different configurations with each other and since this comparison might also hold valuable information, several steps are taken while finding the minimal COE.

The first step is to find the minimal COE per rotor diameter for each blade number and generator-gearbox configuration. The minimal COE is stored in a separate matrix together with the index of this configuration.

Out of these minimal values per rotor size, the absolute minimum per generator-gearbox is selected and its index stored.

The stored indices are now used to find cost and configuration information of the optimal configurations. This is first done per rotor size and afterwards for the optimal configuration per generator-gearbox system.

The final step in the model is to place the wanted information in a cell array of strings, which is written into excel. This spreadsheet is saved into a folder which is specified by the user. The tool checks if this folder already exists on the computer of the user and creates the folder when required.